A WAVELENGTH DIVERSITY TECHNIQUE FOR SMOOTHING OF SPECKLE

Thesis by

Atul Jain

In Partial Fulfillment of the Requirements

For the Degree of

Doctor of Philosophy

California Institute of Technology

Pasadena, California

1974

(Submitted August 30, 1973)

ACKNOWLEDGMENTS

I would like to thank my advisor, Dr. Nicholas George, for initially suggesting the problem to me. I also wish to thank him for his constant encouragement, his first rate guidance during the course of this work and his most refreshing outlook on the subject.

I wish to thank Dr. Ed Posner for the many valuable discussions I have had with him on the statistical aspects of speckle.

I wish to thank David MacQuigg, Alexis Livanos, and Dr. Richard MacAnally for many helpful conversations on the subject.

And I wish to give special thanks to Miss Dian Rapchak and Mrs. Karen Current for typing the manuscript.

ABSTRACT

Theoretical and experimental results are given for the wavelength dependence of speckle, thus establishing a method for the reduction of speckle noise in holographic microscopy with the use of multitoned illumination and a panchromatic viewing system. A model is presented for a partially diffuse phase type of object and the statistical behavior of the speckle produced in the image of this object is studied. A calculation is made for the spectral auto-correlation function which gives a wavelength spacing required to decouple the speckle patterns produced by two tones, this spacing being found to be inversely proportional to the standard deviation of the heights of the scatterers on the object. A criteria is defined for the degradation of an image due to speckle and the resultant improvement is found to depend on the square root of the number of independent tones used.

The wavelength dependence of speckle is verified in a series of experiments where we illuminate the object by both laser and bandlimited light. We first demonstrate the averaging of speckle in the image of a pap smear when we use four tones of an argon laser (5145, 4965, 4880 and 4765 Å). We then show that the image of a rough object is speckly even for bandwidths up to 5Å ;

and then we demonstrate the smoothing of speckle when both a scotch tape diffuser and a section of an optic nerve is illuminated by six equally spaced bandlimited tones scanning 1,500Å .

Thus, in this study, we demonstrate the feasibility of eliminating objective speckle in holographic microscopy using a multimonochromatic source and also provide a theoretical basis for studying the properties of rough surfaces by studying the wavelength diversity of the speckle produced by them.

TABLE OF CONTENTS

Chapter I

Introduction

1.1 Statement of the Problem

The image of a rough object, illuminated with coherent light, appears granular in structure and a lot of the detail on the image is hard to discern for this reason. This granular nature of the image is due to the interference from the phase variations of the light due to the randomly distributed heights within a resolution cell for the optical system forming the image. The same kind of granular structure is observed in the scattered light from a rough object and is known as speckle. With incoherent light, the phases at various points change with time and the speckle pattern, averaged over a normal period of observation time, has a negligible contrast.

This speckle has been a subject of numerous studies in the past[1-25]. One of the major reasons for this interest is because speckle is a detrimental factor in many aspects of holography, particularly in holographic microscopy and has been called the "enemy number one"[15] of holography. Most of these studies, however, had been restricted to the case of monochromatic illumination and the wavelength dependence of speckle in the image of an object had not been studied so far.

The subject of this thesis is to study speckle with the objective of understanding its occurrence, its spatial variations as the wavelength of the illuminating beam is scanned through the visible spectrum and its averaging when the object is illuminated with a set of

monochromatic tones. Although both imaged and non-imaged speckle is of interest, we treat only the imaged case in our study since it is more general and reduces readily to the latter case. We therefore present both theory and experiments on the spectral dependence of speckle. Also from these studies we find that one method for reducing speckle in holography is to illuminate the object with a series of independent wavelengths to record a multicolor hologram and then to view this hologram with a panchromatic viewing system.

In the rest of this chapter, we first give a review of the previous work done on speckle. We then give a short preview of the material in the rest of this thesis.

1.2 Review of Previous Studies on Speckle

One of the first detailed studies of speckle in monochromatic illumination was made by M. Von Laue[1] in 1914 when, using a glass plate with lykopodium powder on it, he demonstrated the existence of speckle in the light scattered by this plate. For his illumination, he used an arc lamp source and a filter which provided blue light spanning the wavelengths between 4.2×10^{-5}cm and 4.3×10^{-5}cm. For the non-imaged case, he also developed a theory where he assumed that the scattered radiation can be given as radiation scattered by a sum of N equally oriented scattering particles, and for an incident wave represented by

$$\psi(\alpha,\beta)\,\frac{e^{-ikR}}{R} \quad ,$$

where α_o, β_o, γ_o are the direction cosines and R is the distance

between the point of origin of the wave and the scatterers, the scattered radiation is given by

$$\psi(\alpha,\beta)\ \frac{e^{-ikR}}{R}\sum_{n}^{N} e^{ik[x_n(\alpha-\alpha_o)+y_n(\beta-\beta_o)]}$$

where (x_n, y_n) represent the coordinates of the scatterers.

Speckle was rediscovered immediately after the advent of the visible helium-neon laser, and Rigden and Gordon[2], Langmuir[3] and Oliver[4] have photographed and discussed the causes of this phenomenon and correctly attributed it to the fact that irregularities in the reflecting surface cause a random diffraction effect in the beam. Rigden and Gordon note that the size of the speckle depends upon the limiting aperture of the optical system in which the speckle is observed and present an analytical argument for this size dependence of speckle. Langmuir notes that this speckle phenomenon is analogous to radar "clutter", while Oliver notes that the existence of the speckle depends upon the monochromaticity of the illumination and the stationarity of the scatterers.

Goodman[5] studied the analytical properties of the speckle formed from light scattered by a diffuser, and his work contains the only prior consideration of the frequency dependence of speckle. He modeled the diffuser to be a set of randomly spaced antennas and used for the electric field a Gaussian distribution and the intensity a Rayleigh distribution. He then calculated the first order and second order statistics of the speckle as well as the spatial averages of the intensity.

The second order statistics of the speckle pattern formed by light scattered from a rough surface were also calculated by Goldfischer[6]. He took his model to be a set of densely packed scatterers. For an incident power density $P(u,v)$ and an attenuation by each scatterer α, he took the contribution of each scatterer to the field at some point (x,y) in the observation plane to be

$$[\alpha P(u,v)\Delta u \Delta v/\pi r^2]^{1/2} \cos[2\pi(ct-r)/\lambda+\varphi_{uv}]$$

where c is the velocity of light, r is the distance between the scatterer and the point (x,y) and φ_{uv} is a random phase angle associated with the scatterer at (u,v). He then proceeded to find the intensity by summing over the various random (u,v) and then, by assuming that the distance between adjacent scatterers approached zero, he showed that the autocorrelation function of the speckle intensity is proportional to the far field diffraction pattern of the aperture filled by the area of the diffuse surface. He then proceeded to verify this result experimentally.

So far, the general approach to the problem of speckle reduction in microscopic holography has been by the incoherent superposition of a number of diffusely illuminated holograms of the same object. Martienssen and Spiller[7] first showed that by taking holograms of an object when the object is illuminated through a diffuser and taking different holograms for different positions of the diffuser, and then superimposing the images formed by these different holograms, one can eventually, in the viewing, see a practically

speckle free holographic image.

Enloe[8] made a statistical study of speckle in imaging systems. He also took for his model of a diffuser a set of point scatterers randomly placed on the object, each scatterer radiating light at a different phase. He then proceeded to calculate the first order statistics for the intensity in the image plane with this model of a diffuser and the second order statistics, i.e., the autocorrelation function and the power spectral density of the intensity. He assumed in his calculations that the positions of the scatterers were given by a Poisson distribution while the phases were given by a normal distribution.

There has been a fair amount of interest in the speckle reduction in holograms of objects which are smooth, but have been diffusely illuminated. Since speckle is caused by the fact that light is scattered by the diffuser which does not eventually get collected by the image, Leith and Upatnieks[9] have proposed making a diffuser with very gradual phase variations and placing it in contact with the object so that the light does not get scattered at high enough angles to not be collected by a lens. On the other hand, Gerritson et al[10] have proposed a diffraction grating as an illuminator for the object. This way they can control the angles of illumination and since the diffraction grating gives a series of beams the image of the hologram continues to have the redundancy necessary to reduce noise from dust, etc. On the other hand, for the grating placed very near the object, the illumination is uniform and since the angles of the illumination are low enough to be collected by the lens no speckle is seen. Thus

this is a reasonable way of illuminating a smooth object so as to avoid speckle while at the same time introducing the redundancy in the holograms which reduces noise due to scratches and dust.

In the application of laser holography to microscopy, the speckle effect has been reported to be a severe obstacle[11-13], limiting the working resolution to from a few to several times the classical optics limit. As an example, Cox, Buckles and Whitlow[13] report resolutions of a few microns with biological specimens.

The history of speckle has not been completely preoccupied with methods of reducing speckle. For example, Burch[14] has utilized speckle to study surface vibration. By either looking directly at the scattered light from a rough surface or combining a beam scattered by the rough surface with a reference beam and observing this combination, it is possible to study the vibration of the scattering surface. If the surface moves toward or away from the source, the brightness of the speckles will undergo a cyclic variation, the change from maximum to minimum brightness corresponding to a displacement in the line of sight of one quarter wavelength of light. When the motion is very fast, the speckle becomes blurred and so the nodal areas can be easily picked out since in those regions the speckle will continue to have a high contrast. Although holographic techniques exist to enable the same kinds of studies, the speckle promises to provide a simpler and quicker method of assessing the nature of vibration.

Gabor[15] has classified speckle into two categories: The objective speckle that arises owing to uneven illumination falling on the subject. The subjective speckle that arises from the roughness of

the subject in conjunction with the convolving effect of a finite aperture. The objective type can occur when one holographically records a smooth transparency but with a diffuser placed in the beam illuminating the transparency. While the diffuser creates a helpful redundancy in the recording, it also leads to the deleterious speckle. He has argued that the only effective means for smoothing the subjective type of speckle is to increase the aperture. However, if one draws this conclusion, it is implicitly assumed that operation is at a single wavelength or that separate, independent looks are not being made in the overall process.

Lowenthal et al[16-18] have studied theoretically the reduction of speckle in the images of coherently illuminated rough objects by moving a diffuser in contact with the object. They show that this is equivalent to illuminating the diffuser with incoherent light and report the results of experiments which confirm their theory.

Dainty[19] provides a simplified method of analyzing the second order statistics of speckle using linear filter theory and square law detection theory. He reports some experimental results of the power spectrum of intensity fluctuations in an image with speckle and obtains an expression for the power spectrum of the intensity fluctuations in a speckle pattern produced by a partially coherent system.

Close[21,22] uses the incoherent superposition of holograms to reduce the effect of speckle noise in his high resolution holocamera and obtains resolution of a few microns with this system.

Elbaum, Greenebaum and King[23] have done experiments on the wavelength dependence of speckle. They successively recorded, on film,

the images of a rough bar target when the illumination consisted of the four tones of an argon laser (5145, 4965, 4880 and 4765Å). They then compared the microdensitometer traces of these images to establish that the speckle pattern depended upon the wavelength of illumination.

An interesting application of the speckle effect was reported by Mohon and Rodeman[24]. It was noticed that when an observer moves his head, the motion of the speckle pattern observed by him is directly related to his visual acuity. Thus, if he has perfect vision, i.e., he is an emmotropic person, he observes little or no motion of the speckle pattern when moving his head. If he is myopic he observes that the speckle pattern moves in the opposite direction relative to his head motion. If the observer has hypermetropia he will find that the speckle moves in the same direction as his head. This phenomenon finds itself as a convenient method of checking the visual acuity, especially of children, since the observer does not have to be able to read.

The fact that the wavelength dependence of speckle is related to the root mean square deviations in the scattering heights of a rough object makes speckle a useful tool in studying the roughness of a surface[25]. So far, the only widely used method for measuring roughness is by a profilometer, which consists of a diamond stylus which is traced lightly across a surface contour to produce a time varying voltage output whose magnitude is directly proportional to the height of the surface contour. The voltage output does not pass the very high frequency components, the cutoff being known as the

"roughness width cutoff." However, the profilometer, though adequate, damages the surface under test and so laser speckle has been considered as a possibly useful alternative. Thus, by finding the linewidth of the illumination for which the speckle contrast is negligible, one can measure the standard deviation of the heights of the surface.

1.3 Summary of Research

In the following chapters we study the behavior of the speckle electric field and intensity in the image of a rough object. We calculate the statistical behavior of speckle and demonstrate the averaging of this speckle pattern when the illumination consists of a set of monochromatic tones.

In Chapter II, considering a pure phase diffuser, we derive expressions for the speckle electric field and intensity for the image of this diffuser. We use a physical argument in order to simplify the calculation of the wavelength spacing required to decorrelate the speckle. Experimental results which verify the theory are also given.

In Chapter III we study the statistics of sums of the form $R = \sum_{r}^{N} e^{jah_r}$. We calculate the density functions, the expected values, variances and the autocorrelation functions of R and $|R|^2$. Since the speckle intensity is of the form of R we can use the mathematical results developed in this chapter to calculate the properties of laser speckle.

In Chapter IV, we apply these results more specifically to examine the detailed statistics of laser speckle. We calculate the density functions, the degradation of the image and the spatial and

spectral autocorrelation functions, under monochromatic and band-limited illumination, for the speckle.

Thus, in this thesis we demonstrate, for the first time, a convenient technique for drastically reducing speckle in holographic microscopy. We calculate a wavelength spacing for decorrelation of speckle and demonstrate experimentally this reduction of speckle. We also examine the speckle statistics, a knowledge of which provides us with a powerful tool to study the surfaces of rough objects.

REFERENCES

1. M. Von Laue, Sitzungsberichte der Koenig, Prussiche Akad. der Wissenshaft (1914), pp. 1144-1163.
2. Rigden and Gordon, Proc. IEEE 50, p. 2367 (1962).
3. R. V. Langmuir, Appl. Phys. Lett. 2, p. 29 (1963).
4. B. M. Oliver, Proc. IEEE 51, p. 220 (1963).
5. J. W. Goodman, Stanford University Electronics Labs. Tech. Report SEL-63-140 (TR 2303-1), December 1963.
6. L. I. Goldfischer, J. Opt. Soc. Am. 55, p. 247 (1965).
7. W. Martienssen and S. Spiller, Phys. Lett. 24A, p. 126 (1967).
8. L. H. Enloe, Bell Syst. Tech. J. 46, p. 1479 (1967)
9. E. N. Leith and J. Upatnieks, Appl. Optics 7, p. 2085 (1968).
10. J. H. Gerritson, W. J. Hannan, and E. G. Ramberg, Appl. Opt. 7, p. 234 (1968).
11. R. F. Van Ligten, Opt. Techol. 1, p. 71 (1969).
12. R. F. Van Ligten, J. Opt. Soc. Am. 59, p. 1545 (1969).
13. M. E. Cox, R. G. Buckles, and D. Whitlow, J. Opt. Soc. Am. 59, p. 1545 (1969).
14. E. Archbold, J. M. Burch, A. E. Ennas, and P. A. Taylor, Nature 222AF, p. 263 (1969).
15. D. Gabor, IBM J. Res. Develop. 14, p. 509 (1970).
16. H. Arsenault and S. Lowenthal, Optics Communications II, p. 451 (1970).
17. S. Lowenthal, H. Arsenault, and D. Joyeux, Applications of Holography (Besancon Conference 6-11 July 1970), p. 2-2.

18. S. Lowenthal and D. Joyeux, J. Opt. Soc. Am. 61, p. 847 (1971).

19. J. C. Dainty, Opt. Acta 17, p. 761 (1970).

20. H. H. Hopkins and H. Tiziani, Applications of Holography (Besancon Conference 6-11 July 1970), p. viii.

21. D. H. Close, IEEE J. Quantum Electron. QE-7, p. 312 (1971).

22. D. H. Close, J. Opt. Soc. Am. 61, p. 649 (1971).

23. M. Elbaum, M. Greenebaum, and M. King, Opt. Comm. 5, p. 171 (1972).

24. N. Mohon and A. Rodeman, NAVTRADEVCEN TN-34 (1972).

25. R. A. Sprague, J. Opt. Soc. Am. 62, p. 723A (1972).

CHAPTER II

Speckle Physics

2.1 Introduction

In this chapter we establish a physical basis for understanding the wavelength diversity of speckle and report some experimental results which verify our theory. Thus, in section 2.2 we give a conceptual argument for an order of magnitude estimate for the wavelength spacing required to decorrelate the speckle. In the next section, we derive an expression for the speckle electric field and intensity in the image of a pure phase diffuser. We calculate the wavelength change for which the average of the magnitude squared change in the electric field at a given point on the image plane is equal to the variance of that field, and this gives us the wavelength spacing for the speckle to decorrelate.

In Chapters III and IV, we calculate the density function and the spatial and spectral autocorrelation functions for the speckle and estimate the improvement in image quality under multitoned and band-limited illumination. The results of sections 2.2 and 2.3, therefore, provide for us a physical basis for understanding the results of the next two chapters.

In section 2.4 we report experiments using collimated band-limited light from a carbon arc source and an argon laser to demonstrate the wavelength dependence of speckle and the averaging of speckle under multitoned illumination. Thus in this chapter, we show conclusively that the speckle pattern depends on wavelength and give an expression for the wavelength spacing to decorrelate the speckle.

2.2 Estimate of the Wavelength Spacing Required to Decorrelate the Speckle

When we have a wave, in a medium with refractive index n, of linewidth $\Delta\nu$ we have that its phase is correlated over a length,[1]

$$L = \frac{\lambda_o^2}{(2\pi n)\Delta\lambda} \qquad (2\text{-}1)$$

where L is now the coherence length of this wave. Thus if some length ℓ is greater than the length given by $\lambda_o^2/\Delta\lambda\ (2\pi n)$ then the two end-points of length ℓ will be uncorrelated in phase. Thus if we illuminate by two waves whose wavelength interval is greater than $\Delta\lambda > \frac{\lambda_o^2}{2\pi n L}$ then these two waves will be uncorrelated in phase over the length L.

Now if the standard deviation of the heights of the scatterers on the diffuser is h_o, then following from the above argument the two waves with a wavelength space $\Delta\lambda > \frac{\lambda_o^2}{2\pi n h_o}$ will be uncorrelated in phase over this interval. Thus this decorrelation carries over onto the image plane, and we will have the speckle decorrelation when the two waves have a wavelength spacing

$$\Delta\lambda > \frac{\lambda_o^2}{2\pi n h_o} \qquad (2\text{-}2)$$

2.3 Diffuser Imaging Results

We model the diffuser to be a pure phase object and, in the geometrical optics approximation, for a plane wave incident on the diffuser at an angle θ_o to the normal, the wave exiting on the other

side of the diffuser will have a spatial phase variation depending upon the distance each part of the wave had to travel through the diffuser. Thus if we model the diffuser to consist of a plane sheet of some average thickness and with scatterers of height h_r and width w_r superposed on this sheet (see fig. 2, Appendix A, p. 98) then the one-dimensional electric field transmitted by this diffuser can be written as

$$f(\xi) = e^{-\left(\frac{i2\pi}{\lambda_o}\right)n_o \xi \sin\theta_o}\left[1 + \sum_r \text{rect}\left(\frac{\xi-\xi_r}{w_r}\right)\left\{e^{-\left(\frac{i2\pi}{\lambda_o}\right)n_3 h_r} - 1\right\}\right] \qquad (2\text{-}3)$$

where λ_o is the wavelength of illumination, θ_o the polar angle of the incident wave, ξ the coordinate in the exit plane of the diffuser, n_3 given by the quantity $(n_1/\cos\theta_1 - n_o/\cos\theta_o)$, n_1 and n_o the refractive indices of the diffuser and air respectively, θ_1, θ_o the polar angles of propagation in these two media, and h_r the height of the scatterer at the r^{th} coordinate.

Although the details of the derivation of (2-3) are outlined in Eqs. (5) through (8) in Appendix A, we give an alternate derivation for this equation. The multiplicative term $\exp[-i(2\pi/\lambda_o)n_o\xi\sin\theta_o]$, with the linear phase taper in (ξ) , occurs for a plane wave incident at an angle θ_o , as shown in Fig. 2. With nonoverlapping steps assumed in the

$$\sum_r \text{rect}[(\xi - \xi_r)/w_r] ,$$

the term within the square brackets, [], is either 1 or

$\exp\pi\text{-}i(2\pi/\lambda_o)n_3 h_r]$. This holds for an arbitrary value of ξ , hence $|f(\xi)| \equiv 1$ as it must for a pure phase object.

We could adapt this transmitted field to fit a variety of models for the diffuser. Thus we can consider the height of a step given by $h_r(\xi)$ to be roughly constant over the width w_r . On the other hand, if one prefers the randomly positioned lenslets of Hopkins and Tiziani, then h_r becomes the quadratic phase transmission for each lens, i.e., $h_r(\xi) = [(\xi - \xi_r)^2/f_r]$, where f_r is the focal length of the lenslet centered at ξ_r .

We now consider the electric field in the image of this diffuser. If this diffuser is placed on the (ξ,η) plane and a lens of focal length F and aperture D is placed a distance s' from this diffuser in the (u,v) plane, while the image is formed a distance s from the lens in the (x,y) plane (fig. 1, Appendix A, p. 97), then by the successive application of Rayleigh Sommerfeld's formula, as detailed in Eqs. (1), (2), (3), and (11) in Appendix A, we obtain the one dimensional electric field at the (x,y) plane to be

$$E_1(x) = e^{-\frac{i\pi n_o}{\lambda_o}\left(\frac{x^2}{Ms'}\right)} \int_{-\infty}^{\infty} dx'\, f\left(-\frac{x'}{M}\right) e^{-\frac{i\pi n_o (x')^2}{\lambda_o M^2 s'} - \left(\frac{(x-x')}{\Delta w}\right)^2} \qquad (2\text{-}4)$$

where M is the magnification of the optical system and $f(\xi)$ is given in (2-3).

Now, if we make the assumption that the width of each random step is much less than the resolution cell size, i.e., $w_r \ll \Delta w_o$, where Δw_o is the size of the resolution cell, then insofar as integrations

of the form of Eq. (2-4) we can replace the rect $[(\xi - \xi_r)/w_r]$ by the Dirac delta function, i.e., by $w_r\delta(\xi - \xi_r)$. Thus, we obtain for the speckle electric field and intensity the result

$$E(x) = \Delta w\sqrt{\pi}\; e^{-\frac{i\pi n_o}{\lambda_o}\left\{\frac{x^2}{Ms'} - \frac{2x\sin\theta_o}{M}\right\} - \frac{4\pi n_o^2 x^2 \sin^2\theta_o}{\lambda^2 M^2}} + e^{-\frac{i\pi n_o}{\lambda_o}\left(\frac{x^2}{Ms'}\right)} \sum_r e^{-\left(\frac{x-x'_r}{\Delta w}\right)^2 + \frac{i\pi n_o}{\lambda_o}\left\{\frac{2x'_r\sin\theta_o}{M} - \frac{(x'_r)^2}{M^2 s'}\right\}} Mw_r \left\{e^{-\frac{i2\pi}{\lambda_o} n_3 h_r} - 1\right\} \tag{2-5}$$

and

$$I(x) = \pi(\Delta w)^2 e^{-2\alpha} + 2\sqrt{\pi}\,\Delta w\, e^{-\alpha} \sum_r e^{-\left(\frac{x-x'_r}{\Delta w}\right)^2} Mw_r \left\{\cos(\chi - \phi_{1r} + \phi_{2r}) - \cos(\chi - \phi_{1r})\right\}$$
$$+ 2\sum_r e^{-2\left(\frac{x-x'_r}{\Delta w}\right)^2} (Mw_r)^2 \left\{1 - \cos\phi_{2r}\right\} + \sum_m \sum_{\substack{r \\ m\neq r}} e^{-\left(\frac{x-x'_m}{\Delta w}\right)^2 - \left(\frac{x-x'_r}{\Delta w}\right)^2 + i(\phi_{1m} - \phi_{1r})}$$
$$\cdot\, M^2 w_m w_r \left\{e^{-i\phi_{2m}} - 1\right\}\left\{e^{+i\phi_{2r}} - 1\right\} \tag{2-6}$$

in which $\alpha = 4\pi(n_o x\sin\theta_o/\lambda_o M)^2$, $\chi = \left(\frac{2\pi}{\lambda_o}\right)\frac{n_o x\sin\theta_o}{M}$,

$\phi_{1r} = \frac{\pi n_o}{\lambda_o}\left\{\frac{2x'_r\sin\theta_o}{M} - \frac{(x'_r)^2}{M^2 s'}\right\}$, and $\phi_{2r} = \frac{2\pi}{\lambda_o} n_3 h_r$.

We next obtain a form for $E(x)$ where the phase factors have been suppressed. We obtain from Eq. (15), Appendix A, the result

$$E_1(x) = A - BN + B \sum_{r=1}^{N} e^{+iph_r}$$

We have defined $A = \Delta w\sqrt{\pi}$, $B = Mw_c\, e^{-\frac{i\pi n_o x^2}{\lambda_o M^2 s'}}$ and p as

$$p = -\frac{2\pi n_3}{\lambda_o} \qquad (2\text{-}7)$$

If we restrict our study to the worst speckle case we consider ΔB negligible with wavelength and can assume B independent of λ. Thus for the purposes of future analysis we take B to be constant.

In Eq. (2-7) the summation $r = 1, 2, \ldots . N$ extends only over the N scatterers within a resolution cell size. For smooth objects $E_1(x)$ is equal to A and the speckle which occurs for rough objects is inherent in the terms containing B; and the ratio $\frac{BN}{A}$ is equivalent to the fractional surface occupied by the scatterers in a resolution cell.

We note that the expected value for the electric field is some complex number, while the variance is a real number since it is defined by $\sigma^2[E_1] = \langle |E_1 - \langle E_1 \rangle|^2 \rangle$. Thus $\sigma^2[E_1]$ gives us the square of the radius of a circle centered around the expected value within which roughly half of our values of E_1 lie. The intensity at some fixed point x can thus be considered to have changed

significantly when the magnitude of the change in $E_1(x)$ with wavelength is of the order of the standard deviation. Thus, we adopt the criterion that the speckle is decoupled when the wavelength change causes the average of the magnitude squared change in $E_1(x)$ to be equal to the variance for a particular wavelength λ_o, i.e., decorrelation occurs whenever

$$\langle \Delta E_1(x) \Delta E_1^*(x) \rangle \geq \sigma^2 [E_1(x)] \tag{2-8}$$

Substituting (2-7) into this criterion and going through the steps as detailed in Eqs. (17) through (29) in Appendix A, we find that the wavelength spacing required to decouple the speckle in the case of a rough diffuser, i.e. $ph_o \gg 1$, for h_o the standard deviation for the scatterer heights, is

$$\Delta\lambda = \frac{\lambda_o^2}{2\pi n_3 h_o} \tag{2-9}$$

2.4 Experimental Results

We discuss here some of the experimental results as presented in Appendices A and B. Since at the time of the experiments we did not have a dye laser, we simulated a tunable monochromatic collimated source by using a spectrometer to bandlimit the light emitted by a carbon arc source and collimating the output of the spectrometer using the pinhole P_1, as shown in Fig. 3, Appendix A. The speckle in this case is readily seen to move with wavelength by the normal

eye, which has been in the dark for about 15 minutes, with a characteristic decorrelation wavelength of between 30 to 100Å . This compares well with the value of 80Å for a scotch tape diffuser computed from Eq. (2-9) where $n_3 = 0.6$, $\lambda_o = 0.5$ μm and $h_o \geq 8$ μm . Fig. 5 in Appendix A shows the speckle pattern produced by the bandlimited source while Fig. 4, Appendix A, shows the speckle pattern produced by laser illumination. Figs. 6, 7, 8 and 9 in Appendix A show the image of an optic nerve in laser illumination, white light, illumination from a single 5Å spectral width source and illumination consisting of 6 separate bandlimited wavelengths scanning 4,300Å to 5,800Å respectively. We note the considerable improvement in resolution in Fig. 6 over that in Fig. 5, demonstrating the speckle reduction when the illumination consists of a superposition of wavelengths.

Similarly Figs. 3a, 3b and 3c in Appendix B show the image of a pap smear illuminated by one tone of an argon laser source, white light and 4 tones of an argon laser (5145, 4965, 4880 and 4765 Å). We note the resultant improvement in the resolution of the image when we have a multitoned illumination.

REFERENCES

1. A. C. S. Van Heel, "Advanced Optical Techniques," North-Holland Publishing Co., Amsterdam (1967), ch. 6.

Chapter III

The Problem of Random Vibrations

3.1 Introduction

In the previous chapter we developed an expression for the imaging of a diffuser in monochromatic collimated illumination, and the resultant creation of speckle. The speckle pattern changes with wavelength and so it is proposed that by superposing the image of a diffuser at various wavelengths we would get an averaging out of speckle, while at the same time the image quality would not be degraded. Thus, this technique offers us a promising possibility of reducing speckle in microscopic holography.

However, in order to understand precisely the wavelength spacings and the optimum number of tones required to average out the speckle, it is necessary to understand the statistics of the speckle. In this chapter we therefore review the statistics of functions of the form of $R = \sum_{r=1}^{N} e^{iah_r}$ where h_r is a random variable and N may or may not be taken as a random variable. In the next chapter we then extend the results of this chapter to consider the specific properties of laser speckle which we see in our imaging systems.

The statistics of the function $R = \sum_{r=1}^{N} e^{iah_r}$ were first considered by Lord Rayleigh[1] in connection with scattering of sound by a random distribution of particles. Since then this kind of statistical problem has occurred in a variety of other physical situations. Karl Pearson[2] has stated this as the problem of random walk and he formulated it in the following terms:

"A man starts from a point O and walks ℓ yards in a straight line; he then turns through any angle and walks another ℓ yards in a second straight line. He repeats this process n times. I require the

probability that after these n stretches he is at a distance r and r + dr from his starting point O."

While Lord Rayleigh solved this problem in the case of $N \to \infty$ the general solution of this problem was obtained by J. C. Kluyver[3] and independently by M. von Smoluchowski.[4] A. A. Markoff[5] also formulated the problem of random flights in its most general form and outlined a method for its solution. S. Chandrasekhar[6] has considered this problem in connection with stellar dynamics. If we take the gravitational force acting on a star (per unit mass) by

$$F = G \sum_{i=1}^{N} M_i \frac{\vec{r}_i}{|\vec{r}_i|^3}$$

where M_i, $\vec{r}_i$ denote the mass and distance of a typical field star, and G the gravitational constant, then it is of interest to calculate the probability distribution for the force on the star given the probability laws for the spatial distributions and the masses of the neighboring stars. Similar problems have come up in x-ray scattering,[7] diffuse scattering of electromagnetic waves from the earth's surface,[8] in considering the statistical properties of random noise currents,[9] and in the study of photon noise in multimode lasers.[10]

Thus, given a distribution function for the random variables h_r and N we derive in this chapter the distribution functions of R and $|R|^2$. We illustrate these results by two specific examples which have been of interest in the literature. We then compare the properties of the random variables $R(a)$ and $R(a+\Delta a)$ and examine the conditions when they become independent.

3.2 The Density Functions of $\sum_{r=1}^{N} e^{jah_r}$ and $\sum_{m=1}^{N}\sum_{n=1}^{N} e^{ja(h_m-h_n)}$

We now consider the sum

$$R(a) = \sum_{r=1}^{N} e^{jah_r} \quad , \tag{3-1}$$

where h_r is a random variable and the random variables h_1, h_2, $h_3 \ldots h_N$ are all independent. We also assume that the density function of each h_r, r=1....N is f(h) and is the same. In this sum, a is taken to be a given number. N is also, in general, a random variable with a distribution function g(N) ; however, for the purposes of our calculations, we take N to be a constant number; and in the double sum, we take the set of variables represented by h_m to be the same as the set represented by h_n. We now derive the result for W(R), the density function for R, as originally outlined by A. A. Markoff[5] and reviewed by Chandrasekhar[11]. The details of this derivation are given in Appendix C and we only outline the results of interest to us.

We note from Eqs. (C-18), (C-19) and (C-20), that if we have a vector R which is a superposition of a number of N vectors $\vec{r}_i$, each one having an independent probability distribution τ_i, i.e.

$$\vec{R} = \sum_{i=1}^{N} \vec{r}_i \tag{3-2}$$

where the probability that the ith displacement lies between r_1 and r_i+dr_i is given by

$$\tau_i(x_i,y_i,z_i)\, dx_i dy_i dz_i = \tau_i d\vec{r}_i \qquad (i = 1,\ldots,N)$$

then we have that the probability distribution $W_N(\vec{R})d\vec{R}$ is given by

$$W_N(\vec{R}) = \frac{1}{8\pi^3}\int_{-\infty}^{\infty} e^{-i\vec{\rho}\cdot\vec{R}}\, A_N(\vec{\rho})d\vec{\rho} \qquad (3\text{-}3)$$

for

$$A_N(\vec{\rho}) = \prod_{j=1}^{N}\int_{-\infty}^{\infty} \tau_j(\vec{r}_j)e^{-i\vec{\rho}\cdot\vec{r}_j}\, d\vec{r}_j \qquad (3\text{-}4)$$

To apply this result to our sum given in (3-1), we take e^{jah_r} to be a unit vector $\vec{r}_j = (x_j, y_j)$ where x_j gives the real part of the phasor and y_j the imaginary part. We also assume that the random variables h_r all have a uniform distribution and have density $\frac{a}{2\pi}$ for the interval $[-\frac{\pi}{a}, \frac{\pi}{a}]$ and zero otherwise. In our diffuser language, this corresponds to the case of a rough diffuser. Thus, in spherical co-ordinates we can write the probability density function for $\vec{r}_j$ as

$$\tau_j(\vec{r}_j) = \frac{1}{2}\,\delta(|\vec{r}_j|^2 - 1)\delta(\omega) \qquad (j = 1,2,\ldots,N) \qquad (3\text{-}5)$$

where ω is the azimuthal angle of the co-ordinate system. We thus obtain the density function $W_N(\vec{R})$, after going through the steps (C-22) through (C-28), for the sum $\vec{R}$ as,

$$W_N(\vec{R}) = \frac{1}{2\pi^2|\vec{R}|}\int_0^{\infty} \sin(|\vec{\rho}||\vec{R}|)\,\{\mathrm{sinc}|\vec{\rho}|\}^N\, |\vec{\rho}|\, d|\vec{\rho}| \qquad (3\text{-}6)$$

We further evaluate (3-6) for the cases $N=3,4,6$ and $N\to\infty$ and get the following results:

Case (1) - N=3

$$W_3(\vec{R}) = \frac{1}{8\pi} \qquad (0<|\vec{R}|<1)$$

$$= \frac{1}{16\pi|\vec{R}|}\ (3 - |\vec{R}|), (1<|\vec{R}|<3) \tag{3-7}$$

$$= 0 \qquad (3<|\vec{R}|<\infty)$$

Case (2) - N=4

$$W_4(\vec{R}) = \frac{1}{64\pi|R|}\ (8|\vec{R}| - 3|\vec{R}|^2) \quad (o<|\vec{R}|<2)$$

$$\frac{1}{64\pi|\vec{R}|}\ (4 - |R|)^2 \qquad (2<|\vec{R}|<4) \tag{3-8}$$

$$0 \qquad (4<|\vec{R}|<\infty)$$

Case (3) - N=6

$$W_6(R) = \frac{1}{2^8\pi|R|}\ (16|\vec{R}| - 4|\vec{R}|^3 + (5/6)|R|^4) \quad (0<R<2)$$

$$= \frac{1}{2^8\pi|\vec{R}|}\ (-20 + 56|\vec{R}| - 30|\vec{R}|^2 + 6|\vec{R}|^3 - (5/12)|\vec{R}|^4)\ (2<\vec{R}<4)$$

$$= \frac{1}{2^8\pi|\vec{R}|}\ (108 - 72|\vec{R}| + 18|\vec{R}|^2 - 2|\vec{R}|^3 + (1/12)|\vec{R}|^4)\ (4<|\vec{R}|<6) \tag{3-9}$$

$$= 0 \qquad (6<|R|\infty)$$

Case (4) - $N=\infty$

$$W(\vec{R}) = \frac{1}{(2\pi N/3)^{1/2}} e^{-3|\vec{R}|^2/2N} \quad \text{as } N \to \infty \tag{3-10}$$

We note here that our distribution for $W(\vec{R})$ in the case of large N is the same as obtained by Goodman[12] and Dainty[13] by a direct application of the central limit theorem.

It is sometimes possible that the number N is also a random number. In this case it is obvious that the probability distribution function $W(\vec{R})$ is given by (using problem 8-11 in Ref. (14))

$$W(\vec{R}) = \sum_{k=1}^{\infty} P\{N = k\} W_N(\vec{R}) \tag{3-11}$$

If N has a Poisson distribution then $P(N = k) = e^{-d} \frac{d^k}{k!}$, and we get for $W(\vec{R})$, for d some constant

$$W(\vec{R}) = \sum_{k=1}^{\infty} \left[e^{-d} \frac{d^k}{k!}\right] W_k(\vec{R}) \tag{3-12}$$

In our later considerations, the quantity of interest is $Q = |\vec{R}|^2$. To evaluate the probability density function of $|\vec{R}|^2$ from the density for $W(\vec{R})$ we simply use the transformation[14] (also equivalent to Eq (D-5))

$$W_Q(Q) = \begin{cases} \frac{1}{\sqrt{Q}} W(|\vec{R}| = \sqrt{Q}) & Q>0 \\ 0 & Q<0 \end{cases} \tag{3-13}$$

where we have assumed that $W(\vec{R})$ is an even function.

3.3 Expected Values and Variance of R, $|R|^2$

We now calculate the expected value of the sum $\sum_{r=1}^{N} e^{iah_r}$ and $\sum_{m=1}^{N}\sum_{n=1}^{N} e^{ia(h_m-h_n)}$. Using the definition of expected value we have,

$$\langle t(h)\rangle = \int_{-\infty}^{\infty} f(h)\,t(h)\,dh \qquad (3\text{-}14)$$

where $\langle\ \rangle$ stands for the expectation value and t(h) is some function of the random variable h. Also we have defined the characteristic function of a random variable h to be, for F(a) the characteristic function

$$F(a) = \int_{-\infty}^{\infty} e^{iah}\, f(h)\,dh \qquad (3\text{-}15)$$

Thus if each h_r has the same expectation value, we obtain for the expectation values of R and Q the quantities,

$$\langle R\rangle = NF(a) \qquad (3\text{-}16)$$

and

$$\langle Q\rangle = N + N(N-1)F(a)F^*(a) \qquad (3\text{-}17)$$

Similarly using the definition for the variance as

$$\sigma^2[t(h)] = \langle t(h)t^*(h)\rangle - \langle t(h)\rangle\langle t(h)\rangle^* \qquad (3\text{-}18)$$

we obtain the variance for R and Q as,

$$\sigma^2[R] = N[1 - F(a)F^*(a)] \qquad (3\text{-}19)$$

and

$$\sigma^2[Q] = N(N-1)+2N(N^2-4N+1)F(a)F^*(a)-2N(2N^2-5N+3)[F(a)F^*(a)]^2+N(N-1)F(2a)F^*(2a)$$
$$+N(N-1)(N-2)[[F^*(a)]^2F(2a)+F^*(2a)F^2(a)] \qquad (3\text{-}20)$$

3.4 Second order statistics of R, $|R|^2$

We now proceed to a consideration of the higher order statistics of R and Q. Suppose we have a function P(a). Then its autocorrelation function is defined by

$$\psi(\Delta a)= \lim_{T\to\infty} \frac{1}{2\pi}\int_{-T}^{T} P(a)P^*(a+\Delta a)\,da \qquad (3\text{-}21)$$

If P(a) is a random variable, then this autocorrelation function will also be a random variable. If $\psi(\Delta a)$ is the autocorrelation function, we can then describe it as a random variable with an appropriate distribution function, an expected value and a standard deviation. If P(a) is a function of some random variable h then $\psi(\Delta a)$ is also a function of the random variable h and so the expected value of $\psi(\Delta a)$ will become

$$\langle\psi(\Delta a)\rangle = \int_{-\infty}^{\infty} f(h)\psi(\Delta a)dh = \lim_{T\to\infty}\frac{1}{2T}\int_{-\infty}^{\infty}\int_{-T}^{T} f(h)P(a)P(a+\Delta a)\,da\,dh \qquad (3\text{-}22)$$

where f(h) is the density function of h.

When $\langle\psi(\Delta a)\rangle$ is zero we define the two variables P(a) and P(a + Δa) to be wide-sense independent.[15] Thus in order to find the length Δa for the quantities R(a) and R(a + Δa) to become independent and also Q(a) and Q(a + Δa) to become independent we simply consider their autocorrelation function. If we assume that N is fixed we get

$$\langle \psi_R(\Delta a) \rangle = \frac{1}{2T} \int_{-\infty}^{\infty} \cdots \int_{-\infty}^{\infty} \int_{-T}^{T} \left\{ \left[\prod_{r=1}^{N} dh_r f(h_r) \right] \left[\sum_{r=1}^{N} e^{iah_r} \right] \left[\sum_{r=1}^{N} e^{-i(ah_r + \Delta a h_r)} \right] \right\}$$

$$= \lim_{T \to \infty} \frac{1}{2T} \int_{-\infty}^{\infty} \cdots \int_{-\infty}^{\infty} \int_{-T}^{T} \left\{ \left[\prod_{r=1}^{N} dhr\ f(h_r) \right] \sum_{m=1}^{N} \sum_{n=1}^{N} e^{i[a(h_m - h_n) + \Delta a h]} da \right\}$$

$$= NF(\Delta a) \tag{3-23}$$

where $F(\Delta a)$ is the characteristic function of $f(h)$. Thus when the function $\langle \psi_R(\Delta a) \rangle$ is sufficiently small, we can consider the two functions $R(a)$ and $R(a + \Delta a)$ to be sufficiently independent.

We can do a similar computation for $Q(a)$

$$\langle \psi_Q(\Delta a) \rangle = \lim_{T \to \infty} \frac{1}{2T} \int_{-\infty}^{\infty} \cdots \int_{-\infty}^{\infty} \int_{T}^{T} \left\{ \left[\sum_{m=1}^{N} \sum_{n=1}^{N} e^{ja(h_m - h_n)} \right] \left[\sum_{p=1}^{N} \sum_{q=1}^{N} e^{-ja(h_p - h_q)} \right. \right.$$

$$\left. \left. \cdot e^{-j\Delta a(h_p - h_q)} \right] da \prod_{r=1}^{N} f(h_r) dh_r \right\}$$

$$= \lim_{T \to \infty} \frac{1}{2T} \int_{-\infty}^{\infty} \cdots \int_{-\infty}^{\infty} \int_{-T}^{T} \left\{ \left[\sum_{m}^{N} \sum_{n}^{N} \sum_{p}^{N} \sum_{q}^{N} e^{ja(h_m + h_p - h_n - h_q) + j\Delta a(h_p - h_q)} \right] \right.$$

$$\left. \left[\prod_{r=1}^{N} f(h_r) dh_r \right] \right\} da$$

$$= N + N(N-1)\ F(\Delta a)\ F^*(\Delta a) \tag{3-24}$$

Similarly we can calculate the spectral density functions $S_R(\omega_a)$ and $S_Q(\omega_a)$ for R and Q respectively by taking the integral

$$S_A(\omega_a) = \frac{1}{2\pi}\int_{-\infty}^{\infty} e^{-i\omega\Delta a} A(\Delta a)\, d\Delta a \tag{3-25}$$

where A stands for R or Q .

3.5 Statistics of Sums of Independent Sums of Random Vibrations

Now suppose that we have a sum of $R(a_1)....R(a_M)$ where $a_1, a_2....a_M$ are sufficiently separated so that the random variables $R(a_1).....R(a_M)$ can be considered to be independent. In this case, if we denote by $\Phi_R(\omega)$ the characteristic function of $R(a_1)$ we get for the probability density function of

$$L = \sum_{n=1}^{M} R(a_n) \tag{3-26}$$

the function (using Eq. 8-40, Ref. (14))

$$W_L(L) = \mathfrak{F}^{-1}\left[\prod_{j=1}^{M} \Phi_R(\omega, a_j)\right] \tag{3-27a}$$

where $\mathfrak{F}^{-1}$ is the inverse fourier transform and is defined by

$$\mathfrak{F}^{-1}(\Phi(\omega)) = \frac{1}{2\pi}\int_{-\infty}^{\infty} e^{-i\omega t}\, \Phi(\omega)\, d\omega \tag{3-27b}$$

In the same way we can calculate the density function for $\sum_{j=1}^{M} Q(a_j) = H$ where the a_j's are sufficiently apart so that $Q(a_j)$ are wide sense independent. We therefore get the result

$$W(H) = \mathfrak{F}^{-1}\left(\prod_{j=1}^{M} \Phi_H(\omega, a_j)\right) \tag{3-28}$$

We also obtain the following results for the mean and variance of $\vec{L}$ and H (from Eq. 8-99, Ref.(14)).

$$\langle \vec{L} \rangle = \sum_{j=1}^{M} \langle \vec{R}_j \rangle \quad , \qquad \sigma^2[\vec{L}] = \sum_{j=1}^{M} \sigma^2(\vec{R}_j) \tag{3-29}$$

and

$$\langle H \rangle = \sum_{j=1}^{M} \langle Q_j \rangle \quad , \qquad \sigma^2[H] = \sum_{j=1}^{M} \sigma^2(Q_j) \tag{3-30}$$

where $\langle A \rangle$ stands for the expectation value of A and $\sigma^2(A)$ for the variance of A.

3.6. Summary and Conclusions

In this chapter we have studied the statistics of the random variables $R(a) = \sum_{r=1}^{N} e^{jah_r}$ and $Q(a) = R(a)R^*(a)$. We have derived expressions for their density functions in Eqs. (3-6) and (3-13), when N is fixed and h_r are random variables. We have also derived an expression given in Eq. (3-11) for the density function of R when N has some probability distribution. Eqs. (3-16), (3-17), (3-19) and (3-20) give us the expectation values and the variances of $R(a)$ and $Q(a)$ in terms of the characteristic function of h. In Eqs. (3-23) and (3-24) we have also derived the expected values of the auto-correlation function of $R(a)$ and $Q(a)$. We have also considered sums of the type $L = \sum_{j=1}^{M} R(a_j)$ and $H = \sum_{j=1}^{M} Q(a_j)$ and have derived their density functions in Eqs. (3-27) and (3-28). We have also calculated their expected values and variances in Eqs. (3-29) and (3-30).

Thus, in this chapter, we have considered some of the pertinent results referring to the problem of random vibrations with a finite number of steps. In the next chapter we use these results to study the statistical behaviour of speckle in the image of diffuse objects and derive some of the important experimental properties which will enable us to understand the properties of the diffuse object, knowing the properties of the image speckle, and also establish for us the necessary guidelines for removing speckle in these images.

REFERENCES

1. Lord Rayleigh, Philosophical Magazine, Vol. x, 73 (1880).

2. K. Pearson, Nature 77, 294 (1905).

3. J. C. Kluyver, Konink. Acad. Wetenschap. Amsterdam 14, 325 (1905).

4. M. von Smoluchowski, Bull. Acad. Cracovie, 203 (1906).

5. A. A.Markoff, "Wahrshienlichkeitsrechnung," Liepzig (1912), Chapters 16 and 33.

6. S. Chandrasekhar, Astrophys. J. 94, 511 (1941).

7. Charles Kittel, "Introduction to Solid State," New York, London, Sydney (1968), Chapter 1.

8. P. Beckmann and A. Spizzichino, "The Scattering of Electromagnetic Waves from Rough Surfaces," Pergamon Press, Oxford (1963).

9. S. O. Rice, Bell S ystem Technical Journal, 23 and 24.

10. H. Hodara and N. George, IEEE J. Quantum Electron. QE-2, 237 (1966).

11. S. Chandrasekhar, Reviews of Modern Physics 15, 1 (1943).

12. J. W. Goodman, Stanford University Electronics Labs. Tech. Rept. WEL-63-140 (TR 2303-1), December 1963.

13. J. C. Dainty, Optica Acta 17, 761 (1970).

14. A. Papoulis, "Probability, Random Variables and Stochastic Processes," McGraw Hill Book Company, New York (1965), Chs. 5 and 8.

15. D. Middleton, "An Introduction to Statistical Communication Theory," McGraw Hill Book Company, New York (1960), p. 187.

Chapter IV

Image Speckle Statistics

4.1 Introduction

In this chapter, we apply the results of the previous chapter to study the statistics of speckle in the image of a diffuser. We calculate the distribution of speckle intensities, the average speckle size, the wavelength spacing to decorrelate two speckle intensity patterns, the improvement in the quality of the image with the superposition of speckle intensity patterns for different wavelengths, and the spectral autocorrelation function for the speckle electric field and intensity.

In the previous chapter we studied the properties of two random variables, $R = \sum_{r=1}^{N} e^{jah_r}$ and $Q = |R|^2$. We derived their density functions, found their mean and standard deviation and derived their autocorrelation function in order to find Δa for which the variables $R(a)$, $R(a+\Delta a)$ and $Q(a)$, $Q(a+\Delta a)$ become wide sense independent. We also derived the density functions, mean and variance for the variables $L = \sum_{n=1}^{M} R(a_n)$ and $H = \sum_{n=1}^{M} Q(a_n)$ for $R(a_1)$, $R(a_2)\ldots R(a_M)$ independent and $Q(a_1)$, $Q(a_2)\ldots Q(a_M)$ independent. We apply these results to study the statistics of speckle in this chapter.

Speckle can be classified according to two chief optical configurations,[1] i.e. when the observation is made of (a) the far field pattern and (b) the image of a diffuser illuminated by coherent light.

There have been a large number of investigations on the statistics of speckle in both of these configurations,[1-7] the questions of major interest in the past being the spatial autocorrelation function and the power spectral density of the speckle observed under monochromatic illumination.

In this chapter we concentrate on the statistics of the speckle arising in imaging systems, although the essential results for the wavelength dependence of speckle in the far field region follow from our calculations. Thus, in section 4.2 we derive the probability densities for the speckle intensity and electric field in the image of a diffuser. We also derive the mean and the variances of these quantities in terms of the characteristic function for the distribution of the heights of the scatterers in the diffuser and define a criteria for measuring the degradation of an image due to speckle noise.

We review a calculation, in section 4.3, of the spatial autocorrelation function of the speckle using some results from communication theory,[1],[3] and show that for a large diffuser this quantity is simply the magnitude square of the spatial autocorrelation function of the pupil function of the system. We thus derive the result that the average speckle size is equal to the size of a resolution cell for the optical system.

In section 4.4 we derive the autocorrelation functions of the speckle electric field and intensity with the wavelength as a variable and then calculate the expected value and the standard deviation for these autocorrelation functions in terms of the characteristic function of the heights of the scatterers on the diffuser. We also calculate

the spectral density function of the speckle and derive from these results the wavelength spacing for two speckle patterns to become wide sense independent to be $\frac{\lambda_0^2}{2\pi n_3 h_0}$ where λ_0 is the mean wavelength of illumination, n_3 the difference in the refractive index of the air and the object and h_0 the standard deviation for the heights of the scatterers on the diffuser. In the next section we derive the same result using the definition that two random variables are uncorrelated if the product of their expected values is equal to the expected value of their product.

In section 4.7 we derive the density functions, mean and variances of the speckle intensity and electric field when the illumination consists of M independent tones. We also calculate the degradation of the image due to speckle noise and show that this quantity decreases directly in proportion to $\frac{1}{\sqrt{M}}$.

We then calculate the speckle electric field mean and standard deviation, in section 4.8, when the illuminating beam has some given linewidth. From these calculations, we note that as the linewidth of the beam approaches the wavelength decorrelation spacing the speckle noise becomes negligible. We also derive the expected value and the variance of the autocorrelation function as well as the spectral density function for this case and show that the wavelength spacing to decorrelate the speckle now is given by the expression

$$\Delta\lambda > \frac{\lambda_0^2}{2\pi n_3 h_0} \left[1 + \left(\frac{2\pi n_3 h_0}{\lambda_0} \right)^2 \left(\frac{\sigma_\lambda}{\lambda_0} \right)^2 \right]^{\frac{1}{2}}$$

where σ_λ is the spectral bandwidth of the illumination.

Thus in this chapter we lay the basis for understanding some important aspects of speckle and derive results which enable us to calculate the important parameters for using wavelength diversity techniques to reduce speckle noise. We thus establish a wavelength spacing to decorrelate the speckle, a spectral bandwidth for the speckle to be laser like and estimate the reduction of speckle image degradation when the illumination consists of a set of independent monochromatic tones.

4.2 The Probability Density of Speckle Intensity in the Diffuser Image

From Chapter II, Eq. (2-7) we obtain the result that the electric field at any point x in the image of a diffuser can be approximated by

$$E_1(x) = A - BN + B \sum_{r=1}^{N} e^{iph_r} \qquad (4\text{-}1)$$

where we have defined $A = \Delta w\sqrt{\pi}$, $B = Mw_c$ and p as

$$p = \frac{-2\pi n_3}{\lambda_0}$$

Here Δw refers to the half width of a resolution cell, w_c the average width of a scatterer and the sum N is taken over the scatterers in the region $x - \Delta w \leq x \leq x + \Delta w$.

Since it is of interest to consider objects of varying roughness, we notice that for smooth objects $E_1(x) = A$. The speckle that occurs for diffuse objects is inherent in the terms containing B; and the ratio $\frac{BN}{A}$ is equivalent to the fractional surface area occupied by the scatterers in a resolution cell and is always less than unity.

We first calculate the density function of $E_1(x)$. Rewriting (3-6), we have for a vector $\vec{R} = \sum_{r=1}^{N} e^{jah_r}$, the density function for the random variable $\vec{R}$, if N is fixed,

$$W_{\vec{R}}(\vec{R}) = \frac{1}{2\pi^2|\vec{R}|} \int_0^\infty \sin(|\vec{\rho}||\vec{R}|)[\mathrm{sinc}|\vec{\rho}|]^N|\vec{\rho}|\,d|\vec{\rho}| \quad . \tag{4-2}$$

From the derivation in Appendix D we obtain the density function for the electric field (4-1) to be, (see Eq. (D-6))

$$W_{\vec{E}_1}(\vec{E}_1) = \frac{1}{2\pi^2\left|\frac{\vec{E}_1-(A-BN)}{B}\right|} \int_0^\infty \sin\left(|\vec{\rho}|\left|\frac{\vec{E}_1-(A-BN)}{B}\right|\right)[\mathrm{sinc}|\vec{\rho}|]^N|\vec{\rho}|\,d|\vec{\rho}| \tag{4-3}$$

Similarly, the density function for the intensity is given by Eq. (D-9),

$$W_{I_1}(I_1) = \frac{1}{I_1^{\frac{1}{2}}}\left[F_{I_1}(I_1,\phi=0) + F_{I_1}(I_1,\phi=\pi)\right] U(I_1)$$

$$F(I_1,\phi) = \frac{1}{2\pi^2\left|\frac{e^{i\phi}(I_1)^{\frac{1}{2}}-(A-BN)}{B}\right|} \int_0^\infty \sin|\vec{\rho}|\left|\frac{e^{i\phi}\sqrt{I_1}-(A-BN)}{B}\right| [\mathrm{sinc}|\vec{\rho}|]^N|\vec{\rho}|\,d|\vec{\rho}| \tag{4-4}$$

where $U(I_1)$ is the unit step function.

We now wish to calculate the expected value and the variance of the electric field and the intensity. If the characteristic function of the random variable h_r, given by the integral $\int_{-\infty}^{\infty} e^{iph} f(h)dh$ is denoted by $F(p)$, we note that for the expected value and variance of the random variable e^{iph} we get

$$\langle e^{iph}\rangle = F(p) \tag{4-5}$$

$$\sigma^2(e^{iph}) = 1 - F(p)F^*(p) \tag{4-6}$$

where $\langle\ \rangle$ denotes the expected value. If we also assume that the random variables h_r, represented by different scattering points, are independent, then we can calculate the expected value and variance of our amplitude defined by Eq. (4-1). Thus we obtain

$$\langle E_1(x)\rangle = A\text{-}NB+BNF(p) \tag{4-7}$$

$$\sigma^2[E_1(x)] = N[1\text{-}F(p)F^*(p)]BB^* \tag{4-8}$$

where $BB^* = (Mw_c)^2$.

Similarly we outline a calculation for the expected value and the variance of the intensity $I_1 = E_1E_1^*$. Given a random variable X which is the sum of the random variable bx and a constant c, where b is a constant, i.e.

$$X = c + bx, \tag{4-9}$$

we have

$$XX^* = c^2 + cbx + cbx^* + bbxx^* \quad . \tag{4-10}$$

Thus the expected value of XX^* becomes

$$\langle XX^*\rangle = c^2 + cb\langle x\rangle + cb\langle x^*\rangle + bb\langle xx^*\rangle \tag{4-11}$$

Similarly, we have

$$(XX^*)^2 = c^4 + 2bxc^3 + 2bx^*c^3 + c^2b^2x^2 + b^2c^2(x^*)^2 + 4b^2c^2xx^* + 2b^3cx^2x^* + 2b^3c(x^*)^2x + b^4(xx^*)^2 \qquad (4\text{-}12)$$

Thus the expected value of $\langle (XX^*)^2 \rangle$ becomes

$$\langle (XX^*) \rangle^2 = c^4 + 2bc^3\langle x \rangle + 2bc^3\langle x^* \rangle + c^2b^2\langle x^2 \rangle + b^2c^2\langle (x^*)^2 \rangle + 4b^2c^2\langle xx^* \rangle + 2b^3c\langle x^2x^* \rangle + 2b^3c\langle (x^*)^2x \rangle + b^4\langle (xx^*)^2 \rangle \qquad (4\text{-}13)$$

We now calculate the values of $\langle x \rangle$, $\langle x^* \rangle$, $\langle xx^* \rangle$, $\langle x^2 \rangle$, $\langle (x^*)^2 \rangle$, $\langle x^2x^* \rangle$, $\langle (x^*)^2x \rangle$, $\langle (xx^*)^2 \rangle$ where

$$x = \sum_{r=1}^{N} e^{iph_r} \quad . \qquad (4\text{-}14)$$

We get

$$\langle x \rangle = NF(p) \quad , \qquad (4\text{-}15a)$$

$$\langle x^* \rangle = NF^*(p) \quad , \qquad (4\text{-}15b)$$

$$\langle xx^* \rangle = N + N(N\text{-}1)F(p)F^*(p) \quad , \qquad (4\text{-}15c)$$

$$\langle x^2 \rangle = N(N\text{-}1)F^2(p) + NF(2p) \quad , \qquad (4\text{-}15d)$$

$$\langle (x^*)^2 \rangle = N(N\text{-}1)(F^*(p))^2 + NF^*(2p) \quad , \qquad (4\text{-}15e)$$

$$\langle x^2x^* \rangle = (2N^2-N)F(p) + (N^2-N)F(2p)F^*(p) + (N^3-3N^2+2N)F^2(p)\,F^*(p) \quad (4\text{-}15f)$$

$$\langle x(x^*)^2 \rangle = (2N^2-N)F^*(p) + (N^2-N)F^*(2p)F(p) + (N^3-3N^2+2N)[F^*(p)]^2F(p) \quad (4\text{-}15g)$$

and

$$\langle (xx^*)^2 \rangle = N(N-1)F(2p)F^*(2p) + N(N-1)(N-2)\{F(2p)[F^*(2p)]^2+F^*(2p)F^2(p)\} + 4N(N-1)^2F(p)F^*(p) + (2N^2-N) \quad . \quad (4\text{-}15h)$$

Substituting Eqs (4-15) into (4-11) and (4-13) we obtain,

$$\langle XX^* \rangle = c^2 + bcNF(p) + bcNF^*(p) + bbN + bbN(N-1)F(p)F^*(p) \quad , \quad (4\text{-}16)$$

and

$$\begin{aligned}\langle (XX^*)^2 \rangle = {} & c^4 + 2bc^3NF(p) + 2bc^3NF^*(p) + c^2b^2[N(N-1)F^2(p)+NF(2p)] \\ & + b^2c^2[N(N-1)[F^*(p)]^2 + NF^*(2p)] + 4b^2c^2[N + N(N-1)F(p)F^*(p)] \\ & + 2b^3c\{[(N^2-N)F(2p)F^*(p) + (2N^2-N)F(p)+(N^3-3N^2+2N)F^2(p)F^*(p)] \\ & + \text{complex conjugate}\} \\ & + b^4[N(N-1)(N-2)F^*(2p)F^2(p)+N(N-1)(N-2)(F^*(p))^2F(2p) \\ & + 4N(N-1)^2F(p)F^*(p) + (2N^2-N) + N(N-1)(N-2)(N-3)(F(p)F^*(p))^2] \quad . \end{aligned} \quad (4\text{-}17)$$

Simplifying (4-17) we obtain the result,

$$\begin{aligned}\langle (XX^*)^2 \rangle = {} & [\{\tfrac{1}{2}[c^4 + 4b^2c^2N + (2N^2-N)b^4] + 2NbcF(p)[c^2+b^2(2N-1)] \\ & + c^2b^2N(N-1)F^2(p) + Nc^2b^2F(2p) + 2b^3c(N^2-N)F(2p)F^*(p) \\ & + 2b^3cN(N-1)(N-2)F^2(p)F^*(p) + N(N-1)(N-2)b^4F^*(2p)F^2(p)\end{aligned}$$

$$+ 2Nb^2[c^2(N-1)+b^2N(N-1)]F(p)F^*(p)+\tfrac{1}{2}b^4N(N-1)(N-2)(N-3)[F(p)F^*(p)]^2$$

$$+ \text{complex conjugate}]. \qquad (4\text{-}18)$$

Also we have for $\langle XX^*\rangle^2$, from Eq. (4-16),

$$\langle XX^*\rangle^2 = \{\tfrac{1}{2}[c^2+b^2N]^2 + 2[c^2+b^2N]bcNF(p) + (bcN)^2F^2(p)$$

$$+ 2b^3cN^2(N-1)F^2(p)F^*(p) + [(c^2+b^2n)b^2N(N-1)+(bcN)^2]F(p)F(p)$$

$$+ \tfrac{1}{2}[F(p)F(p)]^2[b^2N(N-1)]^2\} \quad + \text{complex conjugate} \quad . \qquad (4\text{-}19)$$

We now use the definition that the standard deviation square of XX^* is given by

$$\sigma^2(XX^*) = \langle(XX^*)^2\rangle - \langle XX^*\rangle^2 \qquad . \qquad (4\text{-}20)$$

Thus we have

$$\sigma^2(XX^*) = \{b^2c^2N^2 + \tfrac{1}{2}N(N-1)b^4 - N^3c^2b^2F^2(p)$$

$$+ Nc^2b^2F(2p) + 2b^3cN(N-1)F(2p)F^*(p) - 2b^34N(N-1)F^2(p)F^*(p)$$

$$+ N(N-1)(N-2)b^4F^*(2p)F^2(p) + F(p)F^*(p)b^2N[3b^2N-5b^2N^2+2b^2N^3-c^2]$$

$$- [F(p)F^*(p)]^2b^4[2N^3+5N^2-3N]$$

$$+ \text{complex conjugate}\} \qquad . \qquad (4\text{-}21)$$

To find the expected value and the variance for $I_1(x)$ we simply substitute $E_1(x)$ for X, A - NB for c and B for b in Eqs (4-16) and (4-21). We therefore get,

$$\langle I_1(x)\rangle = (A-NB)^2 + (A-NB)BNF(p) + (A-NB)NBF^*(p) + B^2N(N-1)F(p)F^*(p), \tag{4-22}$$

and

$$\begin{aligned}\sigma(I_1(x)) = \{ & B^2(A-NB)^2N+\tfrac{1}{2}(N^2-N)B^4-N^3B^2(A-NB)^2F^2(p) \\ & + NB^2(A-NB)^2F(2p) + 2B^3N(N-1)(A-NB)F(2p)F^*(p) \\ & - 4N(N-1)B^3(A-NB)F^2(p)F^*(p) + (N-1)(N-2)B^4F^*(2p)F^2(p) \\ & + B^2N[3B^2N-5B^2N^2+2B^2N^3-(A-NB)^2]F(p)F^*(p)-F^2(p)[F^*(p)]^2 \\ & + B^4[4N^3+10N^2-6N] + \text{complex conjugate}\}^{\frac{1}{2}} \end{aligned} \tag{4-23}$$

We now define a criterion for deciding when a particular diffuser will give a large amount of speckle. If we take the ratio of the standard deviation to the expected value of the intensity, we obtain the average fractional change in amplitude among different resolution cells of width $2\Delta w$. When this ratio is very small, we have the case when most cells have the same intensity; and there is practically no speckle. In the case where this ratio approaches one, we have a badly speckled case. Thus we define the ratio

$$R(I_1)=\frac{\sigma(I_1)}{\langle I_1\rangle}= \frac{\text{Eq. (4-23)}}{\text{Eq. (4-22)}} \tag{4-24}$$

as a measure of our image degradation.

We note that this quantity is the inverse of the speckle signal to noise ratio as defined by Dainty[1]

$$\frac{S}{N} = \frac{\langle I_1 \rangle}{\sigma(I_1)} \tag{4-25}$$

where S/N stands for the signal to noise ratio. We approximate R for the case $F(p) \ll 1$ since Eq. (4-24) is very cumbersome to analyze. We therefore write $R(I_1)$ neglecting terms of order higher than $F(p)$. We get

$$R(I_1) = \frac{[2B^2(A-NB)^2N + N(N-1)B^4]^{\frac{1}{2}}}{[(A-NB)^2 + \{F(p) + F^*(p)\}\{(A-NB)BN\}]} \tag{4-26}$$

We note from Eq. (4-26), that the quantity $R(I_1)$ is proportional to $\frac{1}{\sqrt{N}}$. Thus a badly speckled case occurs with a small number of scatterers per resolution cell. And, as N becomes very large, the amount of speckle is drastically reduced. We can define a similar quantity for the electric field, $R(E_1)$

$$R(E_1) = \frac{\sigma(E_1)}{\langle E_1 \rangle} \tag{4-27}$$

Substituting the results from Eqs. (4-7) and (4-8) into Eq. (4-27) we obtain for the speckle electric field,

$$R(E_1) = \frac{N^{\frac{1}{2}}[1 - F(p)F^*(p)]^{\frac{1}{2}}B}{[A-NB + BNF(p)]}, \tag{4-28}$$

We note that the quantity $R(E_1)$ is also proportional to $1/\sqrt{N}$. Also when $F(p) = 1$, we have $R(E_1)$ tending to zero, which corresponds to the case of no speckle, this being the case when the standard deviation for the heights of the scatterers tends to zero, i.e., the scatterers have the same height.

4.3 Speckle Size and the Spatial Autocorrelation Function of the Diffuser Image

We now estimate a value for the average speckle size. This is given by the half width of the spatial autocorrelation function for the speckle intensity. The autocorrelation function becomes negligible for $\Delta x > 4\Delta w$ since from Eq. (4-1) the contribution to the intensity in the two cells, each of width $2\Delta w$, come from different scatterers. Thus the speckle size must have an average value of $2\Delta w$ where Δw is the half width of the resolution cell in the image plane. To see this result more explicitly we can make a detailed calculation of the spatial autocorrelation function of the intensity. Such a calculation has been done by a variety of authors including Dainty[1], Enloe[2], and Burckhardt[3] and we outline one derivation of the spatial autocorrelation function of the intensity in the image of a diffuser.

Let us consider the complex electric field transmitted by the diffuser to have the value $f(\xi,\eta)$, and express the resulting electric field distribution in the image plane as

$$E_1(x,y) = f(x,y) \textcircled{x} k(x,y) \qquad (4\text{-}29)$$

where the symbol $\textcircled{x}$ denotes convolution and where $k(x,y)$ is the transfer function of the imaging system.

Now suppose that the Fourier transform of the transfer function is expressed as $K(\omega_x,\omega_y)$ and the electric field exiting the diffuser is looked upon as a stationary stochastic process, with a power spectrum $N_o(\omega_x,\omega_y)$. The power spectrum of the image intensity is given by, using direct substitution,

$$\begin{aligned} N'_{E_1}(\omega_x,\omega_y) &= \mathfrak{F}\{[f(x,y)\textcircled{x}k(x,y)]\textcircled{x}[f(x,y)\textcircled{x}k(x,y)]\} \\ &= \mathfrak{F}[f(x,y)\textcircled{x}k(x,y)]\,\mathfrak{F}[f(x,y)\textcircled{x}k(x,y)] \\ &= |K(\omega_x,\omega_y)|^2 N_o(\omega_x,\omega_y) \qquad . \quad (4\text{-}30) \end{aligned}$$

In the same way we obtain the output power fluctuation of the intensity $N'_I(\omega_x,\omega_y)$ to be given by[1]

$$\begin{aligned} N'_I(\omega_x,\omega_y) &= \mathfrak{F}[E_1(x,y)E_1^*(x,y)\textcircled{x}E_1(x,y)\,E_1^*(x,y)] \\ &= N'_{E_1}(\omega_x,\omega_y)\textcircled{x}N_{E_1}(\omega_x,\omega_y) \qquad (4\text{-}31) \end{aligned}$$

Thus, if we combine Eqs. (4-31) and (4-30) we obtain

$$N'_I(\omega_x,\omega_y) = |K(\omega_x,\omega_y)|^2 N_o(\omega_x,\omega_y)\textcircled{x}|K(\omega_x,\omega_y)|^2 N_o(\omega_x,\omega_y) \quad . (4\text{-}32)$$

If the diffuser is relatively large, we can approximate $N_o(\omega_x,\omega_y) = 1$. Then the spectral density function of the intensity becomes,

$$N_I'(\omega_x,\omega_y) = |K(\omega_x,\omega_y)|^2 \textcircled{x} |K(\omega_x,\omega_y)|^2 \quad . \quad (4\text{-}33)$$

as shown in Eq. (8) of Ref. (1).
If we define the spatial autocorrelation function of the intensity by $\Psi_I(\Delta x,\Delta y)$, we obtain the result,

$$\Psi_I(\Delta x,\Delta y) = \mathfrak{F}^{-1}[|K(\omega_x,\omega_y)|^2 \textcircled{x} |K(\omega_x,\omega_y)|^2]$$

$$= |k(x,y) \textcircled{x} k(x,y)|^2 \quad . \quad (4\text{-}34)$$

Thus the autocorrelation function for the speckle intensity is equal to the magnitude square of the autocorrelation function for the transfer function of the optical system. Since the width of this transfer function is equal to the size of a resolution cell in the image plane, the width of the autocorrelation function is twice this size and so the average speckle size is $2\Delta w$.

4.4 Wavelength Diversity of Speckle

Since our main interest is to understand the behavior of speckle with respect to wavelength we derive in this section the autocorrelation function of the speckle image intensity as a function of wavelength, a number for the wavelength spacing required to decorrelate the speckle patterns and an expression for the resulting spectral density function of the image of a diffuser illuminated by a monochromatic source.

We rewrite (3-21) which says that if we have a function P(a) then the autocorrelation function for this function is given by

$$\psi_P(\Delta a) = \lim_{T\to\infty} \frac{1}{2T} \int_{-T}^{T} P(a)\, P^*(a+\Delta a)\, da \qquad (4\text{-}35)$$

However, if $P(a)$ is also a function of a random variable h which has a density function $f(h)$, then the quantity of interest is the average value of the autocorrelation function. This quantity will then tell us on the average how much the value of $P(a)$ is changing from its original value a when it is measured at the new point $(a+\Delta a)$. We therefore rewrite Eq. (3-22) to give the expected value of the autocorrelation function as

$$\langle \Psi_P(\Delta a) \rangle = \int_{-\infty}^{\infty} f(h)dh \left[\lim_{T\to\infty} \frac{1}{2T} \left\{ \int_{-T}^{T} P(a)\, P^*(a+\Delta a)da \right\} \right] \qquad (4\text{-}36)$$

We first find the autocorrelation function of the electric field. If we write the electric field as,

$$E_1(x) = c + bR(p), \quad R(p) = \sum_{r=1}^{N} e^{iph_r}, \qquad (4\text{-}37)$$

$$c = A - NB, \quad b = B$$

we get

$$\psi_{E_1}(\Delta p) = \lim_{T\to\infty} \frac{1}{2T} \int_{-T}^{T} [c + bR(p)][c + bR(p+\Delta p)]^* dp$$

$$= c^2 + b^2 \Psi_R(\Delta p) \qquad (4\text{-}38)$$

where $\Psi_R(\Delta p)$ is the autocorrelation function of $R(p)$.

Using (3-23) that the expected value for the autocorrelation function for $R(p)$ is $NF(\Delta p)$, where $F(p)$ is the characteristic function for the distribution of the heights of the scatterers, we obtain the result

$$\langle \psi_{E_1}(\Delta p) \rangle = c^2 + b^2 NF(\Delta p) \qquad (4\text{-}39)$$

Now, substituting the values (A-NB) for c and B for b we obtain the expected value for the autocorrelation function of the electric field to be

$$\langle \psi_{E_1}(\Delta p) \rangle = (A-NB)^2 + B^2 NF(\Delta p) \qquad (4\text{-}40)$$

We now calculate the expected value of the autocorrelation function for the intensity. Using the definitions for R(p), c and b in Eq. (4-37), we rewrite the intensity as,

$$\begin{aligned} I_1 &= E_1 E_1^* \\ &= [c + bR(p)][c + bR^*(p)] \\ &= c^2 + cbR(p) + cbR^*(p) + RR^*(p) \end{aligned} \qquad (4\text{-}41)$$

Thus for the product $I_1(p)I_1^*(p+\Delta p)$ we obtain

$$\begin{aligned} I_1(p)I_1^*(p+\Delta p) = {} & [c^2 + cbR(p) + cbR^*(p) + b^2 R(p)R^*(p)] \cdot \\ & [c^2 + cbR(p+\Delta p) + cb\, R(p+\Delta p) \\ & + b^2 R(p+\Delta p)\quad R^*(p+\Delta p)] \\ = {} & c^4 + c^3 bR(p+\Delta p) + c^3 bR^*(p+\Delta p) + c^2 b^2 R(p+\Delta p)R^*(p+\Delta p) \end{aligned} \qquad (4\text{-}42)$$

$$+ c^3bR(p) + (cb)^2R(p)R^*(p+\Delta p) + (cb)^2R(p)R(p+\Delta p)$$

$$+ cb^3R(p)R(p+\Delta p)R^*(p+\Delta p) + c^3bR^*(p) + (cb)^2R^*(p)R(p+\Delta p)$$

$$+ (cb)^2R^*(p)R^*(p+\Delta p) + cb^3R^*(p)R^*(p)R(p+\Delta p)$$
$$+ (cb)^2R(p)R^*(p) + cb^3R(p)R^*(p)R(p+\Delta p) + cb^3R(p)R^*(p)R^*(p+\Delta p)$$

$$+ b^4R(p)R^*(p)R(p+\Delta p)R^*(p+\Delta p)$$

Collecting terms and rearranging, we get

$$I_1(p)I_1(p+\Delta p) = c^4 + c^3b[R(p+\Delta p)+ R^*(p+\Delta p) + R(p) + R^*(p)]$$

$$+ cb^3[R(p)R(p+\Delta p)R^*(p+\Delta p) + R^*(p)R^*(p)R(p+\Delta p)$$

$$+ R(p)R^*(p) \quad R(p+\Delta p) + R(p)R^*(p)R^*(p+\Delta p)]$$

$$+ c^2b^2[R(p+\Delta p)R^*(p+\Delta p)+R(p)R^*(p+\Delta p)$$
$$+ R(p)R(p+\Delta p)+R^*(p)R(p+\Delta p)+R^*(p)R^*(p+\Delta p)$$

$$+ R(p)R^*(p)]$$

$$+ b^4 R(p)R^*(p)R(p+\Delta p)R^*(p+\Delta p) \qquad (4\text{-}43)$$

We now note the following results,

$$\lim_{T\to\infty} \frac{1}{2T}\int_{-T}^{T} R(p+\Delta p)dp = \frac{1}{2T}\int_{-T}^{T} R^*(p+\Delta p)dp = \frac{1}{2T}\int_{-T}^{T} R(p)dp = \frac{1}{2T}\int_{-T}^{T} R^*(p)dp = 0 \qquad (4\text{-}44a)$$

$$\lim_{T\to\infty} \frac{1}{2T}\int_{-T}^{T} R(p)R(p+\Delta p)R^*(p+\Delta p)dp = 0 \qquad (4\text{-}44b)$$

$$\lim_{T\to\infty} \frac{1}{2T} \int_{-T}^{T} R^*(p)R^*(p)R(p+\Delta p)dp = 0 \qquad (4\text{-}44c)$$

$$\lim_{T\to\infty} \frac{1}{2T} \int_{-T}^{T} R(p)R^*(p+\Delta p)R(p+\Delta p)dp = 0 \qquad (4\text{-}44d)$$

$$\lim_{T\to\infty} \frac{1}{2T} \int_{-T}^{T} R(p)R^*(p)R^*(p+\Delta p)dp = 0 \qquad (4\text{-}44e)$$

$$\lim_{T\to\infty} \frac{1}{2T} \int_{-T}^{T} R(p+\Delta p)R^*(p+\Delta p)dp = N \qquad (4\text{-}44f)$$

$$\lim_{T\to\infty} \frac{1}{2T} \int_{-T}^{T} R(p)R^*(p+\Delta p)dp = \sum_{r=1}^{N} e^{-i\Delta p h_r} = \psi_R(\Delta p) \qquad (4\text{-}44g)$$

$$\lim_{T\to\infty} \frac{1}{2T} \int_{-T}^{T} R(p)R(p+\Delta p)dp = 0 \qquad (4\text{-}44h)$$

$$\lim_{T\to\infty} \frac{1}{2T} \int_{-T}^{T} R^*(p)R(p+\Delta p)dp = \psi_R^*(\Delta p) \qquad (4\text{-}44i)$$

$$\lim_{T\to\infty} \frac{1}{2T} \int_{-T}^{T} R^*(p)R^*(p+\Delta p)dp = 0 \qquad (4\text{-}44j)$$

$$\lim_{T\to\infty} \frac{1}{2T} \int_{-T}^{T} R(p)R^*(p)dp = N$$

$$\lim_{T\to\infty} \frac{1}{2T} \int_{-T}^{T} R(p)R^*(p)R(p+\Delta p)R^*(p+\Delta p)dp = \psi_{RR}(\Delta p) = \sum_{m=1}^{N} \sum_{n=1}^{N} e^{-i\Delta p(h_m - h_n)} \qquad (4\text{-}44k)$$

We therefore find that the autocorrelation function of the quantity $I_1(\Delta p)$ is given by the result, using Eqs. (4-44), (4-43) and the definition (4-35)

$$\psi_{I_1}(\Delta p) = \lim_{T\to\infty} \frac{1}{2T} \int_{-T}^{T} I_1(p) I_1^*(p+\Delta p)\,dp$$

$$= c^4 + 2Nc^2b^2 + c^2b^2[\psi_R(\Delta p) + \psi_R^*(\Delta p)] + b^4\psi_{RR}^*(\Delta p) \qquad (4\text{-}45)$$

where $\psi_R(\Delta p)$ and $\psi_{RR}^*(\Delta p)$ are defined in Eqs. (4-44g) and (4-44k) respectively. We thus, using the definition (4-36) and the relations given in Eqs. (3-23) & (3-24), obtain for the expected value of the autocorrelation function of the intensity,

$$\langle \psi_{I_1}(\Delta p) \rangle = c^4 + 2Nc^2b^2 + Nc^2b^2[F(\Delta p) + F^*(\Delta p)] + b^4[N + N(N-1)F(\Delta p)F^*(\Delta p)] \qquad (4\text{-}45)$$

Thus substituting the values (A-NB) for c and B for b we obtain for the expected value for the autocorrelation function of the intensity as

$$\langle \psi_{I_1}(\Delta p) \rangle = [(A-NB)^4 + NB^4 + 2N(A-NB)^2B^2] + N(A-NB)^2B^2[F(\Delta p) + F^*(\Delta p)] + B^4N(N-1)F(\Delta p)F^*(\Delta p) \qquad (4\text{-}46)$$

Eq. (4-46) thus gives us the expected value of the autocorrelation function for the intensity in terms of the number of scatterers per resolution cell, N, and the characteristic function for the heights of the scatterers, $F(\Delta p)$.

We now study expression (4-46) to find out when the two speckle patterns, one at p and the other at $(p+\Delta p)$, are sufficiently different to be considered as independent functions. Since $\langle \psi_{I_1}(\Delta p) \rangle$ consists of a constant plus a constant times $F(\Delta p)$ plus a constant times $|F(\Delta p)|^2$, the expression (4-46) can be considered to be near its lowest value when $F(\Delta p)$ is near its lowest value. Thus if we calculate the value of Δp for which $F(\Delta p)$ becomes small, then that Δp will give us the spacing over which the intensity decorrelation of the speckle pattern occurs. We note first that if we have some function $f(x)$ and its fourier transform $F(\omega)$ and if the function $f(x)$ can be assigned a certain bandwidth, i.e. a quantity $\Delta x = B_x$ over which $f(x)$ has any appreciable value, and if $F(\omega)$ can also be given a certain bandwidth $\Delta\omega = B_\omega$, then we obtain the result that the product $B_x B_\omega$ is always equal to one.[6] Since the bandwidth for the density function for the distribution of the heights of the scatterers is the standard deviation for the heights of the scatterers, say h_0, then the characteristic function for the heights of the scatterers, which is the fourier transform of the density function, must have a bandwidth which is the reciprocal of the standard deviation for the heights of the scatterers, i.e. the characteristic function is negligibly small, when

$$\Delta p = \frac{1}{h_0} \tag{4-47}$$

where h_0 = standard deviation for the heights of the scatterers. Now, we have defined $p = \frac{-2\pi n_3}{\lambda_0}$. Thus we obtain Δp to be, for small changes in λ_0,

$$\Delta p = \frac{dp}{d\lambda_0} \Delta\lambda = \frac{2\pi n_3}{\lambda_0^2} \Delta\lambda \quad . \tag{4-48}$$

Combining Eqs. (4-47) and (4-48), we obtain the wavelength spacing for the value of the characteristic function to become negligible to be given by

$$\Delta\lambda = \frac{\lambda_0^2}{2\pi n_3 h_0} \quad . \tag{4-49}$$

Since, when the characteristic function is negligible, the expected value of the autocorrelation function for the intensity of the speckle pattern approaches its minimum, we can consider the two speckle patterns, one at λ and the other at $\lambda+\Delta\lambda$, to be <u>wide-sense independent</u> when

$$\Delta\lambda > \frac{\lambda_0^2}{2\pi n_3 h_0} \qquad \underline{\text{decorrelated case}} \quad . \tag{4-50}$$

Also since the value of the characteristic function has not decreased much if $\Delta\lambda$ is, say, less than a tenth of the value as given in Eq. (4-48), we can consider the speckle pattern to still be laserlike for

$$\Delta\lambda < \frac{1}{10}\frac{\lambda_0^2}{2\pi n_3 h_0} \qquad \underline{\text{Laserlike Case}} \qquad . \quad (4\text{-}51)$$

We note that we would get the same result for the speckle pattern to become <u>wide-sense independent</u> had we studied only the electric field of the speckle pattern.

Suppose that the density function of the heights of the scatterers is even. Then the characteristic function $F(p)$ is real,[8] and so we can rewrite Eq. (4-46) as

$$\begin{aligned}\langle \psi_{I_1}(\Delta p)\rangle = {} & [(A-NB)^4 + NB^4 + 2N(A-NB)^2B^2] \\ & + 2N(A-NB)^2B^2F(\Delta p) \\ & + B^4N(N-1)F^2(\Delta p) \qquad , \quad (4\text{-}52)\end{aligned}$$

where $F(\Delta p) = F^*(\Delta p)$. Thus if we do an experiment where we record the speckle intensity patterns at a bunch of wavelengths and therefore p, and if we then optically measure the expected value of the autocorrelation function of these patterns as a function of the difference from the original p, then we can, in principle, from the experimentally determined autocorrelation function, calculate the characteristic function for the heights of the scatterers in the diffuser. Then a

simple fourier transform will give us the density of the heights of the scatterers. Thus from Eq. (4-52), we obtain for the characteristic function and the density function the values,

$$F(\Delta p) = \frac{-b \pm \sqrt{b^2 - 4ac}}{2a}$$

where

$$b = 2N(A-NB)^2B^2$$

$$c = [(A-NB)^4 + NB^4 + 2N(A-NB)^2B^2 - \langle \psi_{I_1}(\Delta p)\rangle]$$

$$a = B^4N(N-1) \quad , \tag{4-53a}$$

and

$$f(h) = \int_{-\infty}^{\infty} e^{-i\Delta ph} F(\Delta p)d\Delta p \tag{4-53b}$$

Also, suppose we can do an experiment to measure the autocorrelation function of the electric field as a function of wavelength. Then we can similarly calculate the characteristic function and the resulting density function for the heights of the scatterers and using Eq. (4-40) we obtain the results,

$$F(\Delta p) = \frac{\langle \psi_{E_1}(\Delta p)\rangle - (A-NB)^2}{B^2N} \tag{4-54a}$$

and

$$f(h) = \frac{1}{B^2N}\int_{-\infty}^{\infty}[e^{-i(\Delta p)h}\langle \psi_{E_1}(\Delta p)\rangle d(\Delta p)] + \frac{(A-NB)^2}{B^2N}\delta(0) \tag{4-54b}$$

Now suppose we had an experiment where we made a measurement of the autocorrelation functions, as a function of wavelength, of various

small sections of the image. Then, in general, we can assign a standard deviation to this experimentally measured random function as a function of the interval Δp. We therefore make a calculation of the standard deviation of the autocorrelation function for the speckle electric field and the speckle intensity. We first calculate the variance for the autocorrelation function of the electric field.

Now, we have already calculated, in Eq. (4-8) the variance of a random variable X where X is the sum of a constant c and the product of another constant b times a random variable x where now x is a sum of the random variables e^{iah_r}. We get this value to be

$$\sigma^2(X) = N[1 - F(a)F^*(a)]b^2 \tag{4-55}$$

where $X = c + bx$, $x = \sum_{r=1}^{N} e^{iah_r}$, $F(a) = \int_{-\infty}^{\infty} f(h_r)e^{iah_r}dh_r$.

Now, comparing Eqs. (4-9) and (4-38) we obtain, using the substitutions,

$$c = (A-NB), \quad b = B, \quad \text{and } a = \Delta p \quad , \tag{4-56}$$

the following value for the variance of the autocorrelation function of the electric field

$$\sigma^2[\psi_{E_1}(\Delta p)] = N[1-F(\Delta p)F^*(\Delta p)]B^4 \ . \tag{4-57}$$

We now compute the standard deviation for the autocorrelation function of the intensity. Eq. (4-45) gives us the expression for the autocorrelation function of the intensity, and we note that this can be written as, comparing with Eq. (4-38),

$$\psi_{I_1}(\Delta p) = 2Nc^2b^2 + \psi_{E_1}(\Delta p)\psi_{E_1}^{*}(\Delta p) \tag{4-58}$$

where, again, $c = (A-NB)$, and $b = B$.

Now, in deriving Eq. (4-8), we have used the result that if we have a random variable X which is equal to a constant plus the random variable x, then the variance of X is the same as the variance of x, i.e.,

given $X = c + x$, we have

$$\begin{aligned}\sigma^2(X) &= \langle XX^* \rangle - \langle X \rangle \langle X \rangle^* \\ &= [c^2 + c\langle x \rangle + c\langle x^* \rangle + \langle xx^* \rangle][c^2 + c\langle x \rangle + c\langle x \rangle^* + \langle x \rangle \langle x \rangle^*] \\ &= \langle xx^* \rangle - \langle x \rangle \langle x \rangle^* \\ &= \sigma^2(x)\end{aligned} \tag{4-59}$$

where we have used the result $\langle x^* \rangle = \langle x \rangle^*$. Thus we obtain from Eq. (4-58) and (4-57) that the standard deviation of the autocorrelation function of the intensity is equal to the standard deviation of the absolute square of the autocorrelation function of the electric field. It is now a straightforward procedure to calculate the desired variance

$\sigma^2[\psi_{I_1}(\Delta p)]$ by simply substituting for $\psi_{E_1}(\Delta p)$ as given by Eq. (4-38) into Eqs. (4-9) through (4-23). We therefore obtain the result

$$\begin{aligned}\sigma^2[\psi_{I_1}(\Delta p)] = [\{ & B^4(A-NB)^4N + \tfrac{1}{2}N(N-1)B^4 \\ & - N^3B^4(A-NB)^4F^2(\Delta p) + NB^4(A-NB)^4F(2\Delta p) \\ & + B^6(N-1)(A-NB)^2F(2\Delta p)F^*(\Delta p) - 4N(N-1)B^6(A-NB)^2F^2(\Delta p)F^*(\Delta p) \\ & + NB^8F^*(2\Delta p)F^2(\Delta p) + B^4N[3B^2N - 5B^2N^2 + 2B^2N^3 - (A-NB)^2] \\ & - F^2(\Delta p)[F^*(\Delta p)]^2 B^8[4N^3 + 10N^2 - 6N] \\ & + \{\text{complex conjugate}\}] \qquad . \quad (4\text{-}60)\end{aligned}$$

We recall that while the expected value of the autocorrelation function of a random variable tells us how much on the average the value of the random variable has changed from its original position, we note that the variance of the autocorrelation function tells us how differently the random variable is changing at various points. Intuitively then, it is reasonable to say that, if the standard deviation is very large, then the distribution of speckle intensities is completely uncorrelated since now the change from the original speckle electric field or intensity is widely different at different points on the image. Thus we can consider the speckle patterns to become independent for Δp such that the standard deviation becomes a maximum. We note from Eqs. (4-57) and (4-60) that both the standard deviations of the autocorrelation functions of the electric field and the intensity tend to a maximum as $F(\Delta p)$ tends to zero. Thus for $F(\Delta p) = 0$ the standard deviation

of the autocorrelation function for the electric field becomes

$$\sigma[\psi_{E_1}(\Delta p)] = N^{\frac{1}{2}}B^2 \qquad \text{for } F(\Delta p) = 0 \qquad . \quad (4\text{-}61)$$

Similarly the standard deviation of the autocorrelation function of the intensity has the value

$$\sigma[\psi_{I_1}(\Delta p)] = NB^2(A-NB)^2+\tfrac{1}{2}N(N-1)B^4 \qquad \text{for } F(\Delta p) = 0 \qquad . \quad (4\text{-}62)$$

Thus from (4-60) we again obtain the result that the speckle is independent when

$$\Delta\lambda > \frac{\lambda_0^2}{2\pi n_3 h_0} \qquad \underline{\text{decorrelated case}} \qquad . \quad (4\text{-}63)$$

Now suppose we look at one speckle point in the image plane and vary the wavelength of the illuminating beam. Then, in general, the electric field and the intensity at that point will go from a high to a low and high again with some periodicity. Also, in general, this periodicity will be different for different speckle points. We can thus assign an average power spectral density function for the speckle electric field and intensity which gives us the probabilities for the electric field and the intensity to have various periodicities of oscillation. We note first that the spectral density function is simply the fourier transform of the autocorrelation functions, i.e.

$$S_{E_1}(\omega_p) = \frac{1}{2\pi}\int_{-\infty}^{\infty} e^{-i\omega_p(\Delta p)}\langle\psi_{E_1}(\Delta p)\rangle d\Delta p \qquad (4\text{-}64)$$

$$S_{I_1}(\omega_p) = \frac{1}{2\pi}\int_{-\infty}^{\infty} e^{-i\omega_p(\Delta p)}\langle\psi_{I_1}(\Delta p)\rangle d\Delta p \qquad (4\text{-}65)$$

Thus, first considering the electric field, we note using Eqs. (4-40) and (4-64) that the power spectrum of the electric field is given by

$$S_{E_1}(\omega_p) = \frac{1}{2\pi}\int_{-\infty}^{\infty} e^{-i\omega_p\Delta p}[(A-NB)^2 + B^2NF(\Delta p)]d(\Delta p)$$

$$= (A-NB)^2\delta(0) + B^2N\, f(\omega_p)\ , \qquad (4\text{-}66)$$

where $f(h)$ is the function which gives the density of the heights of the scatterers having a given value h. We note from Eq. (4-66) that the speckle electric field has a component of magnitude $(A-NB)^2$ which does not change with electric field. The second term on the right hand side of Eq. (4-66) gives us, however, the probabilities of ω_p, i.e. the number ω_p cycles that the speckle electric field has varied per unit change in p. If the standard deviation of the density function $f(h)$ is h_0, then we observe from Eq. (4-66) that the average rate at which most of the speckle change is h_0 cycles per unit change in p. Therefore, since $\Delta p = \frac{2\pi n_3}{\lambda_0^2}\Delta\lambda$, a result that we obtained in Eq. (4-49), we note that half of the speckles take more than $\Delta\lambda = \frac{\lambda_0^2}{2\pi n_3 h_0}$ wavelength spacing to go through one full cycle of

variation in their electric field amplitudes, i.e. from a high value to a low value and then to a high value again. We therefore note that the wavelength spacing, $\Delta\lambda = \frac{\lambda_0^2}{2\pi n_3 h_0}$ is the appropriate minimum separation of wavelengths before we can consider the two speckle electric fields to be sufficiently decorrelated.

We now calculate the spectral density function for the variations of the speckle intensity. Again, substituting Eq. (4-45) into Eq. (4-65) we obtain for the spectral density function of the speckle intensity,

$$
\begin{aligned}
S_{I_1}(\omega_p) = \frac{1}{2\pi}\int_{-\infty}^{\infty} e^{-i\omega_p(\Delta p)} d(\Delta p)\{&[(A-NB)^4 + NB^4 + 2N(A-NB)^2B^2] \\
&+ N(A-NB)^2B^2[F(\Delta p) + F^*(\Delta p)] \\
&+ B^4N(N-1)F(\Delta p)F^*(\Delta p)\} \\
= \{&\delta(0)[(A-NB)^4+NB^4+2N(A-NB)^2B^2] + 2N(A-NB)^2B^2 f(\omega_p) \\
&+ B^4N(N-1)[f(\omega_p) \otimes f(\omega_p)]\}
\end{aligned}
\tag{4-67}
$$

Again, inspecting Eq. (4-67) we note that the term $[(A-NB)^4 + NB^4 + 2N(A-NB)^2B^2]$ gives us the component of the speckle intensity that never changes with wavelength, the second term on the right hand side tells us that half of the speckle take more than $\frac{\lambda_0^2}{2\pi n_3 h_0}$ change in wavelength, $\Delta\lambda$, to go through one cycle of intensity, where this intensity has magnitude $2N(A-NB)^2B^2$ and the

third term has the standard deviation $2h_0$ and so gives us the result that $B^4N(N-1)$ of the speckles have variations with the wavelength spacing of $\Delta\lambda > \frac{\lambda_0^2}{4\pi n_3 h_0}$ to go through one cycle.

As we change the wavelength of the illuminating beam, different points on the image plane will have different correlations with the electric field and the intensity in the image plane at the original wavelength. It is therefore of interest to assign a density function for the autocorrelation function of the speckle electric field and the speckle intensity. We therefore do a calculation for these two density functions. For the electric field, we proceed to calculate the probability density function using the same procedure that we have used to derive Eq. (4-3). We then obtain as the density function the result,

$$W_{\psi_{E_1}(\Delta p)}(\psi_{E_1}(\Delta p)) = \frac{1}{2\pi^2\left|\psi_{E_1}-(A-BN)^2\right|}\int_0^\infty\left(\sin|\vec{p}|\left|\frac{\psi_{E_1}-(A-BN)^2}{B^2}\right|\right)$$

$$[\mathrm{sinc}|\vec{p}|]^N|\vec{p}|\,d|\vec{p}| \qquad (4\text{-}68)$$

To derive the probability density function for the intensity, we first note from Eq. (4-59) that $\psi_{I_1}(\Delta p)$ is simply a constant plus the absolute value square of $\psi_{E_1}(\Delta p)$. We therefore first obtain the probability density function for $\psi_{E_1}\psi_{E_1}^*$ and then by a straightforward

substitution as given by Eq. (D-3), we obtain for the density function of $\Psi_{I_1}(I_1)$

$$W_{\psi_{I_1}}(\psi_{I_1}) = \left[F_{\Psi_{I_1}}(\Psi_{I_1}, \phi=0) + F_{\Psi_{I_1}}(\Psi_{I_1}, \phi=\pi) \right] \cdot U(\Psi_{I_1} - 2Nc^2B^2) \qquad (4\text{-}69)$$

for

$$F_{\psi_{I_1}}(\psi_{I_1}, \phi) = \frac{1}{2\pi^2 \left| e^{i\phi}(\psi_{I_1} - 2Nc^2B^2)^{\frac{1}{2}} - c^2 \right| (\psi_{I_1} - 2Nc^2B^2)^{\frac{1}{2}}} \left[\int_0^\infty \{ \sin(|\vec{\rho}| \frac{e^{i\phi}(\psi_{I_1} - (2Nc^2B^2)^{\frac{1}{2}} - c^2}{B^2}) \right.$$

$$\left. [\mathrm{sinc}|\vec{\rho}|] |\vec{\rho}|^N d|\vec{\rho}| \} \right], \qquad (4\text{-}70)$$

where $c = (A - NB)$ and $U(\psi_I - 2Nc^2B^2)$ is the unit step function.

4.5 Illustration of Speckle Image Statistics for a Particular Case--the Gaussian Distribution Function for Scatterer Heights.

We now illustrate the results of the previous sections with a particular example. We assume that the heights of the scatterers are distributed normally where our expected value and variance for the heights have already been taken to be zero and h_0, respectively. Thus we can write for the density function of h_r as

$$f(h_r) = \frac{1}{h_0\sqrt{2\pi}}\, e^{-h_r^2/2h_0^2} \tag{4-71}$$

and the corresponding characteristic function as

$$F(p) = e^{-\frac{1}{2}p^2h_0^2} \tag{4-72}$$

We note that the density functions for the speckle electric field and intensity, given by Eqs. (4-3) and (4-4) respectively, are independent of the density function for the scatter heights. Likewise the density functions for the autocorrelation of the electric field and the intensity given by Eqs. (4-68) and (4-70) are also independent of the densities of scatterer heights. Substituting Eq. (4-72) into Eqs. (4-7) and (4-22) we obtain the expected values of the electric field and the intensity. Thus the expected value of the electric field is given by

$$\langle E_1(x)\rangle = A\text{-}NB + BNe^{-\frac{1}{2}p^2h_0^2} \tag{4-73}$$

and, similarly the expected value of the intensity becomes

$$\langle I_1(x)\rangle = (A\text{-}NB)^2 + 2BN(A\text{-}NB)e^{-\frac{1}{2}ph_0^2}B^2N(N\text{-}1)e^{-ph_0^2} \tag{4-74}$$

Similarly, we obtain for the variance of the electric field, from Eq. (4-8),

$$\sigma^2[E_1(x)] = N[1\text{-}e^{-p^2h_0^2}]B^2 \quad , \tag{4-75}$$

and from Eq. (4-23) we obtain the variance of the intensity to be

$$\sigma^2[I_1(x)] = 2\{ B^2(A-NB)^2N + \tfrac{1}{2}N(N-1)B^4$$
$$- N^3B^2(A-NB)^2e^{-p^2h_0^2} + NB^2(A-NB)^2e^{-2p^2h_0^2}$$
$$+ 2B^3N(N-1)(A-NB)e^{5/2p^2h_0^2} - 4N(NO1)B^3(A-NB)e^{-3/2p^2h_0^2}$$
$$+ N(N-1)(N-2)B^4e^{-3p^2h_0^2} + B^2N[3B^2N-5B^2N^2+2B^2N^3-(A-NB)]$$
$$- B^4[4N^3-10N^2-6N]e^{-2p^2h_0^2}\} \quad . \quad (4\text{-}76)$$

Eq. (4-28), which gives us the ratio of the standard deviation to the expected value of the electric field, becomes

$$R(E_1) = \frac{N^{\frac{1}{2}}[1-e^{-p^2h_0^2}]^{\frac{1}{2}}B}{[A-NB+BNe^{-\frac{1}{2}p^2h_0^2}]} \quad . \quad (4\text{-}77)$$

The expected value of the autocorrelation function for the electric field, Eq. (4-40), for a change in p becomes

$$\langle \psi_{E_1}(\Delta p)\rangle = (A-NB)^2 + B^2Ne^{-\frac{1}{2}(\Delta p)^2h0^2} \quad , \quad (4\text{-}78)$$

while the expected value of the autocorrelation function for the intensity becomes,

$$\langle \psi_{I_1}(\Delta p)\rangle = [(A-NB)^4 + NB^4 + 2N(A-NB)^2B^2] + 2N(A-NB)^2B^2 e^{-\frac{1}{2}(\Delta p)^2 h_o^2} + B^4 N(N-1) e^{-(\Delta p)^2 h_o^2} \quad , \qquad (4\text{-}79)$$

where

$$p = \frac{-2\pi n_3}{\lambda_o^2} \Delta\lambda \quad .$$

The standard deviation of the autocorrelation function for the electric field is

$$\sigma^2[\psi_{E_1}(\Delta p)] = N\left[1-e^{-p^2 h_o^2}\right] B^4 \quad , \qquad (4\text{-}80)$$

and the corresponding standard deviation for the autocorrelation function for the intensity becomes

$$\begin{aligned}\sigma^2[\psi_{I_1}(\Delta p)] = [&2\{2B^4(A-NB)^4 N + \tfrac{1}{2}N(N-1)B^8 - N^3B^4(A-NB)^4 e^{-(p)^2 h_o^2} \\ &+ NB^4(A-NB)^4 e^{-2(\Delta p)^2 h_o^2} + 2B^6(N-1)(A-NB)^2 e^{-5/2(\Delta p)^2 h_o^2} \\ &- 4N(N-1)B^6(A-NB)^2 e^{-3/2(\Delta p)^2 h_o^2} + N(N-1)(N-2)B^8 e^{3(\Delta p)^2 h_o^2} \\ &+ B^4 N[3B^4 N - 5B^4 N + 2B^4 N^3 - (A-NB)^4] e^{-(\Delta p)^2 h_o^2} \\ &- e^{-2(\Delta p)^2 h_o^2} B^8[4N^3 + 10N^2 - 6N] \quad . \qquad (4\text{-}81)\end{aligned}$$

The power spectral density for the electric field becomes, substituting Eq. (4-71) into Eq. (4-66),

$$S_{E_1}(\omega_p) = (A-NB)^2 \delta(0) + \frac{B^2 N}{h_o\sqrt{2\pi}} e^{-\omega_p^2/2h_o^2} \quad . \qquad (4\text{-}82)$$

Similarly the power spectral density for the intensity becomes

$$S_{I_1}(\omega_p) = \delta(0)[(A-NB)^4 + NB^4 + 2N(A-NB)^2B^2] + \frac{2N(A-NB)^2}{h_o\sqrt{2\pi}} B^2 e^{-\omega_p^2/2h_o^2}$$

$$+ \frac{B^4N(N-1)}{2h_o\sqrt{\pi}} e^{-\omega_p^2/4h_o^2} \quad . \qquad (4\text{-}83)$$

We can likewise derive corresponding results obtained in Eqs. (4-73) through (4-83) for some other distribution of heights such as the uniform distribution with similar substitutions.

4.6 An Intensity Decorrelation Criteria for the Wavelength Spacing

We obtained a wavelength spacing to decorrelate speckle in Eq. (2-9) by equating the expected value of the magnitude square of the change in the electric field to the variance of the electric field. In Eq. (4-50) we obtain this wavelength spacing by finding when the spectral autocorrelation function of the intensity goes to zero. In this section, we again derive the wavelength spacing to decorrelate the speckle by using the definition that two random variables are uncorrelated when the product of their expected values is equal to the expected value of their product.

A convenient starting point is Eq. (2-6) which expresses the intensity at an arbitrary point x in the image plane, $I(x) = EE^*$, with a monochromatic plane wave used to illuminate the diffuser.

We rewrite Eq. (2-6) except that we restrict ourselves to illumination that is normally incident on the diffuser, thus making x

and α equal to zero. Also, if we consider the speckle near the z axis of the image then we can also neglect the term $i \frac{\pi n_o}{\lambda_o} \frac{(x'_r)^2}{M^2 s'}$ and so we can neglect ϕ_{1r}. In this case, the intensity of the image becomes

$$I(x) = \pi(\Delta w)^2 + 2\sqrt{\pi}\,\Delta w \sum_r e^{\frac{-(x-x'_r)^2}{\Delta w}} M w_r \left\{\cos \phi_{2r} - 1\right\}$$

$$+ 2 \sum_r e^{\frac{-2(x-x'_r)^2}{\Delta w}} (M w_r)^2 \left\{1 - \cos \phi_{2r}\right\}$$

$$+ \sum_{\substack{m \\ m \neq r}} \sum_r e^{\frac{-(x-x'_m)^2}{\Delta w}} e^{\frac{-(x-x'_r)^2}{\Delta w}} M^2 w_m w_r \left\{e^{-i\phi_{2m}} - 1\right\} \left\{e^{i\phi_{2r}} - 1\right\}$$

where

$$\phi_{2r} = \frac{2\pi}{\lambda_o} n_3 h_r \qquad . \qquad (4\text{-}84)$$

If we consider there to be N scatters per resolution cell, each of width w_c, then we can write down the intensity of radiation in one resolution cell of the image plane in the same way as we arrived at Eq. (2-7). Thus

$$I(x) \propto A^2 + 2AB \sum_{r=1}^{N} \left\{\cos ph_r - 1\right\} + 2B \sum_r^N \left\{1 - \cos ph_r\right\}$$

$$+ B^2 \sum_{\substack{m \\ m \neq r}}^{N} \sum_r^N \left\{e^{-iph_r} - 1\right\} \left\{e^{iph_m} - 1\right\} \qquad (4\text{-}85a)$$

where again $p = \dfrac{-2\pi n_3}{\lambda_o}$.

Equation (4-85a) can be written as, more simply,

$$I_1(x) = A^2 + 2B \sum_{r=1}^{N} (A-B) \left\{\cos ph_r - 1\right\} + B^2 \sum_{\substack{m=1 \\ m\neq 1}}^{N} \sum_{r=1}^{N} \left\{ e^{ip(h_m - h_r)} + 1 - (e^{-iph_r} + e^{iph_m}) \right\} \quad . \qquad (4\text{-}85b)$$

Let us consider this intensity at one resolution cell of the image plane when the incident radiation consists of a series of discrete monochromatic tones. Then $I_T(x)$, the total intensity, is given by the sum of the individual intensities for the various wavelengths, i.e.

$$I_T(x) = \sum_{n=1}^{L} I_1(\lambda_n, x) \qquad (4\text{-}86)$$

Substituting Eq. (4-86) into Eq. (4-87) we get an equivalent expression for the intensity in a resolution cell, where we now use q_r for the random variable $\left\{\cos ph_r - 1\right\}$, and S_{rm} to denote the random variable $\left\{e^{-iph_r} - 1\right\} \left\{e^{iph_m} - 1\right\}$. We note that S_{rm} and q_r are not independent and so a calculation of the statistics, i.e. the standard deviation of $I_1(x)$ is not algebraically simple. Thus $I_T(x)$ becomes, for M tones,

$$I_T(x) = MA^2 + 2B \sum_{n=1}^{M} \sum_{r=1}^{N} (A-B)\, q_{rn} + B^2 \sum_{n=1}^{M} \sum_{\substack{r=1 \\ r\neq m}}^{N} \sum_{m=1}^{N} S_{rmn} \quad . \qquad (4\text{-}88)$$

If the wavelength interval is large enough, so that the random variables q_{rn} and $q_{r(n+1)}$ and S_{rmn} and $S_{rm(n+1)}$ are uncorrelated, then, for large M, the second and third terms in Eq. (4-88) will tend to their expected value. Thus if the expected value of $\sum_{r=1}^{N} q_r$ is Q and $\sum_{m=1}^{N} \sum_{\substack{r=1 \\ m\neq r}}^{N} S_{rm}$ is equal to S then, for large M, $\frac{I_T(x)}{M}$ will become,

$$\frac{1}{M} I_T(x) = A^2 + 2B(A-B)Q + B^2S \quad . \qquad (4-89)$$

Hence, the intensity at each resolution cell will be the same and this will have the effect of the speckle averaging out. We would now like to find out the wavelength interval for which the random variables q_{rn} and $q_{r(n+1)}$ and S_{rn} and $S_{r(n+1)}$ become independent. To do this we <u>assume</u> independence if the variable $e^{i\phi_r}$ becomes uncorrelated. Thus we wish to find the wavelength interval for which the random variable $e^{i\phi_r}$ becomes uncorrelated.

Two random variables R_1, R_2 are said to be uncorrelated when the product of the expected values of the two is equal to the expected value of their product, i.e., when $\langle R_1\rangle\langle R_2\rangle = \langle R_1 R_2\rangle$. Hence, requiring $e^{i\phi_r}$ and $e^{i\phi_r} + \Delta(e^{i\phi_r})$ to be uncorrelated leads us directly to Eq. (4-90)

$$\langle e^{i\phi_r}\rangle^{*} \langle \Delta e^{i\phi_r}\rangle - \langle e^{i\phi_r} \Delta(e^{i\phi_r})\rangle = \sigma^2(e^{i\phi_r}) \quad . \qquad (4-90)$$

From Eq. (4-6) we have $\sigma^2(e^{iph_r}) = 1-F(p)F^*(p)$,

where $F(p) = \int_{-\infty}^{\infty} e^{iph} f(h)dh$. Also $\langle e^{iph_r} \rangle^* = F^*(p)$. We now have for Δe^{iph_r}

$$\Delta(e^{iph_r}) = e^{iph_r} \left[iph_r (\Delta p) - \frac{(\Delta p)^2 h_r^2}{2} \right] \quad . \qquad (4\text{-}91)$$

Thus for the expected value of $\Delta(e^{iph_r})$ we have

$$\langle \Delta(e^{iph_r}) \rangle = (\Delta p) \frac{dF(p)}{dp} + (\Delta p)^2 \frac{d^2F(p)}{dp^2} \quad , \qquad (4\text{-}92)$$

similarly, for the expected value of $e^{iph_r} \Delta(e^{iph_r})$ we have the result

$$\langle e^{-iph_r} \Delta(e^{iph_r}) \rangle = \langle ih_r(\Delta p) - (\Delta p)^2 h_r^2 \rangle = -h_o^2 \frac{(\Delta p)^2}{2} \quad . \qquad (4\text{-}93)$$

Thus substituting Eq. (4-93), Eq. (4-91), and Eqs. (4-5) and (4-6) into Eq. (4-90) we get

$$F^*(p) \frac{dF(p)}{dp} \Delta p + (\Delta p)^2 F^*(p) \frac{d^2F(p)}{dp^2} + \frac{h_o^2(\Delta p)^2}{2} = 1-F(p)F^*(p) \quad . \qquad (4\text{-}94)$$

Solving the quadratic equation (4-94) for Δp, we get

$$\Delta p = \frac{\left[-F^*(p)\frac{dF(p)}{dp}\right] \pm \sqrt{\left[F^*(p)\frac{dF(p)}{dp}\right]^2 + 4\left[1-F(p)F^*(p)\right]\left[\frac{h_o^2}{2} + F^*(p)\frac{d^2F(p)}{dp^2}\right]}}{2\left[\frac{h_o^2}{2} + F^*(p)\frac{d^2F(p)}{dp^2}\right]} \quad . \quad (4\text{-}95)$$

Noting again that $\Delta p = \frac{2\pi n_3}{\lambda_o^2}\Delta\lambda$, and assuming a gaussian density function, we obtain the wavelength spacing required to decorrelate e^{iph_r} in the case of a rough diffuser $(ph_o > 1)$,

$$\Delta\lambda = \frac{\lambda_o^2}{2\pi n_3 h_o} \quad . \quad (4\text{-}96)$$

4.7 Speckle Statistics When the Illumination Consists of M Independent Tones

Since the proposed method for the reduction of speckle noise in this study is by illuminating the diffuse object by a number of independent tones, making a multicolor hologram of this object, and then viewing the hologram with a color blind system, it is of our interest to understand how the speckle averages under this system. We therefore calculate the density functions for the speckle electric field and intensities when the illuminating beam consists of M independent tones, where by independent we mean that the successive beams are spaced by a wavelength greater than $\lambda_o^2/2\pi n_3 h_o$ units apart, as given by Eq. (4-50). For a typical 50 Å to 100 Å interval and a visible wavelength range from

4,000 to 7,000Å , this would mean that 30 to 60 independent tones are possible.

To calculate the density function for the electric field we first write the total electric field at time t = constant = 0 as

$$E_T(x) = \sum_{m_1}^{M} E_1(\lambda_m x) = M(A-NB) + B^2 \sum_{m=1}^{M} \sum_{r=1}^{M} e^{ip_m h_r} \quad , \qquad (4\text{-}97)$$

where we have assumed that A and B do not change appreciably with wavelength and can be assumed to be constant. For the wavelength spacing such that the $e^{ip_m h_r}$ are independent for the various wavelengths, we obtain for the density function of $W_{E_T}(E_T)$ substituting Eq (4-97) into (D-6)

$$W_{E_T}(E_T) = \frac{1}{2\pi^2 \left| \vec{E}_T \, M(A-NB) \right|} \int_0^{\infty} \sin\left(|\vec{\rho}| \left| \frac{\vec{E}_T (A-NB)M}{B^2} \right| \right)$$

$$\left(\operatorname{sinc} |\rho| \right)^{M+N} |\vec{\rho}| \, d|\vec{\rho}| \qquad . \qquad (4\text{-}98)$$

To derive the density function for the superposed independent intensity patterns we substitute I_1 in Eq. (3-28)

$$W_{I_T}(I_T) = \mathfrak{F}\left[\left[\mathfrak{F}^{-1}\left[W_{I_1}(I_1) \right] \right]^M \right] \qquad (4\text{-}99)$$

where $W_{I_1}(I_1)$ is defined in Eq. (4-4) and

$$\mathfrak{F}(W_{I_1}(I_1)) = \int_{-\infty}^{\infty} e^{-ipI_1} W_{I_1}(I_1) dI_1 \quad , \quad \mathfrak{F}^{-1}(W_{I_1}(I_1)) = \frac{1}{2\pi} \int_{-\infty}^{\infty} e^{ipI_1} W_{I_1}(I_1) dI_1 \qquad (4\text{-}100)$$

and $$I_T(x) = \sum_m^M I(\lambda_m, x) \quad .$$

We now calculate the standard deviation and the expectation values of the electric field and intensity when the illumination is by M independent tones. Thus, using Eq. (3-29) and (3-30) we obtain for the expectation value and the variance of the electric field

$$\langle E_T(x) \rangle = M[A - NB + BNF(p)] \quad , \qquad (4\text{-}101)$$

and

$$\sigma^2 [E_T(x)] = MN[1 - F(p)F^*(p)] B^2 \quad . \qquad (4\text{-}102)$$

Similarly, we obtain for the expectation value and the variance of the intensity the values, using Eq. (3-29) and (3-30)

$$\langle I_T(x) \rangle = M[(A-NB)^2 + (A-NB)BNF(p) + (A-NB)NBF^*(p) + B^2N(N-1)F(p)F^*(p)] \quad , \qquad (4\text{-}103)$$

and

$$\breve{\sigma}^2[I_T(x)] = M\, \sigma^2[I_1(x)] \quad , \qquad (4\text{-}104)$$

where $\sigma^2 [I_1(x)]$ is given in Eq. (4-23), and M is the number of independent illuminating tones.

We now examine the reduction of the speckle image degradation when the illumination consists of M independent tones. We have already defined a quantity which gives us a measure of the speckle noise in Eq. (4-24). Thus we get the expressions $R(E_T)$ and $R(I_T)$ from Eqs. (4-24) and (4-27) and Eqs. (4-101), (4-102), (4-103), and (4-104)

$$R(E_T) = \frac{1}{\sqrt{M}} R(E_1) \qquad \underline{\text{M Tones}} \quad , \qquad (1\text{-}105a)$$

and

$$R(I_T) = \frac{1}{\sqrt{M}} R(I_1) \qquad \underline{\text{M Tones}} \quad , \qquad (1\text{-}105b)$$

where $R(E_1)$ and $R(I_1)$ have the definitions

$$R(E_1) = \frac{\sigma(E_1)}{\langle E_1 \rangle} \qquad \underline{\text{Single Tone}} \quad , \qquad (1\text{-}106a)$$

and

$$R(I_1) = \frac{\sigma(I_1)}{\langle I_1 \rangle} \qquad \underline{\text{Single Tone}} \quad . \qquad (1\text{-}106b)$$

We note that the speckle noise decreases by a factor of $\frac{1}{\sqrt{M}}$ when the illuminating beam has M independent tones. Alternatively we can say that having M independent tones in the illuminating beam gives us a signal to noise ratio improvement by a factor of $\sqrt{M}$.[1] It is interesting to note, both from Eqs. (4-24) and (4-28) that the speckle noise decreases as the number of scatterers per resolution cell increases, this relation being proportional to $\frac{1}{\sqrt{N}}$ where N is the number of scatterers per resolution cell.

4.8 Speckle Statistics when the Illuminating Beam Consists of Spectral Components of Finite Width.

In most experiments, the illuminating beam has some finite spectral width. It is therefore of interest to calculate what the expected value and the variance of the speckle may be when this illumination consists of a beam of finite width. We would also like to calculate the expected values and the variance of the autocorrelation function for the speckle electric field and thus get an estimate for the wavelength spacing necessary to decorrelate the speckle in this case. Since the result for the electric field has been shown to be sufficient to understand the behavior of the speckle, we only derive the relations for the electric field. The corresponding results for the intensity can be calculated in the same way.

Since both the electric field and the intensities are directly expressed in terms of p, we shall find it more convenient to express the wavelength spacing in terms of the interval δp, where $\delta\lambda = \frac{\lambda_o^2}{2\pi n_3}\,\delta p$. Also, we shall assume that the different spectral components in the illuminating beam are distributed normally about some mean λ_o with some standard deviation σ_p, where we consider σ_p to be the spectral width of the illumination. Now we have already written the electric field in Eq. (4-1) as

$$E_1(x) = A - NB + B\sum_{r=1} e^{iphr}$$

and so the electric field at some time, t = 0, for a beam of finite spectral width is

$$E_s(x) = \frac{1}{\sigma_p\sqrt{2\pi}} \int_{-\infty}^{\infty} E_1(x) e^{-(p-p_o)^2/2\sigma_p^2} dp \qquad (4\text{-}107)$$

Substituting $E_1(x)$ in Eq. (4-1) into Eq. (4-107) we obtain

$$E_s(x) = A - NB + B \sum_{r=1}^{N} e^{iph_r} e^{-\frac{1}{2}\sigma_p^2 h_r^2} \qquad (4\text{-}108)$$

We first calculate the expected value of the random variable $E_s(x)$. Since the integral is difficult to evaluate for an arbitrary distribution we study the precise case of a normal distribution of heights, as described by the density function in Eq. (4-71). Thus taking the expected value of $E_s(x)$, we obtain from Eq (4-108),

$$\langle E_s(x)\rangle = \frac{1}{\sqrt{2\pi}\, h_o} \int_{-\infty}^{\infty} E_s(x) e^{-h_r^2/2h_o^2} dh_r$$

$$\text{i.e.} \qquad \langle E_s(x)\rangle = (A-NB) + \frac{BN\, e^{-\frac{1}{2}p_o^2 h_o^2 \left(\frac{1}{1+\sigma_p^2 h_o^2}\right)}}{\sqrt{1+\sigma_p^2 h_o^2}} \qquad (4\text{-}109)$$

In the same way, we calculate the variance of $E_s(x)$ to be

$$\sigma^2[E_s(x)] = \frac{NB^2}{(1 + \sigma_p^2 h_o^2)} \left[\theta - e^{-p_o^2 h_o^2 \left(\frac{1}{1 + \sigma_p^2 h_o^2}\right)}\right] \quad . \quad (4\text{-}110)$$

where $\theta = \dfrac{1+\sigma_p^2 h_o^2}{(1+2\sigma_p^2 h_o^2)^{\frac{1}{2}}}$

Before we consider this expression further, we first transform σ_p into a wavelength spacing. Since $p_o = -\dfrac{2\pi n_3}{\lambda_o}$, we have that

$$\Delta p = \frac{2\pi n_3}{\lambda_o^2} \Delta\lambda \quad . \quad (4\text{-}111)$$

Thus, we define the standard deviation of the wavelength as

$$\sigma_p = - p_o \frac{\sigma_\lambda}{\lambda_o} \quad (4\text{-}112)$$

where σ_p is the bandwidth in terms of p and σ_λ the bandwidth in terms of the wavelength. We now substitute Eq. (4-112) into Eq. (4-110) to obtain

$$\sigma^2[E_s(x)] = \frac{NB^2}{1 + \left(\frac{\sigma_\lambda}{\lambda_o}\right)^2 h_o^2 p_o^2} \left[\theta - e^{-p_o^2 h_o^2 \left(\frac{1}{1 + p_o^2 h_o^2 \left(\frac{\sigma_\lambda}{\lambda_o}\right)^2}\right)}\right]$$

$$\text{and} \quad \theta = \frac{1+\left(\frac{\sigma_\lambda}{\lambda_o}\right)^2 h_o^2 p_o^2}{\left[1+2\left(\frac{\sigma_\lambda}{\lambda_o}\right)^2 h_o^2 p_o^2\right]^{\frac{1}{2}}} \quad . \quad (4\text{-}113)$$

We can subdivide Eq. (4-113) into two cases, (a) when $p_o^2 h_o^2 (\sigma_\lambda/\lambda_o)^2 << 1$ and (b) when $p_o^2 h_o^2 (\sigma_\lambda/\lambda_o)^2 >> 1$. If we consider case (a) first, we can approximate Eq. (4-113) as

$$\sigma^2[E_s(x)] = NB^2[1 - p_o^2 h_o^2 (\frac{\sigma_\lambda}{\lambda_o})^2][1 - e^{-p_o^2 h_o^2 [1-p_o^2 h_o^2 (\frac{\sigma_\lambda}{\lambda_o})^2]}]$$

narrow linewidth case (4-114)

We note that the variance decreases rapidly with increase in the quantity $\sigma_\lambda^2/\lambda_o^2$ and approaches zero as $p_o^2 h_o^2 (\sigma_\lambda/\lambda_o)^2$ approaches one. We note that this condition for the variance to go to zero is the same as the condition used for obtaining the wavelength spacing for the decoupling of speckle, Eq (4-50), we have

$$p_o^2 h_o^2 (\frac{\sigma_\lambda}{\lambda_o})^2 = 1 \quad \text{when}$$

$$\sigma_\lambda = \frac{\lambda_o^2}{2\pi n_3 h_o} \tag{4-115}$$

We now consider the case (b), when $p_o^2 h_o^2 (\frac{\sigma_\lambda}{\lambda_o})^2 >> 1$. Eq. (4-113) now becomes,

$$\sigma^2[E_s(x)] = \frac{NB^2}{(\frac{\sigma_\lambda}{\lambda_o}) p_o h_o}[1 - \frac{\lambda_o^2}{\sigma_p^2 h_o^2 p_o^2}][0 - e^{-p_o^2 h_o^2 \frac{1}{p_o^2 h_o^2 (\frac{\sigma_\lambda}{\lambda_o})^2}[1 - (\frac{\lambda_o}{\sigma_\lambda})^2 \frac{1}{p_o^2 h_o^2}]}]$$

for $p_o^2 h_o^2 (\frac{\sigma_\lambda}{\lambda_o})^2 >> 1$ (4-116)

Simplifying, we obtain,

$$\sigma^2[E_s(x)] = \frac{\lambda_o}{\sigma_\lambda}\frac{NB^2}{p_o h_o}[1 - (\frac{\lambda_o}{\sigma_\lambda h_o p_o})^2][\theta - e^{-(\frac{\lambda_o}{\sigma_\lambda})^2[1 - (\frac{\lambda_o}{\sigma_\lambda p_o h_o})^2]}] \quad (4\text{-}117)$$

broad linewidth case

Thus we note from Eq. (4-117) that as we increase the wavelength spacings, the variance of the electric field rapidly approaches zero because of the factor

$$\{\theta - e^{-(\frac{\lambda_o}{\sigma_\lambda})^2 \quad [1 - (\frac{\lambda_o}{\sigma_\lambda h_o p_o})^2]}\} \quad .$$

We also note that for the case $\sigma_\lambda = o$, i.e. for the incident illumination monochromatic, Eqs. (4-109) and (4-110) reduce to the results previously derived for the ideally monochromatic case, i.e. Eqs. (4-7) and (4-8).

We now derive the autocorrelation function for $E_s(p)$. Following the procedure outlined in Section (4.4) we first calculate the value of $E_s(p)E_s^*(p + \Delta p)$. We obtain

$$E_s(p)E_s^*(p+\Delta p) = [A\text{-}NB + B\sum_{r=1}^{N} e^{iphr} e^{-\frac{1}{2}\sigma_p^2 h_r^2}][A\text{-}NB+B\sum_{r=1}^{N} e^{-i(p+\Delta p)} e^{-\frac{1}{2}\sigma_p^2 h_r^2}]$$

$$= (A\text{-}NB)^2 + (A\text{-}NB)B\sum_{r=1}^{N} e^{iphr} e^{-\frac{1}{2}\sigma_p^2 h_r^2} + \sum_{r=1}^{N} e^{-i(p+\Delta p)h_r} e^{-\frac{1}{2}\sigma_p^2 h_r^2}$$

$$+ B^2[\sum_{m=1}^{N}\sum_{n=1}^{N} e^{ip(h_m - h_n) - i\Delta p h_n - \frac{1}{2}\sigma_p^2(h_m^2 - h_n^2)}] \quad (4\text{-}118)$$

Now taking the average of (4-118) over p, we obtain the result

$$\psi_{E_s}(\Delta p) = \lim_{T\to\infty} \frac{1}{2T}\int_{-T}^{T} E_s(p)E_s(p+\Delta p)dp \tag{4-119}$$

$$= (A - NB)^2 + B^2 \sum_{r=1}^{N} e^{-i\Delta p h_r - \frac{1}{2}\sigma_p^2 h_r^2} \tag{4-120}$$

We now find the expected value of this autocorrelation function. We get,

$$\langle\psi_{E_s}(\Delta p)\rangle = (A - NB)^2 + B^2 N \frac{e^{-\frac{1}{2}(\Delta p)^2 h_o^2 [\frac{1}{1+\sigma_p^2 h_o^2}]}}{\sqrt{1+\sigma_p^2 h_o^2}} \tag{4-121}$$

Similarly, the standard deviation of this autocorrelation function becomes

$$\sigma^2[\psi_{E_s}(\Delta p)] = \frac{B^4 N^2}{(1+\sigma_p^2 h_o^2)}\left[\theta - e^{-(\Delta p)^2 h_o^2 (\frac{1}{1+\sigma_p^2 h_o^2})}\right] \tag{4-122}$$

By examining Eqs. (4-121) and (4-122), we would like to find a criteria when the speckle pattern decorrelates. We therefore follow the argument used in Section (4.4) and consider the speckle patterns to be independent when

$$\Delta p^2 h_o^2 (\frac{1}{1+\sigma_p^2 h_o^2}) > 1 \quad \underline{\text{uncorrelated case}} \tag{4-123}$$

Using the substitutions, $\Delta p = - p_o(\Delta\lambda/\lambda_o)$, $\sigma_p = -p\sigma_\lambda/\lambda$, we solve for

$$(\Delta\lambda)^2 \frac{p_o^2 h_o^2}{\lambda_o^2} \left(\frac{1}{1 + \frac{p_o^2 h_o^2}{\lambda_o^2}\sigma_\lambda^2}\right) > 1 \quad . \quad (4\text{-}124)$$

We obtain the result then,

$$\Delta\lambda > \frac{\lambda_o^2}{2\pi n_3 h_o}\left[1 + \left(\frac{2\pi n_3 h_o}{\lambda_o}\right)^2 \left(\frac{\sigma_\lambda}{\lambda_o}\right)^2\right]^{\frac{1}{2}} \quad \underline{\text{decorrelated case}} \quad . \quad (4\text{-}125)$$

We now consider the case when $\sigma_p h_o << 1$, which would correspond to the case of illumination by a narrowband source which would have a σ_λ narrow enough to give speckle. Then (4-125) reduces to

$$\Delta\lambda > \frac{\lambda_o^2}{2\pi n_3 h_o}\left[1 + \tfrac{1}{2}\left(\frac{2\pi n_3 h_o}{\lambda_o}\right)^2 \left(\frac{\sigma_\lambda}{\lambda_o}\right)^2\right] \quad , \quad \underline{\text{narrowband decorrelation case}} \quad (4\text{-}126)$$

where $p_o^2 h_o^2 \frac{\sigma_\lambda^2}{\lambda_o^2} << 1$.

Alternatively, we consider the case when the illumination is by a broadband source and there is hardly any speckle. We then get, substituting $p_o^2 h_o^2 (\sigma_\lambda^2/\lambda_o^2) >> 1$ into (4-136),

$$\Delta\lambda > \sigma_\lambda\left[1 + \left(\frac{1}{2}\right)\frac{\lambda_o^2}{(2\pi n_3 h_o)^2 \sigma_\lambda^2}\right] \quad \underline{\text{broadband decorrelation case}} \quad . \quad (4\text{-}127)$$

We can now take the fourier transform of (4-121) to also calculate the spectral density function of the electric field and we get the expression

$$S_{E_s}(\omega_p) = (A - NB)^2 \delta(o) + \frac{B^2 N}{h_o \sqrt{2\pi}} e^{-\frac{\omega_p^2 (1+h_o^2 \sigma_p^2)}{2h_o^2}} \quad . \quad (4\text{-}128)$$

We note here that the width of the spectral density function is $h_o/(1 + h_o^2 \sigma_p^2)^{\frac{1}{2}}$ which will give us the same result as Eq. (4-123) for the wavelength spacing before an appreciable decorrelation of the speckle occurs.

4.9 Summary and Conclusions

In this chapter we have applied the results of Chapter III to understand the statistical behavior of speckle. We have taken the electric field and the intensity of the speckle to be a random variable and then computed the expectation values and the variance of these quantities, in Eqs. (4-7) and (4-22) and Eqs. (4-8) and (4-23). We have calculated the density functions for the electric field and intensity in Eqs. (4-3) and (4-4). We have computed the spatial autocorrelation function in Eq. (4-34), and so estimated the average speckle size to be the size of a resolution cell in the image plane. We have defined a criteria to determine the degradation of the image due to speckle, Eq. (4-24) and found that this quantity is proportional to $1/\sqrt{N}$ where N is the number of scatterers per resolution cell.

We then investigated the wavelength diversity of speckle. We calculate the spectral autocorrelation functions in Eqs. (4-38) and (4-45). We find the expectation values of these functions in Eqs. (4-37) and (4-45). We compute the variance of the autocorrelation functions in Eqs. (4-57) and (4-60). We investigate the spectral density functions for the electric field and the intensity which give us the distribution of how rapidly the speckle is changing, in Eqs. (4-66) and (4-67). We derive the intensity decorrelation criteria in a completely different way and obtain the same result for speckle decorrelation as we obtained by a consideration of the autocorrelation functions in Eq. (4-50).

We then investigate the statistics of the averaged speckle patterns when the diffuser is illuminated by a set of M independent monochromatic tones and obtain the density functions for the electric field and the intensity in Eqs. (4-99) and (4-100). We obtain the expected values and the standard deviations of the electric field and the intensities in Eqs. (4-101), (4-102), (4-103) and (4-104) respectively. We calculate the image degradation due to speckle in (4-105) and find an improvement by a factor of $1/\sqrt{M}$ over the single tone case.

In Section 4.9 we study the statistics of the speckle when the illuminating beam is not monochromatic but has a finite bandwidth σ_p. We derive an expression for the electric field for such a case in Eq.(4-108) and calculate the expected value and the variance of this field in Eqs. (4-109) & (4-110). We examine this expression for the standard deviation to note that the speckle noise decreases rapidly with increase in the spectral width of the illumination and that the image is virtually speckle free if the spectral width of the illumination is equal the wavelength spacing to decorrelate the speckle. We then examine the autocorrelation function for this electric field and calculate a wavelength spacing required to decorrelate the speckle when the illumination has spectral

widths of σ_λ in Eq. (4-125). We calculate the spectral density function of the electric field for beams of finite spectral width in Eq. (4-128) and note that in the limit of σ_λ, the spectral width of the illumination, going to zero, we obtain the same results as for monochromatic speckle.

Thus, in this chapter we have examined the statistical behavior of speckle noise in imaging systems and from our calculations we obtain the wavelength spacing required to decorrelate the speckle, the speckle size, and the resulting improvement in resolution when the illumination is not monochromatic.

REFERENCES

1. J. C. Dainty, Optica Acta 17, 761 (1970).

2. L. H. Enloe, Bell Syst. Tech. J. 46, 1479 (1967).

3. C. B. Burckhardt, Bell Syst. Tech. J. 49, 309 (1970).

4. H. H. Hopkins and H. Tiziani, Applications of Holography (Besancon Conference 6-11 July 1970), viii.

5. L. I. Goldfischer, J. Opt. Soc. Am. 55, 247 (1965).

6. J. W. Goodman, Stanford University Electronics Labs. Tech. Report, SEL-63-140 (TR 2303-1), December 1963.

7. Serge Lowenthal and Denis Joyeux, J. Opt. Soc. Am. 61, 847 (1971).

8. A. Papoulis, "Probability, Random Variables and Stochastic Processes," McGraw Hill Book Company, New York (1965), Ch. 5.

CHAPTER V

Summary and Conclusions

In this thesis we have investigated the wavelength dependence of speckle in the image of a pure phase diffuse object. We have studied both the speckle electric field and intensity and derived expressions for the spatial and spectral dependence of these quantities. We have also demonstrated experimentally the wavelength dependence of speckle and the averaging of speckle under multitoned illumination. As a result of these studies we have demonstrated the feasibility of eliminating speckle in holographic microscopy while still requiring only a single rapid exposure from some multimonochromatic source and also established a theoretical basis for deducing the properties of a rough surface by analyzing the spectral dependence of the speckle due to this surface.

We have developed an analytic model for a diffuser in section 2.2 and Eq. (2-3) gives us the electric field transmitted by this diffuser when a plane wave is incident on it. In Eq. (2-7) we give the electric field in the image of the diffuser and we find that this field is given by a constant, which depends on the area occupied by the scatterers on the diffuser, and a sum of random unit phasors, the angle of each phasor depending on the height of the corresponding scatterer on the diffuser and the number of phasors depending on the number of scatterers in one resolution cell.

We define the image degradation due to speckle in Eq. (4-24) as the ratio of the standard deviation to the electric field for the

speckle intensity and find that this quantity is inversely proportional to the square root of the number of scatterers per resolution cell. Also we note from this equation that this ratio decreases as the standard deviation for the scatterer heights decrease.

We derive that the wavelength spacing for two speckle patterns to decorrelate is $\Delta\lambda > \frac{\lambda_0^2}{2\pi n_3 h_0}$ where $\Delta\lambda$ is the wavelength interval, λ_0 is the mean wavelength, n_3 is the difference in the refractive index of the object and of air and h_0 is the standard deviation for the heights of the scatterers. We obtain this result using four different derivations as described in sections 2.1, 2.2, 4.4 and 4.6. Eq. (2-2) gives this result if we consider h_0 to be the temporal coherence length of a wave of linewidth $\Delta\lambda$. We derive Eq. (2-9) by equating the expected value of the magnitude square change in electric field to the variance of the electric field. Eq. (4-50) comes from determining when the expected value of the spectral autocorrelation function of the intensity is negligible, and Eq. (4-96) is derived by using the definition that two random variables are uncorrelated when the product of their expected values is equal to expected value of their product.

Eq. (4-46) gives us the expected value of the autocorrelation function and we note that this quantity depends on the characteristic function for the heights of the scatterers on the diffusers. Thus, if we can measure this expected value for the speckle autocorrelation function we can determine the density of heights for the scatterers in the diffuser, as calculated in Eq. (4-53).

In Eqs (4-105) and (4-106) we have calculated the image degradation when M independent speckle patterns are added together, such as is the case under illumination with M independent tones. We note that this quantity is inversely proportional to $\sqrt{M}$ and so these results predict the reduction of speckle noise under multitoned illumination.

We calculate the expected value and standard deviation for the speckle electric field when the illumination has a linewidth of σ_λ in Eqs. (4-109) and (4-110). We note from (4-113) that the speckle noise is negligible when the linewidth is equal to the wavelength spacing for the decorrelation of speckle. We also calculate the expected value of the spectral autocorrelation function of the speckle in Eq. (4-121) and the spectral density function in Eq. (4-128).

In section 3.2 we reviewed the calculation for the density function for a sum of random vibrations, when all phases are equally possible, and applied these results to calculate the density function for the speckle electric field and intensity in Eqs. (4-3) and (4-4) respectively. Also in section 4.3 we review the calculation for the spatial autocorrelation function for the speckle intensity, which is given in Eq. (4-34). From this result we deduce that the average speckle size is equal to the resolution of the imaging system.

In section 2.4, we describe the results of two sets of experiments conducted to establish the wavelength dependence of speckle. In one set we illuminate a pap smear by one tone of an argon laser, white light, and four tones of the argon laser (5145, 4965, 4880 and 4765Å) as shown in Figs. 3a, 3b and 3c in Appendix B and we find the

reduction of speckle when the four tones are used. In the next set of experiments, we simulate a tunable monochromatic source by bandlimiting the light from a carbon arc source with a monochromator and then collimating this output. Fig. 5 in Appendix A shows the speckle pattern when the illumination has a linewidth of 5Å and Figs. 6, 7, 8 and 9 in Appendix A show respectively the image of an optic nerve in laser illumination, white light, bandlimited illumination of 5Å linewidth and 6 separated bandlimited tones scanning 4, 300Å to 5,800Å .

Thus we have established, both experimentally and theoretically, that the speckle pattern in the image of a diffuser depends on wavelength and that it averages out in multi-toned illumination and have calculated some of the spectral properties of this speckle.

APPENDIX A

Speckle Reduction Using Multiple Tones of Illumination

In this Appendix we detail the derivations for the electric field and the intensity in the image of a pure phase diffuser, results given in Eqs. (2-5) and (2-6) in section 2.3, chapter II. We also give the details for the calculation of the wavelength spacing required to decorrelate the speckle by equating the expected value of the magnitude square change in the speckle electric field to the variance of this electric field (Eq. (2-9)). In addition we give details of the speckle experiments using collimated bandlimited light from a carbon arc source described in section 2.4.

Speckle Reduction Using Multiple Tones of Illumination

Nicholas George and Atul Jain

The occurrence and smoothing of speckle are studied as a function of the line width for a highly collimated illuminating source. A general theory is presented for speckling in the image of a partially diffuse, phase type of object, which has a variable number of random scattering centers per resolution element. Then, an expression is derived for the wavelength spacing required to decouple the speckle patterns arising from two monochromatic tones in an imaging system, thereby establishing that it is feasible to smooth speckle using multicolor illumination. This theory is verified in a series of experiments using both laser illumination and band-limited light from a carbon arc. With highly collimated sources, we show that speckle appears laserlike for an imaged diffuser even up to line widths of 5 Å. Then, smoothing of speckle is demonstrated in the imaging of a diffuser and for a section of an optic nerve when the illumination is provided by six narrow lines spread over 1500 Å. Since with color-blind, panchromatic viewing the speckle smooths, a direct extension of this method to holographic microscopy, using a multitone laser, should permit one to record and reconstruct holograms of diffraction-limited resolution that are essentially speckle-free.

Introduction

Under monochromatic illumination, objects with a scale of roughness grossly on the order of the wavelength are hard to discern in feature detail, owing to the rapid spatial variations that occur in the scattered radiation. This characteristic of laser illumination to speckle has been studied by many investigators; however, owing to space limitations, we cite only a few of the publications.[1-22] It is difficult to quote a specific numerical value for this resolution loss since it varies widely with the roughness of the object being studied. However, in the application of laser holography to microscopy, this speckle effect has been a severe obstacle,[8-10,12,17,20] limiting the *working* resolution to from a few to several times the classical optics limit. As examples, Young *et al.* report that "the usual resolution criterion should be divided by five or more whenever diffused laser light is used"[12]; Close reports resolutions of a few microns on test samples[17]; and Cox *et al.* have obtained similar resolutions with biological specimens.[10]

Gabor[14] has classified speckle into two categories: The *objective* speckle that arises owing to uneven illumination falling on the subject. The *subjective* speckle that arises from the roughness of the subject in conjunction with the convolving effect of a finite aperture. The objective type can occur when one holographically records a smooth transparency but with a diffuser placed in the beam illuminating the transparency. While the diffuser creates a helpful redundancy in the recording, it also leads to the deleterious speckle. Most prior studies of speckle elimination have considered only this objective type, and good results have been reported, although the subject is far from closed.[5-9,14,22]

In this paper we consider the smoothing of subjective speckle. This is a somewhat neglected topic, since it has been generally argued that the only effective means for smoothing this type is to increase the aperture.[14] However, if one draws this conclusion, it is implicitly assumed that operation is at a single wavelength or that separate, independent looks are not being made in the over-all process. In the method we are to describe, separate wavelengths are used to provide independent looks.[20,21] In this way, we will show that one can smooth subjective speckle at a fixed value of aperture. Probably, too, a method that smooths subjective speckle also smooths the objective type (but not conversely). Hence, in this instance, the need for making the distinction is not great.

An analysis for the wavelength variation of speckle in an imaging system has not been found in the literature; however, Goodman has treated the related problem of the wavelength sensitivity of speckle in the far-field region of a coherently illuminated group of scatterers.[2] Recent experiments have been reported in confirmation of the thesis that speckle patterns vary spatially in a marked way with change in wavelength.[19-21]

We feel that an interesting possibility for dramati-

The authors are with the California Institute of Technology, Pasadena, California 91109.

Received 25 September 1972.

cally reducing the speckle effect in holographic microscopy is to use a multicolor recording process with several widely spaced laser tones spanning the visible optical region. The hologram-volume effects permit one to record and play back these images in a noninteracting way, provided that adequate spatial separation and wavelength intervals have been chosen between each reference beam.[23] In viewing, the same multitone spectra are used for the reference beams so that no spatial distortions occur, but a color-blind monitor with uniform response over the visible spectrum must be provided, e.g., by a vidicon apparatus, in order to average the multitone speckle.

Within this context, we report the first study of the spatial variations of speckle in the imaging system of a microscope as the wavelength of a monochromatic source is scanned through the visible. First, we analyze the imaging of a diffuser in which there is a variable number of random phase heights per resolution cell. This is a good model for the objects of practical interest covering the smooth case, through the troublesome case where five to ten random scatters per resolution element are limiting the resolution, and the case where the number of random contributors per resolution cell is very high. We show that the multicolor speckle will decorrelate when

$$\lambda_2 - \lambda_1 \geq (\lambda_0^2/2\pi n_3 h_0)\{[1-e^{-(ph_0)^2}]/[1 + (N-1)(ph_0)^2 e^{-(ph_0)^2}]\}^{1/2},$$

where the n_3 is the difference in the refractive index of the air and the diffuse object, N is the number of scatterers per resolution cell, and the heights h_r of the scatterers have been assumed to have a normal distribution with an expected value of zero and a standard deviation h_0, $p = -2\pi n_3/\lambda_0$, and $\lambda_0 = (\lambda_1 + \lambda_2)/2$. As an alternative interpretation, speckle will appear laserlike as a given line width increases from the few hertz band up to a small fraction of the above $\lambda_2 - \lambda_1$ (this fraction is typically a few angstroms). We note too that wavelength diversity may also prove useful in *electron microscopy* where the monoenergetic electrons typically have a monochromaticity $d\lambda/\lambda \lesssim 10^{-5}$, where λ is the de Broglie wavelength of the electron. This is easily small enough to cause speckle, however a further consideration of speckle in matter waves is beyond the scope of this paper.

Analysis of Diffuser Imaging

An imaging system for a microscope is idealized by a lens of focal length F and aperture D, an input plane (ξ,η) at a distance $s' = F + \delta$ from the lens (Fig. 1), and thus with the image plane at a distance s given by $1/s + 1/s' = 1/F$. For monochromatic illumination, $e^{i\omega t}$, of an arbitrary object D_0, we describe the transverse scalar component of the input electric field by $f(\xi,\eta)e^{i\omega t}$. In the image plane, this corresponding field amplitude is found by two applications of the usual Fresnel-zone approximation of Sommerfeld's formula[24]; i.e., the output field amplitude $E(x,y)e^{i\omega t}$ is given by

$$E(x,y) = -\frac{\exp[-(i2\pi/\lambda_0)(s+s')]}{\lambda_0^2 ss'} \times \int\int\int\int_{-\infty}^{\infty} d\xi d\eta du dv\, f(\xi,\eta)T(u,v) \times \exp\left\{-\frac{i\pi}{\lambda_0 s'}[(u-\xi)^2 + (v-\eta)^2] - \frac{i\pi}{\lambda_0 s}[(x-u)^2 + (y-v)^2]\right\}, \quad (1)$$

in which (u,v) are Cartesian coordinates in the plane of the lens, $\lambda_0 = 2\pi c/\omega$, and $c = 3 \times 10^8$ m/sec. The transmission function for the lens $T(u,v)$ will be taken with the spherical convergence factor exp $[+(i\pi/\lambda_0 F)(u^2 + v^2)]$ and a pupil function that is Gaussian, i.e., it is given by

$$T(u,v) = \exp[-(i\pi/\lambda_0)(u^2+v^2)/\rho], \quad (2a)$$

where

$$1/\rho = -(1/F) - (i4\lambda_0/\pi D^2), \quad (2b)$$

and D is the diameter of the lens of focal length F.[25] Substitution of Eq. (2) into Eq. (1) and integration over the (u,v) plane, defining the magnification factor $M = s/s'$ and the up-scaled variables $x' = -M\xi$, $y' = -M\eta$, give the result:

$$E(x,y) = -\frac{\exp\{-(i2\pi/\lambda_0)(M+1)s' - (i\pi/\lambda_0)[(x^2+y^2)/Ms']\}}{\lambda_0^2 s'^2 M^3} \times \frac{\pi D^2}{4}\int\int_{-\infty}^{\infty} dx'dy'\, f\left(-\frac{x'}{M}, -\frac{y'}{M}\right) \exp\left\{-\frac{i\pi}{\lambda_0 s'}\left[\frac{(x'^2+y'^2)}{M^2}\right] - \left(\frac{\pi D}{2\lambda_0 s}\right)^2 [(x-x')^2 + (y-y')^2]\right\}. \quad (3)$$

In the basic imaging equation, Eq. (3), the convolving effect of a finite aperture, D, is readily seen. As is well known, subjective speckle arises from this averaging or smearing of the input function $f(-x'/M, -y'/M)$, i.e., for a finite aperture $E(x,y)$ will not be a perfectly resolved scaled replica of $f(-x'/M, -y'/M)$. The departures here from the usual imag-

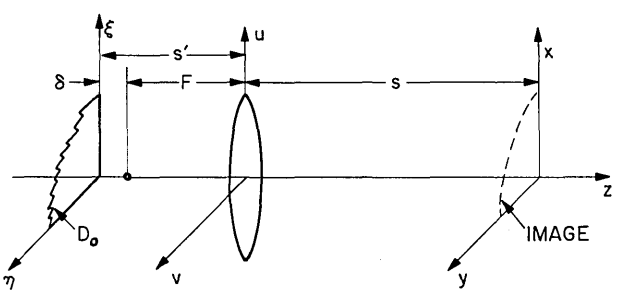

Fig. 1. Single lens magnification with object plane (ξ,η) and image plane (x,y).

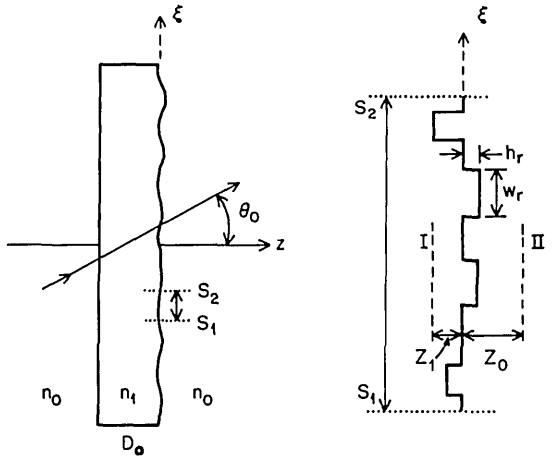

Fig. 2. The idealized diffuser object (D_0) in the (ξ,η) plane showing a magnified inset between S_1S_2 for the computation of the transmission function, Eq. (10). The diffuser has steps of width w_r and random height h_r.

ing formula are that phase terms have been retained and the Gaussian transmission function of Eq. (2) is used. Hence, it is instructive to find the radius of the resolution cell for comparison to the conventional circular pupil function. By integration of Eq. (3) with a delta function impulse as input, i.e., $f = \delta(x',y')$, we find that the output spot size is given by

$$\dot{E}(x,y) \propto \exp[-(\pi D/2\lambda_0 s)^2 (x^2 + y^2)].$$

Thus, in the output plane (x,y), the intensity falls to a $1/e^2$ fraction of its peak at a radius of $0.637\lambda_0 s/D$. From this impulse interpretation, we define the radius of the resolution cell referenced to the (x,y) plane or the (ξ,η) plane, respectively, as

$$\Delta w = (2\lambda_0 s/\pi D) \text{ or } \Delta w_0 = (2\lambda_0 s'/\pi D). \quad (4)$$

If we would have used the usual circ $[(u^2 + v^2)^{1/2}/(D/2)]$ as the pupil function portion of Eq. (2a), the resulting Airy disk would have the function value $[2J_1(z)/z]^2$. This would result in a radius for the $1/e^2$ power down locus of $0.82\ \lambda_0 s/D$, which is close enough for our purposes to the corresponding value of $0.637\ \lambda_0 s/D$, obtained for a Gaussian pupil function.[26]

Model for the Phase-Type Diffuser

There have been various ways, in the past, of describing the electric field transmitted by a rough object. Hopkins and Tiziani,[16] for instance, idealize the diffuser as a series of closely packed lenslets of varying sizes and focal length. Enloe[4] and Goodman,[2] on the other hand, idealize the diffuser as a randomly spaced array of inifinitesimal radiators, each radiating with a random phase.

A semitransparent object of complex-valued amplitude transmission factor $D_0(\xi,\eta)$ is placed in the input plane and illuminated by a monochromatic plane wave incident at the polar angle θ_0 in the (ξ,η) plane (Fig. 2). Thus, the input amplitude function $f(\xi,\eta)$ is given by

$$f(\xi,\eta) = D_0(\xi,\eta) \exp[-i(2\pi/\lambda_0)n_0\xi \sin\theta_0], \quad (5)$$

where n_0 and n_1 are the relative indices of refraction in the two media and $n_0\sin\theta_0 = n_1\sin\theta_1$. For a general object consisting of an amplitude transmittance, denoted by real-valued function $D_1(\xi,\eta)$ and the phase delay $\psi(\xi,\eta)$, we write

$$D_0(\xi,\eta) = D_1(\xi,\eta) \exp[-i\psi(\xi,\eta)]. \quad (6)$$

For the surface contour $h(\xi,\eta)$ of the diffuser (shown between planes I and II spaced by $Z_0 + Z_1$ in Fig. 2), we use a ray optics approximation to $\psi(\xi,\eta)$. Thus, we write the phase delay

$$\psi(\xi,\eta) = (2\pi n_0/\lambda_0)(Z_0 - h)/\cos\theta_0 + (2\pi n_1/\lambda_0)(Z_1 + h)/\cos\theta_1;$$

and suppressing the nonessential constant phase delays, we can rewrite Eq. (5) as follows:

$$f(\xi,\eta) = D_1(\xi,\eta) \exp[-(i2\pi/\lambda_0)n_0\xi \sin\theta_0] \exp\left[-\frac{i2\pi}{\lambda_0} n_3 h(\xi,\eta)\right], \quad (7)$$

in which $n_3 = (n_1/\cos\theta_1 - n_0/\cos\theta_0)$.

Now, consider the simplified one-dimensional case with a pure phase object, i.e., $D_1 = 1$, consisting of randomly positioned steps of height h_r and width w_r centered at $\xi = \xi_r$, i.e.,

$$h(x,y) = \sum_r h_r \text{ rect}[(\xi - \xi_r)/w_r].$$

Then, the one-dimensional idealization of Eq. (7) becomes

$$f(\xi) = \exp[-(i2\pi/\lambda_0)n_0\xi \sin\theta_0] \exp\left\{-\left(\frac{i2\pi}{\lambda_0}\right) n_3 \sum_r h_r \text{ rect}[(\xi - \xi_r)/w_r]\right\}, \quad (8)$$

where the function rect$(x) = 1$ when $|x| < \frac{1}{2}$ and is zero otherwise. If nonoverlapping steps are assumed in the expression

$$\sum_r h_r \text{ rect}[(\xi - \xi_r)/w_r],$$

one can prove the following identity:

$$\exp\{-(i2\pi/\lambda_0)n_3 \sum_r h_r \text{ rect}[(\xi - \xi_r)/w_r]\} = 1 + \sum_r \text{rect}[(\xi - \xi_r)/w_r]\{\exp[-(i2\pi/\lambda_0)n_3 h_r] - 1\}.$$

Substituting this into Eq. (8) we obtain

$$f(\xi) = \exp[-i(2\pi/\lambda_0)n_0\xi \sin\theta_0]$$

$$\left(1 + \sum_r \text{rect}[(\xi - \xi_r)/w_r]\left\{\exp[-i(2\pi/\lambda_0)n_3h_r] - 1\right\}\right). \quad (9)$$

Equation (9) for a pure phase type of diffuser could equally well have been postulated directly, as follows. The multiplicative term $\exp[-i(2\pi/\lambda_0)n_0\xi\sin\theta_0]$, with the linear phase taper in (ξ), occurs for a plane wave incident at an angle θ_0, as shown in Fig. 2. With nonoverlapping steps assumed in the

$$\sum_r \text{rect}[(\xi - \xi_r)/w_r],$$

the term within the square brackets, [ ], is either 1 or $\exp[-i(2\pi/\lambda_0)n_3h_r]$. This holds for an arbitrary value of ξ, hence $|f(\xi)| \equiv 1$ as it must for a pure phase object.

We could adapt this transmitted field to fit a variety of models for the diffuser. Thus we can consider the height of a step given by $h_r(\xi)$ to be roughly constant over the width w_r. On the other hand, if one prefers the randomly positioned lenslets of Hopkins and Tiziani, then h_r becomes the quadratic phase transmission for each lens, i.e., $h_r(\xi) = [(\xi - \xi_r)^2/f_r]$, where f_r is the focal length of the lenslet centered at ξ_r.

If we make the assumption that the width of each random step is much less than the resolution cell size, i.e., $w_r \ll \Delta w_0$, then insofar as integrations of the form of Eq. (3), we can replace the rect $[(\xi - \xi_r)/w_r]$ by the Dirac delta function, i.e., by $w_r\delta(\xi - \xi_r)$. Thus, combining Eqs. (8) and (9), we find a convenient approximation for the one-dimensional input transmittance

$$f(\xi) = \exp\left[-\left(\frac{i2\pi}{\lambda_0}\right)n_0\xi\sin\theta_0\right]$$

$$\left(1 + \sum_r w_r\delta(\xi - \xi_r)\left\{\exp[-(i2\pi/\lambda_0)n_3h_r] - 1\right\}\right). \quad (10)$$

To facilitate the consideration of our diffuser, we arbitrarily define the one-dimensional lens process, reducing Eq. (3), as follows:

$$E_1(x) = \exp[-(i\pi n_0/\lambda_0)(x^2/Ms')]\int_{-\infty}^{\infty} dx' f\left(-\frac{x'}{M}\right)$$
$$\exp\left\{-\frac{i\pi n_0(x')^2}{\lambda_0M^2s'} - \left[\frac{(x-x')}{\Delta w}\right]^2\right\}. \quad (11)$$

Substitution of Eq. (10) into Eq. (11) and integrating give

$$E_1(x) = \Delta w(\pi)^{1/2}\exp\left[-\frac{i\pi n_0}{\lambda_0}\left(\frac{x^2}{Ms'} - \frac{2x\sin\theta_0}{M}\right)\right.$$
$$\left. - \frac{4\pi n_0^2x^2\sin^2\theta_0}{\lambda^2M^2}\right] + \exp\left[-\frac{i\pi n_0}{\lambda_0}\left(\frac{x^2}{Ms'}\right)\right]$$
$$\times\sum_r\exp\left[-\left(\frac{x-x_r'}{\Delta w}\right)^2 + \frac{i\pi n_0}{\lambda_0}\left(\frac{2x_r'\sin\theta_0}{M} - \frac{(x_r')^2}{M^2s'}\right)\right]$$
$$\times Mw_r\left[\exp\left(-\frac{i2\pi}{\lambda_0}n_3h_{r_{-1}}\right) - 1\right]. \quad (12)$$

Now define the intensity or energy density factor by $I(x) = E_1E_1^*$, and from Eq. (12) we find

$$I(x) = \pi(\Delta w)^2e^{-2\alpha} + 2(\pi)^{1/2}\Delta we^{-\alpha}\sum_r Mw_r$$
$$\exp\left[-\left(\frac{x-x_r'}{\Delta w}\right)^2\right]\{\cos(\chi - \phi_{1r} + \phi_{2r}) - \cos(\chi - \phi_{1r})\}$$
$$+ 2\sum_r \exp[-2(x - x_r')^2/(\Delta w)^2](Mw_r)^2\{1 - \cos\phi_{2r}\}$$
$$+ \sum_{\substack{m\\ m\neq r}}\sum_r \exp[-(x - x_m')^2/(\Delta w)^2 - (x - x_r')^2/(\Delta w)^2]$$
$$\times \exp[i(\phi_{1m} - \phi_{1r})]$$
$$\times M^2w_mw_r(e^{-i\phi_{2m}} - 1)(e^{+i\phi_{2r}} - 1), \quad (13)$$

in which $\alpha = 4\pi(n_0x\sin\theta_0)^2/(\lambda_0M)^2$,

$$\chi = (2\pi/\lambda_0)(n_0x\sin\theta_0/M),$$

$\phi_{1r} = (\pi n_0/\lambda_0)\{2x_r'\sin\theta_0/M - (x_r')^2/(M^2s')\}$, and

$$\phi_{2r} = (2\pi/\lambda_0)n_3h_r.$$

Equation (13) is a convenient starting point for the statistical analysis of decorrelation based on combining intensity patterns taken at *separate* wavelengths.[21] Equation (12) is the more useful starting point in the simpler amplitude decoupling criterion presented in Eq. (21) of the following section.

Expected Value and Variance for the Electric Field

To calculate the wavelength spacing required to decouple the speckle pattern described by Eqs. (12) and (13), first we analyze the simpler case when θ_0 is constant, e.g., when $\theta_0 = 0$. Later separate comment is included for the important case when a distributed angular spectrum is used for the illumination.

We assume the response of a panchromatic viewing system is given by $I = E_1E_1^* + E_2E_2^* + \ldots$ when there are multiple tones of monochromatic illumination, i.e., beat terms are negligible with long exposure times. Hence, we must compare the intensities in the image plane at two different wavelengths and find when these two intensity patterns are decorrelated. Since in computing $E_1E_1^*$, common phase terms will cancel, we factor Eq. (12) extracting and suppressing the term $\exp\{(i\pi n_0/\lambda_0)[(2x\sin\theta_0/M) - (x^2/Ms')]\}$. The *remainder* of the electric field we denote by $\mathbf{E}_1$, and rewriting Eq. (12) gives

$$\mathbf{E}_1(x) = \Delta w(\pi)^{1/2} + \sum_r \exp\left[-\left(\frac{x-x_r'}{\Delta w}\right)^2\right.$$
$$\left. - \frac{i\pi n_0(x_r')^2}{\lambda_0M^2s'}\right]Mw_r\left\{\exp\left(-\frac{i2\pi}{\lambda_0}n_3h_r\right) - 1\right\}. \quad (14)$$

Additionally, comparing Eqs. (12) and (14), one will note that we have dropped the quadratic multiplier $\exp[-4\pi n_0^2x^2\sin\theta_0/(\lambda_0^2M^2)]$ from the first term in Eq. (14); and the *small* phase term $\exp\{(i\pi n_0/\lambda_0)[2(x_r' - x)\sin\theta_0/M]\}$ from the summation.

To study the speckle in the image plane, we consider an arbitrary position x. In Eq. (14), the rapid falloff of the Gaussian term, $\exp\{-[(x - x_r')/\Delta w]^2\}$, limits the number of scatterers from among the entire set x_r' that contribute effectively to $\mathbf{E}_1$ at x. Thus, if there are N scatterers remaining from this set that are positioned (in image plane coordinates) with values of x_r' in the range $x - \Delta w < x_r' < x + \Delta w$, then we can approximate Eq. (14) by

$$\mathbf{E}_1(x) = A - BN + B \sum_{r=1}^{N} \exp(+iph_r). \quad (15)$$

We have defined $A = \Delta w(\pi)^{1/2}$,

$$B = Mw_c \exp[-(i\pi n_0 x^2)/(\lambda_0 M^2 s')] \text{ and } p \text{ as}$$

$$p = -(2\pi n_3/\lambda_0). \quad (16)$$

To simplify the analysis, we assume that the step widths w_r are constant for all scatterers and equal to w_c. Also, with negligible error, the Gaussian permits us to approximate the phase term $\exp -[i\pi n_0 (x_r')^2/\lambda_0 M^2 s']$ in Eq. (14) by the term $\exp -[i\pi n_0 x^2/\lambda_0 M^2 s']$ in Eq. (15).

If we assume that the real random variable h_r is distributed according to some known density function, $f(h_r)$, and the corresponding characteristic function for this distribution is given by $F(p) = \int_{-\infty}^{\infty} \exp(+iph)\, f(h)dh$, then we also obtain the following results for the expectation and variance of e^{iph} (Ref. 27):

$$\langle e^{iph} \rangle = F(p), \quad (17)$$

$$\sigma^2(e^{iph}) = 1 - F(p)F^*(p). \quad (18)$$

If we also assume that the random variables h_r represented by different scattering points are independent, then we can calculate the expected value and variance of our amplitude defined by Eq. (15). Thus, we obtain the following expression for the expected value of the electric field at a point in the image plane

$$\langle \mathbf{E}_1(x) \rangle = A - NB + BNF(p). \quad (19)$$

Also, the variance in this electric field, defined by $\sigma^2[\mathbf{E}_1(x)] = \langle (\mathbf{E}_1 - \langle \mathbf{E}_1 \rangle)(\mathbf{E}_1 - \langle \mathbf{E}_1 \rangle)^* \rangle$, is readily computed by substitution of Eq (15) into this form and simplification using Eqs. (17)-(19). The resulting expression for the variance in the electrical field is

$$\sigma^2[\mathbf{E}_1(x)] = N(1 - FF^*)BB^*, \quad (20)$$

where $BB^* = (Mw_c)^2$ and the characteristic function F is given by Eq. (17).

Wavelength Spacing for Speckle Decorrelation

We note that our expected value is some complex number, while the variance is a real number since it is defined by $\sigma^2 = \langle |\mathbf{E}_1 - \langle \mathbf{E}_1 \rangle|^2 \rangle$. Thus, Eq. (20) gives us the square of the radius of a circle centered around the expected value within which roughly half of our values of $\mathbf{E}_1$ lie. The intensity at some fixed point x can thus be considered to have changed significantly when the magnitude of the change in $\mathbf{E}_1(x)$ with wavelength is of the order of the standard deviation. Thus, we *adopt the criterion* that the speckle is decoupled when the wavelength change causes the average of the magnitude squared change in $\mathbf{E}_1(x)$ to be equal to the variance for a particular wavelength λ_0, i.e., *decorrelation occurs whenever*

$$\langle \Delta\mathbf{E}_1(x) \Delta\mathbf{E}_1(x)^* \rangle \geq \sigma^2[\mathbf{E}_1(x)]. \quad (21)$$

The change in the electric field $\mathbf{E}_1(x)$ with wavelength interval $\Delta\lambda$ is given by

$$\Delta\mathbf{E}_1(x) = [\partial\mathbf{E}_1(x)/\partial\lambda]\Delta\lambda.$$

Thus differentiating Eq. (15) with respect to λ and noting that $dp/d\lambda = (+2\pi n_3/\lambda^2{}_0)$, we obtain

$$\Delta\mathbf{E}_1(x) = \left(-\Delta BN + B \sum_{r=1}^{N} ih_r e^{iph_r} \frac{2\pi n_3}{\lambda_0^2} + \Delta B \sum_{r=1}^{N} e^{iph_r}\right)\Delta\lambda, \quad (22)$$

where

$$\Delta B = i\pi n_0 x^2 M w_c/(\lambda_0{}^2 M^2 s') \exp[i\pi n_0 x^2/(\lambda_0 M^2 s')].$$

We now consider the speckle near the axis, i.e., when ΔB is negligible (worst case). In this case Eq. (22) reduces to

$$\Delta\mathbf{E}_1(x) = \simeq B \sum_{r=1}^{N} ih_r \frac{2\pi n_3}{\lambda_0^2} e^{iph_r}\Delta\lambda. \quad (23)$$

If we now compute $\langle \mathbf{E}_1(x)\Delta\mathbf{E}_1(x)^* \rangle$, we obtain the following result, assuming that the expected value of h_r is zero and that the standard deviation is h_0,

$$\langle \Delta\mathbf{E}_1(x)\Delta\mathbf{E}_1(x)^* \rangle = (2\pi n_3 \Delta\lambda/\lambda_0{}^2)^2 \{h_0{}^2 N + (N^2 - N)[(d/dp)F(p)][(d/dp)F(p)]^*\} BB^*. \quad (24)$$

Substituting Eqs. (20) and (24) into the criterion, Eq. (21), we obtain a value for the wavelength spacing $\lambda_2 - \lambda_1$ required to decorrelate the speckle:

$$\lambda_2 - \lambda_1 = \frac{\lambda_0{}^2}{2\pi n_3} \left\{\frac{1 - F(p)F^*(p)}{h_0{}^2 + (N-1)[(d/dp)F(p)][(d/dp)F(p)]^*}\right\}^{1/2} \text{[decoupled case]}. \quad (25)$$

The speckle pattern will therefore be laserlike when the spectral line width of a single tone is much less than is given by Eq. (25), i.e., when the line width $\Delta\lambda$ is given by

$$\Delta\lambda \leq \frac{1}{10}(\lambda_2 - \lambda_1)$$

$$\leq \frac{\lambda_0^2}{20\pi n_3}\left\{\frac{1 - F(p)F^*(p)}{h_0^2 + (N-1)[(d/dp)F(p)][(d/dp)F(p)]^*}\right\}^{1/2}$$

[*laserlike case*]. (26)

To illustrate the above results with an example, assume that the heights of the scatterers are distributed normally, where our expected value and standard deviation for the heights have already been taken to be zero and h_0, respectively. Thus, we write the density function for h_r as

$$f(h_r) = \exp[-h_r^2/(2h_0^2)]/h_0(2\pi)^{1/2} \quad (27a)$$

and the corresponding characteristic function as

$$F(p) = \exp(-\tfrac{1}{2}p^2h_0^2). \quad (27b)$$

Substituting Eq. (27) into Eq. (25) we obtain the wavelength spacing required to decorrelate the speckle pattern as

$$\lambda_2 - \lambda_1 = \frac{\lambda_0^2}{2\pi n_3 h_0}\left[\frac{1 - e^{-p^2h_0^2}}{1 + (N-1)(h_0p)^2e^{-p^2h_0^2}}\right]^{1/2}. \quad (28)$$

We note that for the case of a very rough diffuser, where (ph_0) is greater than 1, Eq. (28) can be approximated by

$$\lambda_2 - \lambda_1 = \lambda_0^2/(2\pi n_3 h_0), \quad \text{when } (ph_0)^2 \gg 1. \quad (29)$$

In the case of a relatively smooth diffuser, Eq. (28) can be reduced to

$$\lambda_2 - \lambda_1 = \frac{\lambda_0}{[1 + (N-1)(ph_0)^2]^{1/2}}, \text{when } (ph_0)^2 \ll 1. \quad (30)$$

Now assuming monochromatic illumination, we study the condition under which we can expect a particular diffuser to give a large amount of speckle. If we take the ratio of the standard deviation to the amplitude of the expected value, i.e., by Eqs. (19) and (20), we obtain the average fractional change in amplitude among different resolution cells of width $2\Delta w$. When this ratio is very small, we have the case when most cells have the same intensity; and there is practically no speckle. In the case where this ratio approaches 1, we have a badly speckled case. Thus, for the normal distribution, as defined by Eq. (27), this ratio is given by

$$R = \frac{(N)^{1/2}(1 - e^{-p^2h_0^2})^{1/2}|B|}{|A - NB + NBe^{-p^2h_0^2/2}|}. \quad (31)$$

By Eq. (31), we note that R goes to zero, i.e., no speckle, when the roughness as characterized by ph_0 decreases. Alternatively, taking A to be of the same order of magnitude as NB, we note that the ratio R is proportional to $1/(N)^{1/2}$. Thus, the badly speckled case occurs with small numbers of scatterers per resolution element. And as N gets very large, say exceeding 100, the amount of speckle is drastically reduced.

If we assume operation at a single wavelength, it is still possible to obtain averaging of speckle by superimposing image intensities formed when the diffuser is illuminated *successively* by plane waves at different angles of incidence. We can calculate the angular difference $\Delta\theta_0$ between successive plane waves incident at angles θ_{01} and θ_{02}, which will decouple these respective image intensities. Since we are considering the sequential recording of intensities, the phase term containing θ_0, which was suppressed in writing Eq. (14), still does not enter: and Eqs. (15) and (16) form a convenient starting point. From $n_3 = (n_1/\cos\theta_1 - n_0/\cos\theta_0)$ and $n_1 \sin\theta_1 = n_0\sin\theta_0$, we compute the angular variation of n_3:

$$dn_3/d\theta_0 = (1/2)(n_0^2/n_1)(\sin 2\theta_0/\cos^3\theta_1) - (n_0\sin\theta_0/\cos^2\theta_0). \quad (32)$$

The variation of p, at fixed wavelength, is found by differentiation of Eq. (16), i.e.,

$$dp/d\theta_0 = (-2\pi/\lambda_0)(dn_3/d\theta_0). \quad (33)$$

Following the same mathematical procedure as we did in deriving Eq. (25) except that now $\Delta\mathbf{E}_1(x) = [\partial\mathbf{E}_1(x)/\partial\theta_0]\Delta\theta_0$, one can readily show that the angular spacing $\Delta\theta_0 = \theta_{02} - \theta_{01}$ is given by

$$\Delta\theta_0 = \left(\lambda_0\left\{\frac{1 - F(p)F^*(p)}{h_0^2 + (N-1)[(d/dp)F(p)][(d/dp)F(p)]^*}\right\}^{1/2}\right)\Big/ \{\pi n_0[2\sin\theta_0/\cos^2\theta_0 - n_0\sin 2\theta_0/(n_1\cos^3\theta_1)]\}. \quad (34)$$

For the case when the heights are distributed normally, by substitution of Eq. (27) into (34), we find the angular separation required to decouple the speckle patterns reduces to

$$\Delta\theta_0 = (\lambda_0\{(1 - e^{-p^2h_0^2})/[1 + (N-1)(h_0p)^2e^{-p^2h_0^2}]\}^{1/2})/\left[\pi n_0 h_0\left(\frac{2\sin\theta_0}{\cos^2\theta_0} - \frac{n_0\sin 2\theta_0}{n_1\cos^3\theta_1}\right)\right]. \quad (35)$$

We will use Eq. (35) in the following section to establish a numerical value for the degree of collimation required to assure that our speckle averaging is due to wavelength variation and not to multiangular illuminating beams.

Experiments with Laser Sources

Three different experiments were conducted using a laser. In the first, a single mode argon laser was used to illuminate a ground glass diffuser and the speckle positions were charted as the wavelength was set to the various principal lines (4579 Å, 4727 Å, 4765 Å, 4880 Å, 4965 Å, 5017 Å, and 5145 Å). In this experiment, the statistical problem is different in the details from the analysis presented herein

(e.g., see Goodman's treatment[2]) in that the number of scatterers that contribute at each point in the output plane is essentially that of the *entire* illuminated diffuser; and this is usually a very large number. Since, in this experiment, the diffuser is *not* being imaged, one should not be thinking in terms of the number of scatterers per resolution cell, i.e., the N of the previous section. Nevertheless, speckle repositioning is readily seen; the bright spots in the image vary quite noticeably for the wavelength shifts of 100 Å or so.

In this first experiment it is also interesting to vary the size of that portion of the diffuser that is being illuminated. The equation for the speckle size in the nonimaged case indicates a speckle size inversely proportional to the entire object dimension.[16] Thus, one can greatly enlarge the mean speckle size by placing a small aperture at the diffuser. It is an experimental convenience to work with these larger speckles. An effective nonmechanical means for providing this variable aperture is to pass the collimated output of the laser directly through a microscope objective. Then, of course, the spot size of the exit beam converges to a small diameter in the rear focal plane of the objective, and thereafter it rapidly expands. The diffuser is placed in this exit beam; axial translation of the diffuser in this region near and beyond the rear focal plane provides a handy method for varying the effective aperture over a wide range. The diffuser is fixed at a specific position that gives large, easily monitored speckles on a screen at 1–2-m distance; and then the wavelength is varied. Again, no imaging is involved; and the speckle positions are readily charted by directly exposing a piece of sheet film placed at the screen. While speckle repositioning is definitely observed at the different wavelengths, we were not satisfied that we had the amount of control necessary to corroborate the theory, e.g., the wavelength spacing and total interval available were limited.

A more persuasive experimental observation of speckle averaging with multiple tones of monochromatic illumination was obtained in the following second experiment using an argon laser source. The prism line selector, not the single mode etalon, is removed so that oscillation is obtained simultaneously on several of the transitions listed in the preceding paragraph. The speckle averages pretty well for these wavelength spacings; photographing an object illuminated first by a single tone and then by the multitone clearly shows this effect. In this imaging experiment, the aperture of the camera is used to control the amount of subjective speckle that is introduced by the camera lens.

Unfortunately, the spread of wavelengths and the single collimated beam of the argon laser are not adequate for the recording and reconstruction of speckle-free holograms as a simple, single exposure process. Both spatial and spectral separation of the multitone reference beams are probably going to be required.[23]

A third experiment was performed using a single mode helium–neon laser at 6328 Å. This laser is continuously tunable over the Doppler-broadened transition (about 1200 MHz) by a piezoelectric control of the cavity length. Using the 3-M Company's Magic Transparent Tape as a standard diffuser, since it is both readily available and reproducible, we carefully measured bright spot positons in speckle patterns as the wavelength was scanned over 1200 MHz. By this experiment, we concluded that the motion is below the threshold of detection for such small shifts in frequency. This null result is in agreement with the prediction of our theory, e.g., Eq. (26). Care was taken to control the angular drift of the laser beam in all of these experiments [see θ_0 in Eq. (12)]. This is particularly important for the argon laser since the wavelength selection consists of angularly positioning a prism in the cavity. Both this and the large temperature changes during warmup cause easily measurable drifts in θ_0. For our experiments, angular control is obtained by passing the laser beam through two high-quality microscope objectives separated by twice their focal length (20 mm) with a 5-μm diam pinhole located at their common focus. The output beam from this unity beam expander–spatial filter device is used as the source. Thus, the angular deviation in θ_0 is maintained at some small portion of 2×10^{-4} rad.

Multicolor Speckle Experiments

A series of experiments was also performed using both the Scotch Magic Tape diffuser and a biological specimen as objects with band-limited light being used to simulate a continuously tunable laser (see Fig. 3). A carbon arc or high-pressure mercury arc

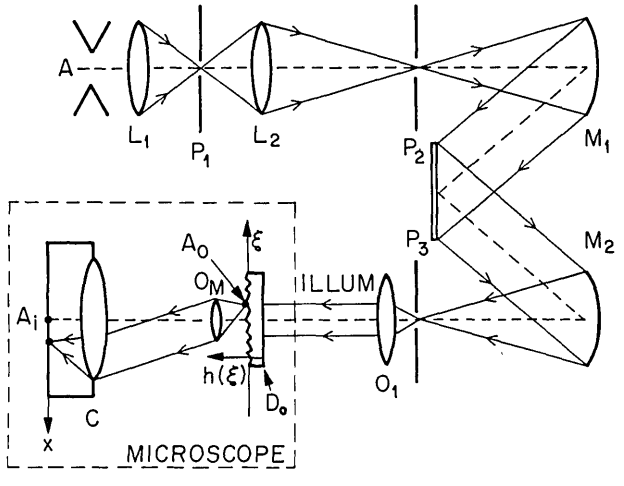

Fig. 3. The experimental arrangement for obtaining laserlike speckle from a band-limited, carbon arc source. The diffuse object D_0, is magnified by the microscope O_M and speckled images are photographed by the camera C. Illumination from the arc (A) is band limited by the Spex monochromater (mirrors M_1, M_2 are 10-cm diam and 75-cm focal length); pinholes P_1 and P_2 are 400 μm, P_3 is 60 μm, and the microscope objective O_1 is used to collimate the illumination at D_0.

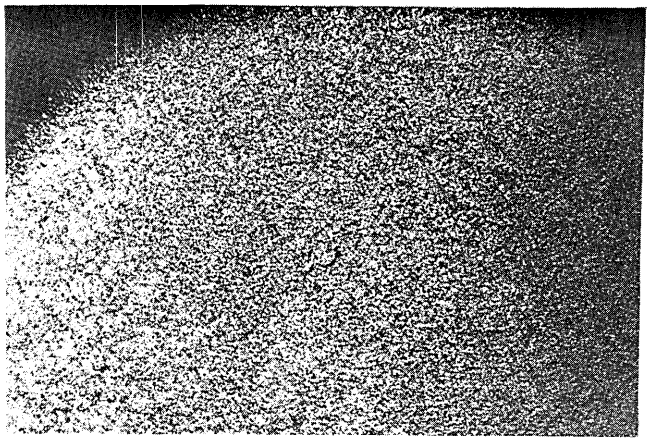

Fig. 4. Speckle pattern with collimated laser illumination at 6328 Å incident on diffuser made from Scotch Magic Tape. Imaging is as shown in Fig. 3.

source (A) is collimated, dispersed by the grating (G) for band limiting by pinholes P_2, P_3; then it is highly collimated by the pinhole–objective lens combination (P_3, O_1 in Fig. 3). The objects are placed at D for magnification by the microscope, O_M, and photographically recorded by the camera (C).

Since the principal objective of this experiment is a detailed study of the averaging of speckle from a multitone source, first we must establish values for the allowable width of the single tone; then, we will take a series of exposures with wavelength differences exceeding the interval given by Eq. (28). The quantitative treatment of the degree of smoothing that results from a number of independent tones is beyond the scope of this paper.[21]

For experimental purposes in the classification of diffusers, it is convenient to recognize that $[\Delta w_0/\langle w_r\rangle]^2$ sets an upper limit to the number of samples per resolution cell and that h_0 and $\langle w_r\rangle$, are coupled, i.e., by coupled, we mean that in making a finer diffuser, $\langle w_r\rangle$ becomes less, but the attainable h_0 usually decreases too. Hence, we rewrite Eq. (28) as follows:

$$\frac{\Delta\lambda}{\lambda} = \frac{\lambda}{2\pi n_3 h_0}\left(\{1-\exp[-(2\pi n_3 h_0/\lambda)^2]\}/\{1+[(\Delta w_0/\langle w_r\rangle)-1]\,[h_0(2\pi n_3/\lambda)]^2\exp[-(2\pi n_3 h_0/\lambda)^2]\}\right), \quad (36)$$

where $\Delta w_0 = 2\lambda F/(\pi D)$.

The Scotch Magic Tape diffuser is relatively rough; separate measurements using a depth microscope fix the depth $h_0 \gtrsim 8\ \mu$m, although it could be as high as 14 μm and the width $\langle w_r\rangle \approx 1\ \mu$m. For $n_3 = 0.6$ and $\lambda_0 = 0.5\ \mu$m, we find $ph_0 = 50$, hence by Eq. (29) we predict that

$$\lambda_2 - \lambda_1 = 80\,\text{Å} \quad (37)$$

decouples, and the speckle should remain laser-like for line widths up to about one tenth of this, i.e., for 8 Å. We note that N does not enter into this computation, since $ph_0 \gg 1$.

For the spectrometer used, the output line width from P_3 in Fig. 3 is just slightly under 5 Å for the input pinhole (P_2) of 400 μm and the exit pinhole (P_3) of 60 μm. In the customary language of partial coherence,[29] an equivalent viewpoint on the need to restrict $\Delta\lambda$, as by Eq. (26), is that we must restrict the temporal coherence so that axial path differences inherent in traversing the diffuser will not smooth out the laserlike speckle. Thus, we have $n_3 h_0 \ll c/\Delta\nu$; hence, we see that $n_3 h_0\,\Delta\lambda/\lambda^2 \ll 1$, which is precisely the expression used to compute the 8-Å limit in the preceding paragraph.

P_2 essentially controls $\Delta\lambda$ in the apparatus; and in a relatively independent manner, the much smaller P_3 controls the transverse coherence. This is the reason for the disparity in our choices of their sizes. This, too, can be understood directly from Eq. (13). A larger pinhole P_3 permits a continuous range of angle θ_0 from zero up to some maximum θ_{02} in the illumination of the sample.

From Eq. (35) and the discussion of the previous section, we obtain the maximum angular bandwidth allowable for laserlike speckle to be

$$\Delta\theta = \frac{1}{10}\left\{\frac{\lambda\cos^2\theta_0}{\pi h_0[n_0-(n_0^2/n_1)]}\right\}^{1/2},$$

in the case of rough diffuser, i.e., $ph_0 \gg 1$, where θ_0 is the mean incident angle. For the Scotch Magic Tape diffuser, this value is 0.02 rad. A simple geometrical consideration gives the illumination on the diffuser (D) in Fig. 3 to have an angular bandwidth of 1.9×10^{-3} rad, and so we are well within the limit to see speckle. (Parenthetically, we note that when the diffuser is very rough, the occurrence of speckle is reasonably estimated using a simple temporal coherence requirement and the usual transverse coherence requirement, which results from the van Cittert-Zernike theorem. However, in the intermediate

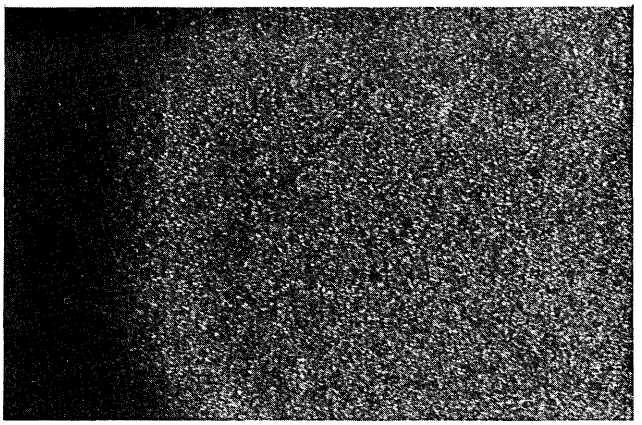

Fig. 5. Speckle pattern for Scotch Magic tape diffuser, as in Fig. 4, but illuminated with band-limited light from a carbon arc (5 Å band limited at 6000 Å and 70 min of exposure using Tri-X film). Beam collimation angle is 2×10^{-3} rad.

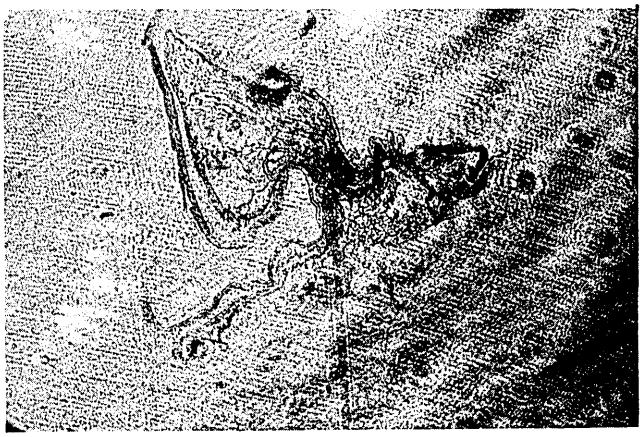

Fig. 6. Section of optic nerve at low magnification illuminated by collimated laser light.

range, $ph_0 \sim 1$, the statistical properties control, and the formulas of the last section should be used.)

Band limiting the source to a 5 Å width and maintaining adequate transverse coherence greatly reduces the illumination level at the camera. A value for the exposure time is estimated in the following discussion. Referring to Fig. 3, and noting that the energy radiated by the source A (carbon arc lamp) is 10^{-2} W sr^{-1} Å^{-1} and that the f numbers of the lenses L_1 and L_2 and mirrors M_1 and M_2 have been matched, we obtain the energy transmitted through the pinhole P_3 to be 3×10^{-6} W in a 5-Å bandwidth. The intensity at the diffuser is approximately 2×10^{-5} W/cm^2. The magnification of the objective and camera system (O_M and C) is 20 and so the intensity of the light hitting the film is 4×10^{-8} W/cm^2. Now the film requires, including the reciprocity loss factor, 50 μJ/cm^2 of energy to be at threshold for recording, and so this gives a minimum exposure time of 20 min.

The speckle pattern using a collimated 6328-Å laser to illuminate the Magic Tape diffuser D in Fig. 3 is shown in Fig. 4. The laserlike speckle pattern using tbe high pressure arc source is shown in Fiq. 5. Even so, some averaging of the speckle pattern is evident with the highly collimated arc source band limited to 5 Å. While a narrower line width would have been desirable, the extremely long exposure times, 70 min for one tone, forced this compromise. With the arc source illumination, the speckle is also easily seen visually through the microscope eyepiece (after 15 min of dark adaptation). A precise motorized scan (Spex monochromator) of the grating G also permits one to observe the speckle variations with wavelength. Visual observation during motorized scanning at 2Å/sec was used in order to establish that the characteristic decorrelation is in the range from 30 Å to 100 Å for the diffusers used. The corroboration with the computed value of 80 Å in Eq. (37) is excellent.

A separate series of exposures to show the averaging effect of multicolor speckle is presented in Figs. 6 through 9. Its an 8-μm thick section from the optic nerve of a crayfish, prepared and stained by Roach.[30] All exposures have the same magnification, and the major characteristic length of the nerve is 1 mm. First, we should compare the appearance of this optic nerve when illuminated in laser light (no diffuser is used in this case, since it would cause speckle) and in white light as is shown in Figs. 6 and 7, respectively. It is to be emphasized that this type of comparison is essential to an understanding of the speckle problem, since the degree of difficulty in seeing things that are illuminated by a laser is highly dependent on their roughness; and of course with biological specimens, a great range of roughness is experienced. For example, from this comparison we conclude that the sample shown is not unusually diffuse, hence its visibility with laser illumination, while low, is by no means representative of a badly speckled case.

Now, a single exposure of 180-min duration for one wavelength of our 5-Å band-limited source is shown in Fig. 8. A multiple exposure with six separate wavelengths each spaced by 300 Å is shown in Fig. 9. Great care is taken to minimize the relative motion as the grating is scanned to each new wavelength. An exposure duration of 50 min is used at each wavelength, the longer total exposure time being a characteristic aspect of the averaging process. A comparison of Figs. 6 and 8 shows the slight smoothing of the laser speckle caused by the finite (5-Å) width of the band-limited carbon arc source. Comparing Figs. 8 and 9 dramatically shows the improved resolution that results from using six tones of the multicolor illumination. In the holographic application, Fig. 6 shows the representative speckle for one-wavelength recording, and Fig. 9 is approximately the improvement that one would expect using six tones spanning 1500 Å.

Conclusions

A theoretical study of the wavelength dependence of speckle that has been so troublesome in holo-

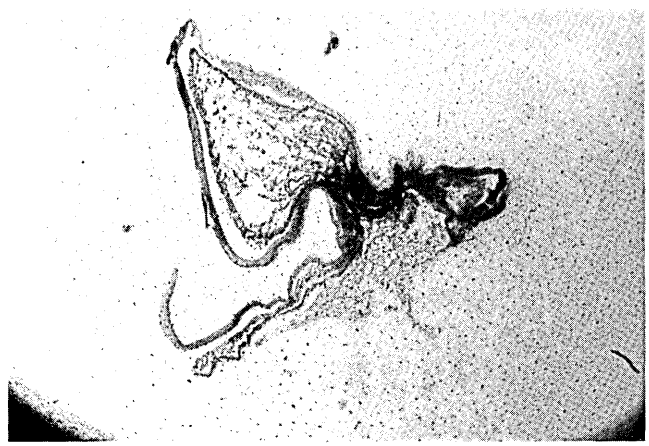

Fig. 7. Optic nerve illuminated in white light. Resolution here is much better than in the speckled image of Fig. 6. The maximum length of this specimen is approximately 1 mm (actual length).

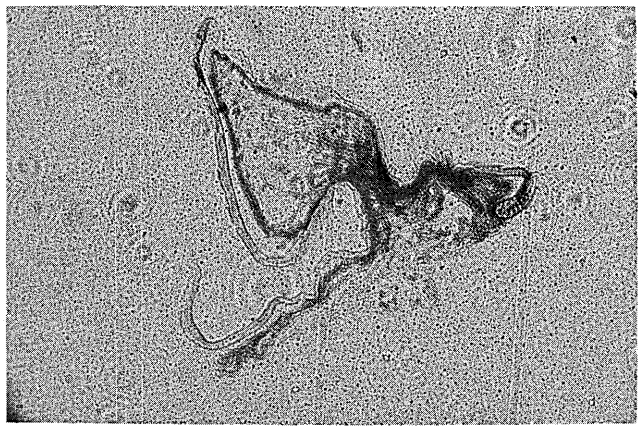

Fig. 8. Optic nerve illuminated by a collimated source at 5500 Å with 5-Å line width (180-min exposure using a high pressure mercury arc and Tri-X film). Note that the image is speckled to a slightly lesser degree than with laser illumination.

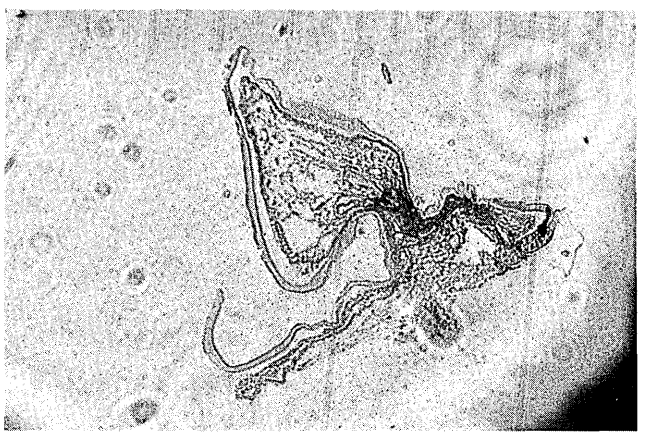

Fig. 9. Optic nerve illuminated by six separate band-limited wavelengths, spanning the spectrum from 4300 Å to 5800 Å. Note that the resolution is considerably improved over that for a single tone as shown in Fig. 8. The beam collimation angle of 2×10^{-3} rad is maintained throughout the series.

graphic microscopy is used to establish general criteria for the wavelength interval required in order to decouple speckle in an imaging system. A simple statistical argument is presented in analysis of Eq. (12) for the imaging of a diffuser with variable roughness; expressions for $\Delta\lambda$ to decouple with speckle or to keep it laserlike are given by Eq. (25) and (26), respectively. These are specialized for a Gaussian distribution of heights in the diffuser in Eq. (28) and then applied and discussed in an experimental context in Eq. (36).

Experiments are described that verify that decorrelation results as the wavelength is scanned. In approximate terms, for highly collimated illumination, speckle is laserlike for $\Delta\lambda \leq 8$ Å and is greatly smoothed for $\Delta\lambda \geq 80$ Å. Perhaps the most significant implication of this study is that it demonstrates the feasibility of eliminating speckle in holographic microscopy while still requiring only a single rapid exposure from some multimonochromatic-toned source, e.g., a dye laser.

We acknowledge that J. H. Wayland's and R. J. Bing's interest in making holograms of microcirculatory blood vessels first stimulated our interest in speckle-free holographic microscopy; also we are pleased to acknowledge helpful discussions with D. MacQuigg and R. B. MacAnally as well as the enthusiastic participation of Francois Bertiere in the first series of experiments with the laser sources.

This work was supported by the Air Force Office of Scientific Research.

References

1. M. v. Laue, Sitzber. Preuss. Akad. 1144, (1914), trans. by H. K. V. Lotsch.
2. J. W. Goodman, Stanford University Electronics Labs. Tech. Rept. SEL-63-140 (TR 2303-1) (Dec. 1963).
3. L. I. Goldfischer, J. Opt. Soc. Am. **55,** 247 (1965).
4. L. H. Enloe, Bell Syst. Tech. J. **46,** 1479 (1967).
5. W. Martienssen and S. Spiller, Phys. Lett. **24A,** 126 (1967).
6. E. N. Leith and J. Upatnieks, Appl. Opt. **7,** 2085 (1968).
7. H. J. Gerritsen, W. J. Hannan, and E. G. Ramberg, Appl. Opt. **7,** 2301 (1968).
8. R. F. van Ligten, Opt. Technol. **1,** 71 (1969).
9. R. F. van Ligten, J. Opt. Soc. Am. **59,** 1545 (1969).
10. M. E. Cox, R. G. Buckles, and D. Whitlow, J. Opt. Soc. Am. **59,** 1545 (1969).
11. E. Archbold, J. M. Burch, A. E. Ennos, and P. A. Taylor, Nature **222,** 263 (1969).
12. M. Young, B. Faulkner, and J. Cole, J. Opt. Soc. Am. **60,** 137 (1970).
13. J. C. Dainty, Opt. Acta **17,** 761 (1970).
14. D. Gabor, IBM J. Res. Develop. **14,** 509 (1970).
15. S. Lowenthal and D. Joyeux, J. Opt. Soc. Am. **61,** 847 (1971).
16. H. H. Hopkins and H. Tiziani, Applications of Holography (Besancon Conference 6–11 July 1970), viii.
17. D. H. Close, J. Quantum Electron. **QE-7,** 312 (1971).
18. J. M. Burch, SPIE Devel. Hologr. **25,** 149 (1971).
19. M. Elbaum, M. Greenebaum, and M. King, Opt. Commun. **5,** 171 (1972).
20. N. George and A. Jain, Opt. Commun. **6,** 253 (1972).
21. N. George and A. Jain, Calif. Inst. of Technol. Sci. Rept. 14, AFOSR-TR-72-1308 (1972).

22. J. Upatnieks and R. W. Lewis, J. Opt. Soc. Am. **62,** 1351A (1972).
23. Hologram volume effects and color holography are fully discussed in the following textbook and will not be treated further herein: R. J. Collier, C. B. Burckhardt, and L. H. Lin, *Optical Holography* (Academic Press, New York, (1971), Chaps. 9 and 17.
24. J. W. Goodman, *Introduction to Fourier Optics* (McGraw-Hill, New York, 1968), Chap. 5.
25. N. George and J. T. McCrickerd, Photogr. Sci. Eng. **13,** 342 (1969).
26. As we have employed it here, the Gaussian transmission function in Eq. (2) is chosen for theoretical convenience, although for electronic optics it is physically appropriate as well. In the results it will not make any qualitative difference; in fact, in deriving the form in Eq. (15) we further approximate the actual case using a simple rect function as the impulse response of the lens.
27. In this simplification, the assumption is that the phase terms in the integrand of Eq. (3) involving the variables x', y' do not vary appreciably within the interval w_r. For a consideration of the extent of this type of phase variation, the reader is referred to D. A. Tichenor and J. W. Goodman, J. Opt. Soc. Am. **62,** 293 (1972).
28. A. Papoulis, *Probability, Random Variables, and Stochastic Processes* (McGraw-Hill, New York, 1965), Chap. 8.
29. M. Born and E. Wolf, *Principles of Optics* (Pergamon Press, Oxford, 1970), Chap. 10.
30. The 8-μm section of the optic nerve is prepared by perfusing the eyestalk in 1% $K_4Fe(CN)_6$ in crayfish saline; it is removed from the crayfish, soaked in saline saturated with picric acid, dehydrated in alcohol, embedded in paraffin, sectioned with a rotary microtome, stained in a Ponceau acid fushin solution, and mounted with Permount on glass.

APPENDIX B

Speckle in Microscopy

In this appendix we give details of an experiment with an argon laser discussed in section 2.4, to demonstrate the averaging of speckle in the magnified image of a pap smear when four tones of the laser are used (5145, 4965, 4880 and 4765Å) as compared to when only the 5145Å line is used.

Volume 6, number 3 OPTICS COMMUNICATIONS November 1972

SPECKLE IN MICROSCOPY†

Nicholas GEORGE and Atul JAIN
California Institute of Technology, Pasadena, California 91109, USA

Received 19 July 1972
Revised manuscript received 1 August 1972

We present some theoretical and experimental results for the averaging of speckle as a function of bandlimited and multi-tone illumination. In imaging various microscope specimens, we find that photographs taken with either 6 narrow lines spread over 1500 Å or white light have comparable resolution.

It has been found that holographic microscopy is severely limited in attainable resolution by speckle noise in the reconstruction. This granular appearance of an image is due to the interference from phase variations of the light caused by the randomly distributed heights of an object which occur within a resolution cell [1–6].

In this communication we outline a theory for the wavelength sensitivity of speckle; and we present data showing speckle averaging as a function of wavelength for typical microscope specimens. These results are directly applicable to multi-tone holographic recording, however our experiments have been limited to the use of various multi-toned sources as simple illuminators and do not include holographic recordings.

Consider the microscope imaging system shown in the enclosed border in fig. 1. A typical point A_0 of the object D, a diffuser, is shown imaged as A_i. For the one-dimensional case of a pure phase object we take the random thickness variations to be $h(\xi)$‡. The index difference between D and the surroundings is denoted by n_3. Assuming monochromatic illumination of wavelength λ_0, normally incident and collimated, we can write the tangential electric field, exiting D, as

$$f(\xi) = \exp\,[(2\pi i/\lambda_0)n_3 h(\xi)]\,, \tag{1}$$

where $\exp(-i\omega t)$ is suppressed.

Useful diffuser models in characterizing speckle are described by [1–8] and others. Both in laser speckle metrology [8] and in microscopy of typical biological specimens, the direct radiation is important in establishing the speckle contrast. Thus, we assume a functional idealization for h given by

$$h(\xi) = \sum_r h_r \mathrm{rect}\left(\frac{\xi-\xi_r}{w_r}\right),$$

consisting of random variables h_r and w_r. In this model the number of scattering centers per resolution cell can be small. By definition the function $\mathrm{rect}(x) = 1$ when $|x| < 1/2$ and is zero otherwise. For the diffuse surfaces of interest in microscopy, the scattering angles are quite large; hence w_r is on the order of a wavelength or smaller. While the following physical picture is hardly defensible rigorously as a model for our choice of h, it may be helpful in visualizing this diffuser to think in terms of a polished glass slide with randomly positioned steps of height h_r and width w_r centered at $\xi = \xi_r$. Similarly, if one prefers the randomly positioned lenslets of Hopkins and Tiziani [2], then h_r becomes a constant plus the quadratic phase trans-

† Research supported in part by the Air Force Office of Scientific Research.

‡ Comparison between pure phase and other diffuser models is made in ref. [7].

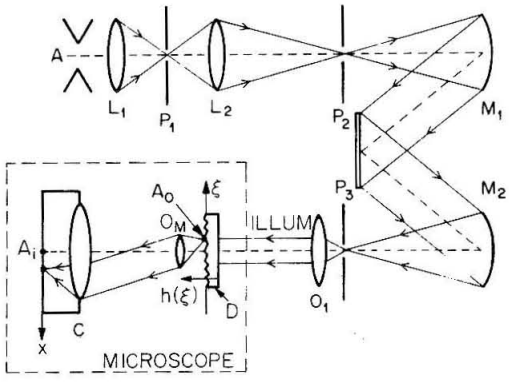

Fig. 1. The experimental arrangement for studying speckle in band-limited light or with the argon laser. The inset, labeled microscope, shows the diffuse object D, the microscope objective O_M and the image recording by the camera C. Band-limited and highly collimated illumination is obtained by passing light from the arc A through the Spex monochromator (mirrors M_1, M_2 are 10 cm diameter and 75 cm focal length and pinholes P_1 and P_2 are 400 μm), the pinhole P_3 of 60 μm, and the collimating 20 mm objective O_1.

mission function for each lens. Thus, substitution of the function choice for $h(\xi)$ in (1), assuming non-overlapping rect functions and rearranging give equivalently:

$$f(\xi) = 1 + \sum_r \operatorname{rect}\left(\frac{\xi-\xi_r}{w_r}\right)\{\exp[(2\pi i/\lambda_0)n_3 h_r] - 1\}. \tag{2}$$

We note that $|f(\xi)| \equiv 1$; and that the integer, minus one, in brackets in the summation properly reduces the direct transmission to account for the energy scattered by the term $\exp[(2\pi i/\lambda_0)n_3 h_r]$.

With the conventional Fresnel-zone approximations of Sommerfeld's formula, one can show that the radiation arriving at A_i comes from a very limited region, i.e., the resolution cell of radius ρ_0, surrounding A_0 [9]. In this integration, we neglect the slight phase taper over ρ_0 as detailed in [9]; and for simplicity, we assume a unity amplitude weighting factor over ρ_0. The radius ρ_0 is approximately given by the Airy disc size, i.e., $1.22\,\lambda_0 f/D$ in which f and D are the focal length and diameter respectively of the objective O_M. Thus, for the imaged diffuser, the tangential electric field at A_i, $E(x_i)$, is approximately given by the following summation over ρ_0:

$$E(x_i) = R - BN + B\sum_{m=1}^{N} \exp(ip h_m), \tag{3}$$

where $p = 2\pi n_3/\lambda_0$. In (3), the summation $m = 1,2,\ldots,N$ extends only over the N scatterers within a radius ρ_0 about A_0. The explicit forms for the parameters R and B follow from the aforementioned integration of (2); however they are not of interest in the statistical argument. It is of interest to consider objects of varying roughness; and we note that for a smooth object $E = R$. Also, the speckle which occurs for diffuse objects is inherent in the terms containing B; and the ratio BN/R is equivalent to the fractional surface occupied by the scatterers in a resolution cell.

For the case of monochromatic illumination, the details of the speckle pattern in an image can be deduced from a statistical consideration of (3) with p fixed. However, what is of central interest to us here is the wavelength sensitivity of E. The following simple argument leads directly to an expression for the wavelength spacing which is required to decouple the speckle patterns for a rough diffuser. The wavelength sensitivity is due mainly to the exponential terms containing p in (3); and as a worst case applicable on-axis, we neglect the wavelength variations of R and B. At a fixed point A_i, we require that the root-mean-square phase difference between an arbitrary pair of scatterers change by $\pi/2$, i.e.,

$$2\pi n_3\left(\frac{1}{\lambda_2} - \frac{1}{\lambda_1}\right) \langle (h_r - h_m)^2\rangle^{1/2} = \tfrac{1}{2}\pi. \tag{4}$$

Simplifying (4), we find that the wavelength spacing $\Delta\lambda = \lambda_2 - \lambda_1$ required to decouple the speckle is given by††:

$$\Delta\lambda = \lambda_0^2/4\sqrt{2}\, n_3 h_0, \tag{5}$$

where h_0 is the standard deviation of the heights of the scatterers.

†† A more careful analysis for $\Delta\lambda$, based on an intensity criterion, is made in ref. [10]. The result which reduces approximately to (5) for a rough diffuser is given by

$$\Delta\lambda = \frac{\lambda_0^2}{2\pi n_3}\left[\frac{1 - F(p)\,F^*(p)}{h_0^2 + (N-1)\{dF(p)/dp\}\{dF(p)/dp\}^*}\right]^{1/2},$$

in which $F(p)$ is the characteristic function (Fourier transform) of the probability density function $f(h_r)$ for the random heights h_r.

Volume 6, number 3 OPTICS COMMUNICATIONS November 1972

The criterion (4) is meaningful only for large h_0, hence (5) is applicable only for a rough diffuser. The limiting case as h_0 goes to zero is readily explained separately. In this case, the speckle is weak since by (3) $E \approx R$ and only a partial decoupling of the low contrast speckle will reduce its deleterious effect.

In our experiments we compare the speckle patterns under monochromatic, bandlimited, and multi-toned illumination. In the first series, we use the Minnesota Mining and Manufacturing Company's Magic Transparent Tape No. 810, for which we measure an $h_0 \approx 8\ \mu$m and $\langle w_r \rangle \approx 1\ \mu$m. With $n_3 = 0.5$ and $\lambda = 5000$ Å, (5) gives us $\Delta\lambda = 110$ Å as the wavelength spacing required for decoupling. Fig. 2 shows the speckle characteristics in the image of this diffuser, placed at D in fig. 1, under illumination from a He–Ne laser or alternately a band-limited arc source. Note, as expected, the similarity of the speckle under laser illumination and the 5 Å light. A low numerical aperture for O_M is used to assure $\rho_0 > \langle w_r \rangle$ and so one is not able to resolve the 1 μm scatterers under white light. Fig. 2 (4) demonstrates a considerable speckle reduction when 6 tones of 5 Å width and spanning 1500 Å are used for the illumination.

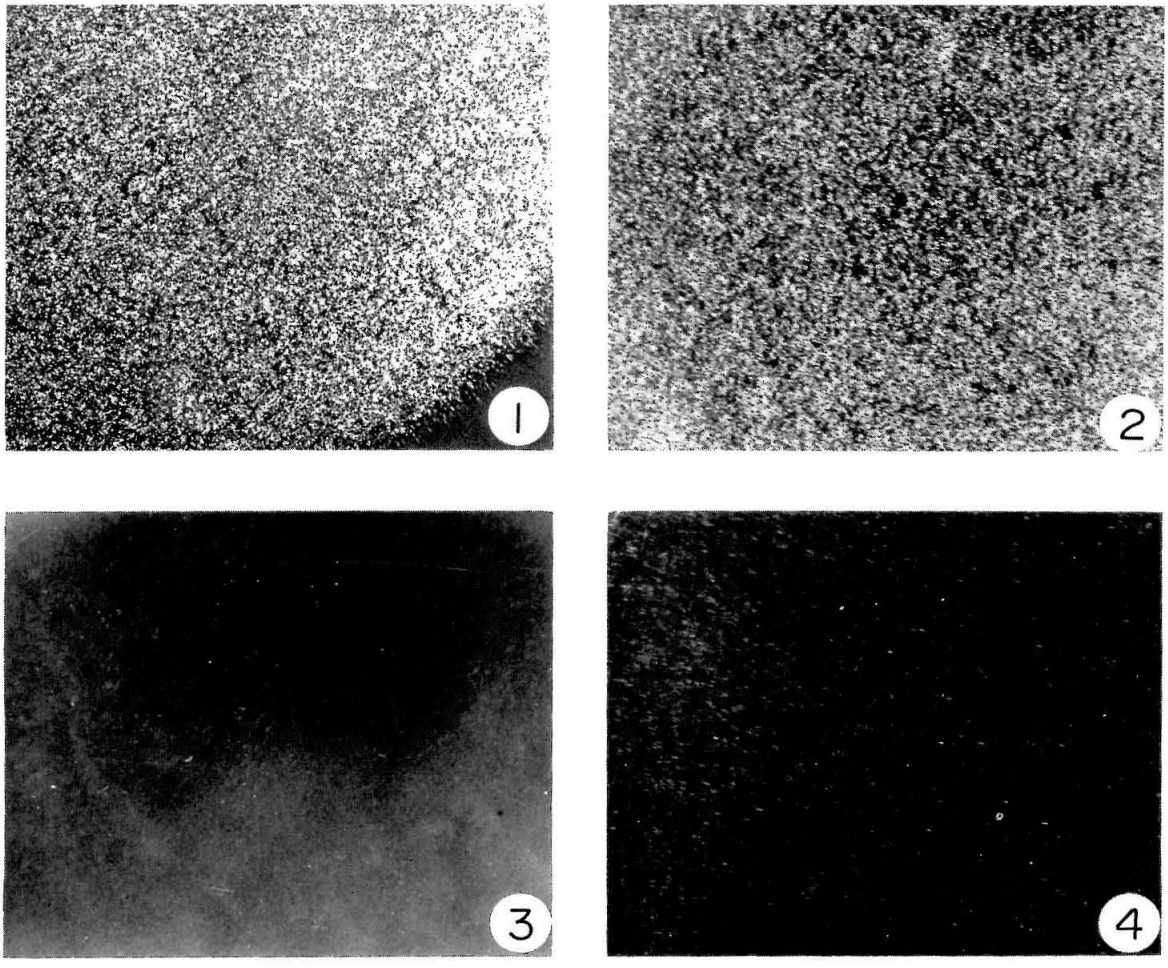

Fig. 2. Image of Scotch-Magic-Tape diffuser for the following illumination: (1) laser source at 6328 Å, (2) light from an arc source band-limited to 5 Å as shown in fig. 1, (3) white light, and (4) six tones of band-limited (5 Å) light spanning 1500 Å.

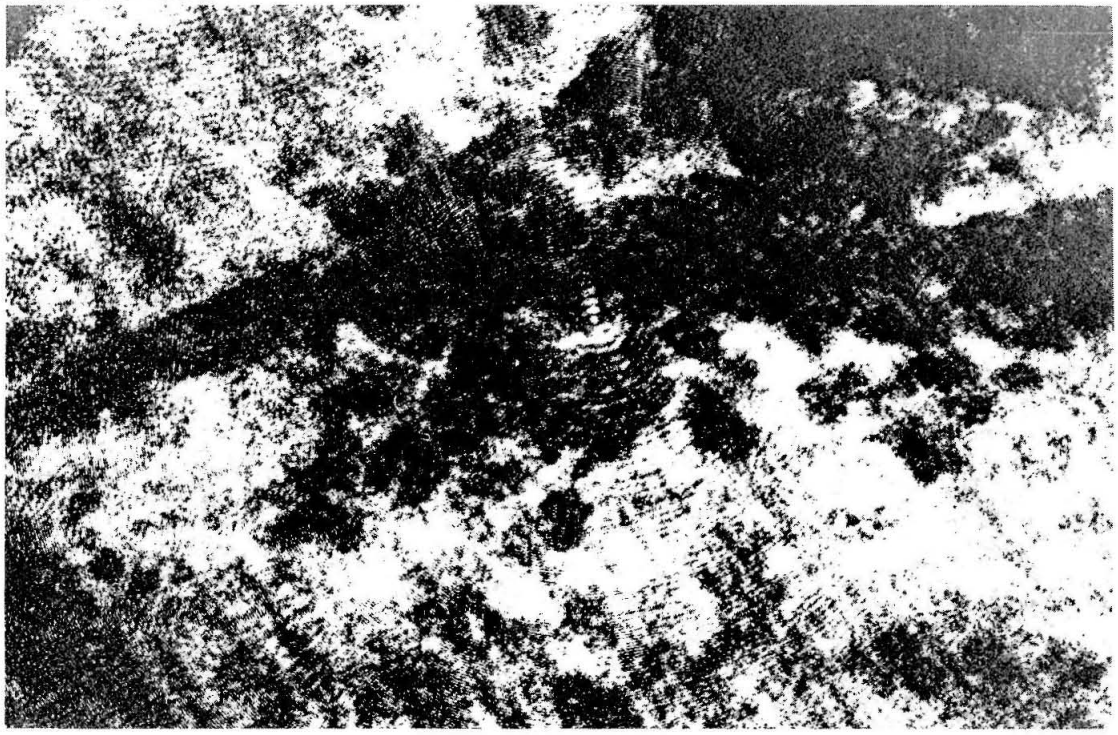

Fig. 3a. Speckled image of a positive PAP-smear under illumination by the 5145 Å line from an argon laser.

Fig 3b →

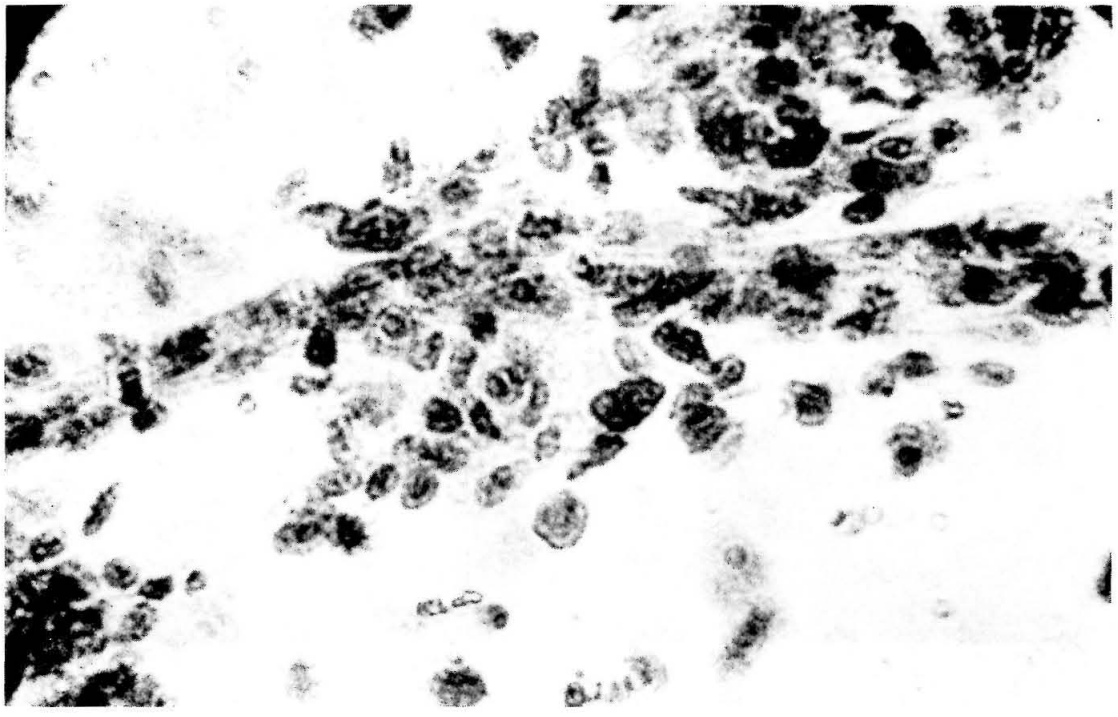

Fig. 3b. Image of the positive PAP-smear illuminated by 4 tones of an argon laser (5145, 4965, 4880, and 4765 Å). Note the improvement of resolution from the case of fig. 3a, although the image is still not as good as under white light.

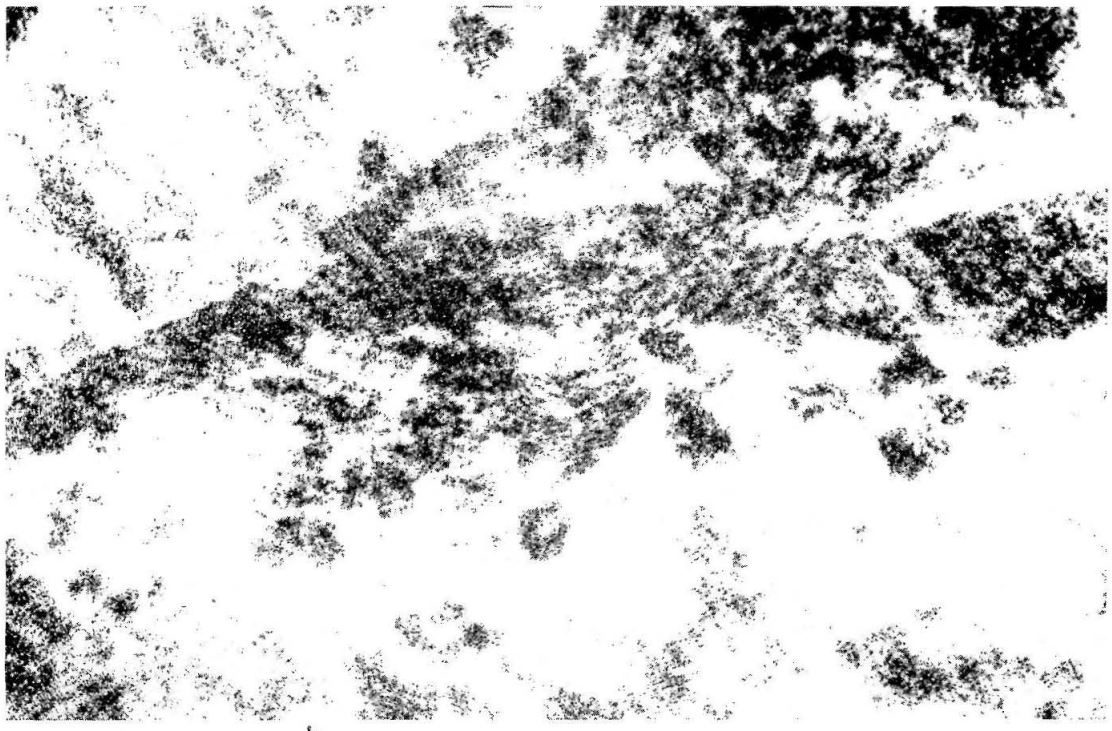

Fig. 3b Image of the positive PAP-smear illuminated by white light.

As one would expect, the roughness and the attendant speckle vary widely in the many biological specimens that have been studied. For example, figs. 3a, b, and c show the highly magnified image of a positive PAP-smear, illuminated without relative motion by a single color of the argon laser (5145 Å), 4 tones from an argon laser (5145, 4965, 4880, and 4765 Å), and with white light, respectively. The size of the centrally located white cell is roughly 14 μm. So that none of the averaging could be attributed to variations in the illumination angle as the argon laser is tuned to its various lines, first the laser beam is passed through a spatial filter (10 mm objective and 5 μm pinhole) and then recollimated. This assures a pointing accuracy of about 10^{-4} radians. While for one color the image is badly speckled, we see that four monochromatic tones averaged on an intensity basis by multiple exposures lead to a good improvement. With the argon laser, one is still too limited in the available wavelength spread. This is evident on comparing to the white light resolution shown in fig. 3c. Similar experiments with 6 to 12 band-limited lines of 5 Å width show considerably more improvement than the 4 lines from the argon laser, if the wavelength spanned exceeds 1500 Å.

Perhaps the most significant implication of this study is that it demonstrates the feasibility of reducing speckle in holographic microscopy while still requiring only a single rapid exposure from some multitoned source such as a dye laser.

References

[1] J.W. Goodman, Stanford University Electronics Labs Tech. Rept. SEL-63-140 (TR2302-1) (1963).
[2] H.H. Hopkins and H. Tiziani, Applications of holography, Besançon Conference (1970), viii.
[3] M. Elbaum, M. King and M. Greenbaum, J. Opt. Soc. Am. 62 (1972) 732A.
[4] S. Lowenthal and H. Arsenault, J. Opt. Soc. Am. 60 (1970) 1478.
[5] L.H. Enloe, Bell Syst. Tech. J. 46 (1967) 1479.
[6] E. Archbold, J.M. Burch, A.E. Ennos and P.A. Taylor, Nature 222 (1969) 263.
[7] S. Lowenthal and D. Joyeux, J. Opt. Soc. Am. 61 (1971) 847.
[8] J.M. Burch, SPIE Develop. Holography 25 (1971) 149.
[9] D.A. Tichenor and J.W. Goodman, J. Opt. Soc. Am. 62 (1972) 293.

APPENDIX C

Probability Distribution for a Sum of Unit Vibrations

In this Appendix we review the derivation of the probability density of the sum

$$\vec{R} = \sum_{i=1}^{N} \vec{r}_i$$

given the probability densities of $\vec{r}_i$'s . Although this derivation has been reviewed by a number of authors[1]-[6], our treatment follows that of Chandrasekhar[6] whose method was originally outlined by A. A. Markoff[5]. In this Appendix we also apply our results to calculate the density function for the sum

$$R = \sum_{r=1}^{N} e^{jah_r} \qquad \text{(C-1)}$$

and specify these functions for the case $N = 3,4,6$ and $N \to \infty$, where the random variables h_r are uniformly distributed from $-\frac{\pi}{a}$ to $\frac{\pi}{a}$.

We therefore first state the problem in its most general form and apply the results to the case defined in (C-1).

Let

$$\vec{\varphi}_j = (\varphi_j{}^1, \varphi_j{}^2, \ldots, \varphi_j{}^n) \qquad (j = 1, \ldots N) \tag{C-2}$$

be N, n-dimensional vectors, the components of each of these vectors being functions of s coordinates

$$\varphi_j{}^k = \varphi_j^k(q_j{}^1, q_j{}^2, \ldots q_j{}^s) \qquad (k = 1, \ldots, n; \quad j = 1, \ldots, N) \tag{C-3}$$

The probability that the $q_j{}^i$'s occur in the range

$$q_j{}^1,\ q_j{}^1+dq_j{}^1; q_j{}^2, q_j{}^2+dq_j{}^2; \ldots;\ q_j{}^s, q_j{}^s+dq_j{}^s, \quad (j=1, \ldots, N) \tag{C-4}$$

is given by $\tau_j(q_j{}^1, \ldots, q_j{}^s)dq_j{}^1 \ldots dq_j{}^s = \tau_j(\vec{q}_j)d\vec{q}_j$. Further, let

$$(\Phi^1, \Phi^2, \ldots, \Phi^n) = \vec{\Phi} = \sum_{j=1}^{N} \vec{\varphi}_j \tag{C-5}$$

The problem is: what is the probability that

$$\vec{\Phi}_o - \tfrac{1}{2}d\vec{\Phi}_o \le \vec{\Phi} \le \vec{\Phi}_o + \tfrac{1}{2}d\vec{\Phi}_o,^{(7)} \text{where } \vec{\Phi}_o \text{ is some preassigned value for } \vec{\Phi}. \tag{C-6}$$

If we denote the probability by

$$W_N(\vec{\Phi}_o)d\Phi_o{}^1 d\Phi_o{}^2 d\Phi_o{}^3 \ldots d\Phi_o{}^N = W(\vec{\Phi}_o)d\vec{\Phi}_o$$

We clearly have

$$W_N(\vec{\Phi}_o)d\vec{\Phi}_o = \int \ldots \int \prod_{j=1}^{N} \{\tau_j(\vec{q}_j)d\vec{q}_j\} \tag{C-7}$$

where the integration is affected over only those parts of the Ns dimensional configuration space where the inequalities (C-6) are satisfied.

We now introduce a factor $\Delta(\vec{q}_1, \ldots, \vec{q}_N)$ having the following properties:

$$\Delta(\vec{q}_1 \ldots . \vec{q}_N) = 1 \quad \text{whenever } \vec{\Phi}_0 - \tfrac{1}{2}d\vec{\Phi}_0 \leq \vec{\Phi} \leq \vec{\Phi}_0 + \tfrac{1}{2}d\vec{\Phi}_0 \qquad (C\text{-}8)$$

$$= 0 \quad \text{otherwise}$$

Then

$$W_N(\vec{\Phi}_0)d\vec{\Phi}_0 = \int \ldots . \int \Delta(\vec{q}_1, \ldots, \vec{q}_N) \prod_{j=1}^{N} \{\tau_j(\vec{q}_j)d\vec{q}_j\} \qquad (C\text{-}9)$$

where now the integration is extended over all the accessible regions of the configuration space. The introduction of the factor Δ under the integral sign in Eq (C-9)in this manner appears at first sight as a very formal device to extend the range of integration over the entire configuration space. But the essence of Markoff's method is that an explicit expression for this factor can be given.

Consider the integrals

$$\delta_k = \frac{1}{\pi} \int_{-\infty}^{\infty} \frac{\sin\alpha_k\rho_k}{\rho_k} \exp(i\rho_k\gamma_k)d\rho_k \quad (k = 1, \ldots, n) \qquad (C\text{-}10)$$

This integral defining δ_k has the property

$$\delta_k = 1 \quad \text{whenever } -\alpha_k < \gamma_k < \alpha_k \qquad (C\text{-}11)$$

$$= 0 \quad \text{otherwise}$$

Now let

$$\alpha_k = \tfrac{1}{2}d\Phi_o^k \quad , \quad \gamma_k = \sum_{j=1}^{N} \varphi_j^k - \Phi_0^k \quad , \quad (k=1, \ldots, n) \qquad (C\text{-}12)$$

Accordingly,

$$\delta_k = 1 \quad \text{whenever} \quad \Phi_0^k - \tfrac{1}{2}d\Phi_0^k < \sum_{j=1}^{N} \Phi_j^k < \Phi_0^k + \tfrac{1}{2}d\Phi_0^k \qquad (C\text{-}13)$$

$$= 0 \quad \text{otherwise}$$

Consequently

$$\Delta = \prod_{k=1}^{n} \delta_k \qquad (C\text{-}14)$$

Substituting for Δ from Eqs. (C-10) and (C-14) in Eq. (C-9) we obtain

$$W_N(\vec{\Phi}_O)d\vec{\Phi}_O = \frac{1}{\pi^n}\int\cdots\int_{(\vec{\rho})}\int\cdots\int_{(\vec{q})}\left\{\prod_{j=1}^{N}\tau_j(\vec{q}_j)d\vec{q}_j\right\}\left\{\prod_{k=1}^{n}\frac{\sin(\frac{1}{2}d\Phi_O^k\rho_k}{\rho_k}\right\}$$

$$\exp\{i[\sum_{k=1}^{n}\sum_{j=1}^{N}\Phi_j{}^k\rho_k - \sum_{k=1}^{n}\Phi_O{}^k\rho_k]\}d\rho_1\ldots d\rho_n \tag{C-15}$$

$$= \frac{d\vec{\Phi}_O}{2^n\pi^n}\int\ldots\int e^{-i\vec{\rho}\cdot\vec{\Phi}_O}\,A_N(\vec{\rho})d\vec{\rho}$$

where we have written

$$A_N(\vec{\rho}) = \prod_{j=1}^{N}\int\ldots\int dq_j{}^1\ldots dq_j{}^s\, e^{+i\vec{\rho}\cdot\vec{\varphi}_j}\,\tau_j(\vec{q}_j{}^1\ldots\vec{q}_j{}^s) \tag{C-16}$$

The case of greatest interest is when all the functions τ_j (of the respective q_j's) are equal. Eq.(C-16)then becomes

$$A_N(\vec{\rho}) = [\int e^{i\vec{\rho}\cdot\vec{\varphi}(\vec{q})}d\vec{q}]^N \tag{C-17}$$

Thus if we have a vector R which is a superposition of a number of N vectors $\vec{r}_i$, each one having an independent probability distribution τ_i, i.e.

$$\vec{R} = \sum_{i=1}^{N}\vec{r}_i \tag{C-18}$$

where the probability that the ith displacement lies between r_1 and r_i+dr_i is given by

$$\tau_i(x_i,y_i,z_i)\,dx_idy_idz_i = \tau_i d\vec{r}_i \qquad (i=1,\ldots,N)$$

then we have that the probability distribution $W_N(\vec{R})d\vec{R}$ is given by

$$W_N(\vec{R}) = \frac{1}{8\pi^3}\int_{-\infty}^{\infty} e^{-i\vec{\rho}\cdot\vec{R}}\,A_N(\vec{\rho})d\vec{\rho} \tag{C-19}$$

$$A_N(\vec{\rho}) = \prod_{j=1}^{N} \int_{-\infty}^{\infty} \tau_j(\vec{r}_j) e^{-i\vec{\rho}\cdot\vec{r}_j} \, d\vec{r}_j \qquad \text{(C-20)}$$

These results can be immediately applied to our original R in (C-1) if we consider e^{iah_r} to be a unit vector $\vec{r}_j = (x_j, y_j)$ with a random direction and the sum $\sum_{r=1}^{N} e^{iah_r}$ is the total displacement vector $\vec{R}$ and where $\tau_j(\vec{r}_j)$ is the joint probability distribution of $\vec{r}_j$.

Proceeding further, we write the probability density function for $\vec{r}_j$ as

$$\tau_j|\vec{r}_j| = \frac{1}{2} \delta(|\vec{r}_j|^2 - 1)\, \delta(\omega) \quad (j=1,..,N) \qquad \text{(C-21)}$$

since we are specifically interested in the behavior of $|\vec{R}|$ it is obvious that it is simplest to work in terms of $\vec{r}_j$, $|\vec{R}|$ rather than in terms of the components of $\vec{r}_j$ and $\vec{R}$.

Substituting (C-21) into (C-20) we obtain our expression for $A_N(\vec{\rho})$ as

$$A_N(\vec{\rho}) = \prod_{j=1}^{N} \frac{1}{2} \int_{-\infty}^{\infty} e^{-i\vec{\rho}\cdot\vec{r}_j} \delta(r_j^2 - 1)\, \delta(\omega) d\vec{r}_j \qquad \text{(C-22)}$$

or using polar coordinates with the z-axis in the direction of $\vec{\rho}$

$$A_N(\vec{\rho}) = \prod_{j=1}^{N} \frac{1}{2} \int_0^{\infty} \int_0^{\pi} \int_0^{2\pi} e^{i|\vec{\rho}| r_j \cos\theta} \delta(r_j^2 - 1) \delta(\omega) r_j^2 \sin\theta \, dr_j \, d\theta \, d\omega \qquad \text{(C-23)}$$

Integrating over the polar angles θ and ω we get

$$A_N(\vec{\rho}) = \prod_{j=1}^{N} \int_0^{\infty} \int_0^{\pi} e^{i|\vec{\rho}|r_j\cos\theta}\delta(r_j^2-1)\sin\theta\, d\theta dr_j$$

$$= \prod_{j=1}^{N} \frac{1}{|\vec{\rho}|} \int_0^{\infty} \sin(|\vec{\rho}|r_j) r_j \delta(r_j^2-1) dr_j \qquad \text{(C-24)}$$

$$= \left[\frac{\sin|\vec{\rho}|}{|\vec{\rho}|}\right]^N$$

Thus

$$W_N(\vec{R}) = \frac{1}{8\pi^3} \int_{-\infty}^{\infty} e^{(-i\vec{\rho}\cdot\vec{R})} \left[\frac{\sin|\vec{\rho}|}{|\vec{\rho}|}\right]^N d\vec{\rho} \qquad \text{(C-25)}$$

Again using polar coordinates with the z-axis pointing in the direction of $\vec{R}$, we have

$$W_N(\vec{R}) = \frac{1}{8\pi^3} \int_0^{\infty} \int_{-1}^{+1} \int_0^{2\pi} e^{-i|\vec{\rho}||\vec{R}|t)} \left\{\frac{\sin|\vec{\rho}|}{|\vec{\rho}|}\right\}^N d|\vec{\rho}||\vec{\rho}|^2 d\omega dt d|\vec{\rho}| \qquad \text{(C-26)}$$

Integrating over and t we get

$$W_N(\vec{R}) = \frac{1}{2\pi^2|\vec{R}|} \int_0^{\infty} \sin(|\vec{\rho}||\vec{R}|) \left\{\frac{\sin|\vec{\rho}|}{|\vec{\rho}|}\right\}^N |\vec{\rho}|\, d|\vec{\rho}| \qquad \text{(C-27)}$$

This expression further reduces to

$$W_N(\vec{R}) = \frac{1}{2\pi^2|\vec{R}|} \int_0^{\infty} \sin(|\vec{\rho}||\vec{R}|) \{\text{sinc}|\vec{\rho}|\}^N |\vec{\rho}|\, d|\vec{\rho}| \qquad \text{(C-28)}$$

We now illustrate this method by evaluating the integral on the right-hand side of (C-28) for finite values of N by considering the cases N = 3 and 4. For N = 3, (C-28) becomes

$$W_3(\vec{R}) = \frac{1}{2\pi^2|\vec{R}|} \int_0^{\infty} \sin(|\vec{\rho}||\vec{R}|) \sin^3|\vec{\rho}| \frac{d|\vec{\rho}|}{|\vec{\rho}|^2} \qquad \text{(C-29)}$$

$$\sin(|\vec{\rho}||\vec{R}|)\sin^3(|\vec{\rho}|) = \frac{1}{8}\{3\cos[(|\vec{R}|-1)-3\cos[(|\vec{R}|+1)|\vec{\rho}|]$$
$$-\cos[(|\vec{R}|-3)|\vec{\rho}|] + \cos[(|\vec{R}|+3)|\vec{\rho}|]\} \qquad \text{(C-30)}$$

Further

$$\int_0^\infty \{\cos[(|\vec{R}|-1)|\vec{\rho}|]-\cos[|\vec{R}|+1)|\vec{\rho}|]\}\ \frac{d|\vec{\rho}|}{|\vec{\rho}|^2}$$

$$= 2\int_0^\infty \{\sin^2\frac{(|\vec{R}|+1)|\vec{\rho}|}{2} - \sin^2\frac{(|\vec{R}|-1)|\vec{\rho}|}{2}\}\ \frac{d|\vec{\rho}|}{|\vec{\rho}|^2} \qquad \text{(C-31)}$$

$$= \tfrac{1}{2}\pi(|\vec{R}| + 1 - \big||\vec{R}|- 1\big|)$$

We have a similar formula for the integral involving the other pair of cosines in Eq (C-30) Combining these results we obtain

$$W_3(\vec{R}) = \frac{1}{32\pi|\vec{R}|}\ \{(2|\vec{R}|-3\big||\vec{R}|- 1\big| + \big||\vec{R}| - 3|\big\} \qquad \text{(C-32)}$$

Or equivalently we get

$$W_3(\vec{R}) = \frac{1}{8\pi} \qquad (0<|\vec{R}|<1)$$

$$= \frac{1}{16\pi|\vec{R}|}\ (3 - |\vec{R}|), (1<|\vec{R}|<3) \qquad \text{(C-33)}$$

$$= 0 \qquad (3<|\vec{R}|<\infty)$$

We now consider the case N = 4. From Eq. (C-28) we get

$$W_4(\vec{R}) = \frac{1}{2\pi^2|\vec{R}|}\ \int_0^\infty \frac{d|\vec{\rho}|}{|\vec{\rho}|^3}\ \sin\ (\vec{\rho}||\vec{R}|)\sin^4(|\vec{\rho}|) \qquad \text{(C-34)}$$

From this equation we derive

$$-\frac{d^2}{d|R|^2}\left[|\vec{R}|W_4(\vec{R})\right] = \frac{1}{2\pi^2}\int_0^\infty \frac{d|\vec{\rho}|}{|\vec{\rho}|}\sin(|\vec{\rho}||\vec{R}|)\sin^4(|\vec{\rho}|) \qquad (C\text{-}35)$$

$$= \frac{1}{32\pi^2}\int_0^\infty \frac{d|\vec{\rho}|}{|\vec{\rho}|}\{\sin[(|\vec{R}|+4)|\vec{\rho}|] + \sin[(|\vec{R}|-4)|\vec{\rho}|]$$

$$-4\sin[(|\vec{R}|+2)|\vec{\rho}|] - 4\sin[|\vec{R}|-2)|\vec{\rho}|] + 6\sin(|\vec{R}||\vec{\rho}|)\} \qquad (C\text{-}36)$$

where the two alternatives in the last two steps of Eq. (C-34) depend, respectively, on the signs of $(|\vec{R}|-4)$ and $(|\vec{R}|-2)$. Thus

$$64\pi\frac{d^2}{d|\vec{R}|^2}\left[|\vec{R}|W_4(\vec{R})\right] = -6 \qquad (0<|\vec{R}|<2)$$

$$= +2 \qquad (2<|\vec{R}|<4) \qquad (C\text{-}37)$$

$$= 0 \qquad (4<|\vec{R}|<\infty)$$

Integrating the foregoing equation working backwards from large values of $|\vec{R}|$ where all derivations must vanish, we find

$$64\pi - \frac{d}{d|\vec{R}|}\left[|\vec{R}|W_4(\vec{R})\right] = 2(|\vec{R}|-4) \quad (2<|\vec{R}|<4)$$

$$= -6|\vec{R}|+8 \qquad (0<|\vec{R}|<2) \qquad (C\text{-}38)$$

where we have used the continuity of the quantity on the left side of this equation at $|\vec{R}| = 2$.

Integrating Eq (C-38) once again, we similarly obtain

$$64\pi\ |\vec{R}|W_4(\vec{R}) = |\vec{R}|^2 - 8\ |R| + 16 \quad (2<|\vec{R}|<4)$$

$$= (4 - |\vec{R}|)^2 \tag{C-39}$$

and

$$64\pi|\vec{R}|W_4(\vec{R}) = -\ 3|\vec{R}|^2 + 8|\vec{R}| \quad (2>|\vec{R}|>o) \tag{C-40}$$

Thus finally we obtain

$$W_4(\vec{R}) = \frac{1}{64\pi|R|}\ (8|\vec{R}| - 3|\vec{R}|^2) \quad (o<|\vec{R}|<2)$$

$$\frac{1}{64\pi|\vec{R}|}\ (4 - |R|)^2 \qquad (2<|\vec{R}|<4) \tag{C-41}$$

$$0 \qquad (4<|\vec{R}|<\infty)$$

In like manner, it is possible in principle to evaluate the integral for $W_N(\vec{R})$ for any finite value of N although the calculations may become very tedious. We may, however, note the following solution obtained for the case $N = 6$.

$$W_6(R) = \frac{1}{2^8\pi|\vec{R}|}\left(16|\vec{R}| - 4|\vec{R}|^3 + (5/6)|R|^4\right) \quad (0<R<2)$$

$$= \frac{1}{2^8\pi|\vec{R}|}\left(-20 + 56|\vec{R}| - 30|\vec{R}|^2 + 6|\vec{R}|^3 - (5/12)|\vec{R}|^4\right) (2<\vec{R}<4)$$

$$= \frac{1}{2^8\pi|\vec{R}|}\left(108 - 72|\vec{R}| + 18|\vec{R}|^2 - 2|\vec{R}|^3 + (1/12)|\vec{R}|^4\right) (4<|\vec{R}|<6)$$

$$= 0 \qquad (6<|R|\infty)$$

(C-42)

We now consider the special case when N is very large, i.e. N>>1. In this case

$$\lim_{N\to\infty} \left(\frac{\sin|\vec{\rho}|}{|\vec{\rho}|}\right)^N = \lim_{N\to\infty} \left(1 - \frac{1}{6}|\vec{\rho}|^2 + \ldots\right)^N \qquad (C-43)$$

$$= e^{-N|\vec{\rho}|^2/6}$$

Accordingly, for large values of N Eq. (C-28) becomes

$$\lim_{N\to\infty} W_N(\vec{R}) = \frac{1}{2\pi^2|\vec{R}|} \int_0^\infty e^{-N|\vec{\rho}|^2/6} |\vec{\rho}| \sin(|\vec{R}||\vec{\rho}| \; d|\vec{\rho}| \qquad (C-44)$$

Therefore,

$$W(\vec{R}) = \frac{1}{(2\pi N/3)^{1/2}} e^{-3|\vec{R}|^2/2N} \quad \text{as } N \to \infty \qquad (C\text{-}45)$$

REFERENCES

1. Lord Rayleigh, Philosophical Magazine, Vol. XXXVI, 429-449 (1918).

2. K. Pearson, Nature 77, 294 (1905).

3. J. C. Kluyver, Konink. Acad. Wetenschap. Amsterdam 14, 325 (1905).

4. M. von Smoluchowski, Bull. Acad. Cracovie, 203 (1906).

5. A. A. Markoff, "Wahrshienlichkeitsrechnung," Liepzig (1912), Chapters 16 and 33.

6. S. Chandrasekhar, Reviews of Modern Physics 15, 1 (1943).

7. This vector inequality as originally stated in Ref. (6) is defined in Eq. (C-13).

APPENDIX D

Probability Density for the Speckle Electric Field and Intensity

In this appendix we derive the probability density for the speckle electric field given in Eq. (4-1) and the speckle intensity given by the absolute value square of the electric field. In order to do this we rewrite the following results:

(a) The speckle electric field is given by Eq (4-1)

$$E_1(x) = A - BN + B\sum_{r=1}^{N} e^{iph_r} \tag{D-1}$$

where h_r is a random variable and A, B, N and p are given numbers

(b) The density function for the random variable $\vec{R}$, where $\vec{R} = \sum_{r=1}^{N} e^{jph_r}$ and ph_r takes on all possible angles, is (see (3-6))

$$W_{\vec{R}}(\vec{R}) = \frac{1}{2\pi^2|\vec{R}|}\int_0^\infty \sin(|\vec{\rho}|\ |\vec{R}|)[\operatorname{sinc}|\vec{\rho}|]^N|\vec{\rho}|\ d\ |\vec{\rho}| \tag{D-2}$$

(c) Given a function $y = ax + b$, where a and b are constants and also given the density function for the random variable x to be $f_x(x)$, the density function for y is, rewriting Eq. (5-7) in Ref. (1),

$$f_y(y) = \frac{1}{|a|} f_x\left(\frac{y-b}{a}\right) \tag{D-3}$$

(d) Given a function $z = |y|$, where the density function for y is $f_y(y)$, the density function for z is (see Eq. (5-12), Ref. 1)

$$f_z(z) = [f_y(z) + f_y(-z)]U(z) \tag{D-4}$$

where $U(z)$ is a unit step function and is 0 for $z < 0$, and unity for $z > 0$.

(e) The density function for $V = z^2$, is given by (Eq. 5-9 , Ref. (1))

$$f_v(v) = \frac{1}{2\sqrt{V}} [f_z(\sqrt{V}) + f_V(-\sqrt{V})]U(V) \tag{D-5}$$

To calculate the density function for the electric field we substitute (D-1) and (D-2) into (D-3) and obtain

$$W_{\vec{E}_1}(\vec{E}_1) = \frac{1}{2\pi^2|E_1-(A-BN)|} \int_0^\infty \sin\left(|\vec{\rho}|\left|\frac{E_1-(A-BN)}{B}\right|\right)[\text{sinc}|\vec{\rho}|]^N|\vec{\rho}|\, d\,|\vec{\rho}| \tag{D-6}$$

The density function of the absolute of the electric field, $|E_1|$ is given by, substituting (D-6) into (D-4)

$$W_{|E_1|}(|E_1|) = [W_{E_1}(|E_1|) + W_{E_1}(-|E_1|)]U(|E_1|) \tag{D-7}$$

Also substituting (D-7) into (D-5) and simplifying the algebra we obtain that the density function of the speckle intensity, $I_1 = |E_1|^2$ is given by

$$W_{I_1}(I_1) = \frac{1}{\sqrt{I_1}} [W_{E_1}(\sqrt{I_1}) + W_{E_1}(-\sqrt{I_1})]U(I_1) \qquad \text{(D-8)}$$

Alternatively (D-8) can be written as

$$W_{I_1}(I_1) = \frac{U(I_1)}{2\pi^2\sqrt{I_1}} \left[\frac{1}{|\sqrt{I_1}-(A-BN)|} \int_0^\infty \sin\left(|\vec{\rho}| \left| \frac{\sqrt{I_1}-(A-BN)}{B} \right| \right) [\text{sinc}|\vec{\rho}|]^N |\vec{\rho}| \, d\,|\vec{\rho}| \right.$$

$$\left. + \frac{1}{|\sqrt{I_1}+(A-BN)|} \int_0^\infty \sin\left(|\vec{\rho}| \left| \frac{\sqrt{I_1}+(A-BN)}{B} \right| \right) [\text{sinc}|\vec{\rho}|]^N |\vec{\rho}| \, d\,|\vec{\rho}| \right] \qquad \text{(D-9)}$$

REFERENCES

1. A. Papoulis, "Probability, Random Variables and Stochastic Processes," McGraw Hill Book Company, New York (1965), Ch. 5.